CHALMERS
UNIVERSITY OF TECHNOLOGY

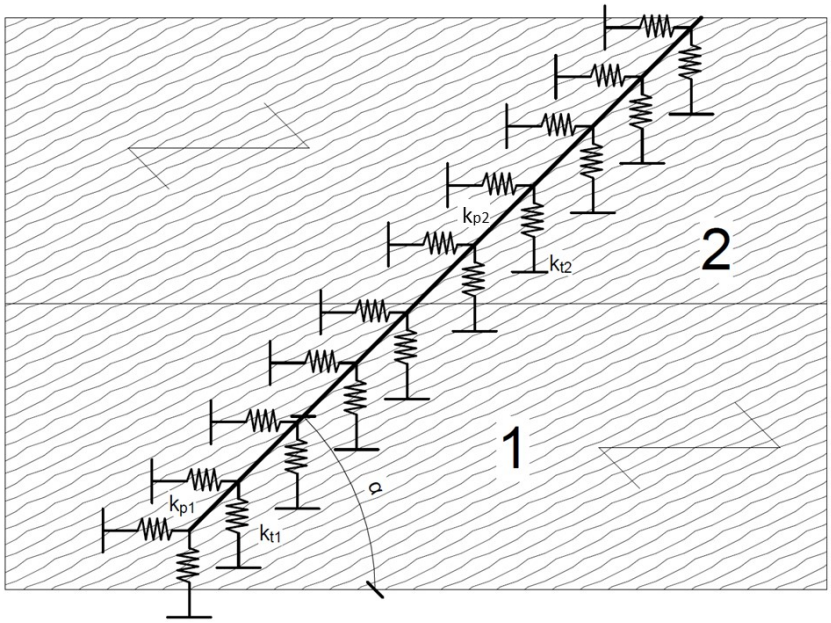

Combined loading of angled screws in timber connections

A study to evaluate the stiffness and load-carrying capacity of inclined screws

Master's Thesis in Structural Engineering and Building Technology

GUSTAV KULLANDER
ALEXANDER SANDSTRÖM

Department of Architecture and Civil Engineering
CHALMERS UNIVERSITY OF TECHNOLOGY
Gothenburg, Sweden 2023
www.chalmers.se

Master's thesis ACEX30

Combined loading of angled screws in timber connections

A study to evaluate the stiffness and load-carrying capacity of inclined screws

GUSTAV KULLANDER
ALEXANDER SANDSTRÖM

Department of Architecture and Civil Engineering
Division of Structural engineering
Research Group for Lightweight Structures
Chalmers University of Technology
Gothenburg, Sweden 2023

Combined loading of angled screws in timber connections
A study to evaluate the stiffness and load-carrying capacity of inclined screws

GUSTAV KULLANDER
ALEXANDER SANDSTRÖM

Supervisor: Linda Jakobsson, ELU Konsult AB
Examiner: Robert Jockwer, Department of Architecture and Civil Engineering

Master's Thesis 2023
Department of Architecture and Civil Engineering
Division of Structural Engineering
Research Group for Lightweight Structures
Chalmers University of Technology
SE-412 96 Gothenburg
Telephone +46 31 772 1000

Cover: An illustration of how the screw is simulated inside the timber

Typeset in LaTeX
Printed by Chalmers Reproservice
Gothenburg, Sweden 2023

Combined loading of angled screws in timber connections
A study to evaluate the stiffness and load-carrying capacity of inclined screws
Gustav Kullander
Alexander Sandström
Department of Architecture and Civil Engineering
Chalmers University of Technology

Abstract

Connections have a deciding role in the design of timber structures as they often present complex solutions and behaviour, which makes them critical areas during the design process. As wood has orthotropic properties the structural behaviour of connections becomes highly influenced by fastener- and force orientation. For connections with inclined screws, this behaviour is not fully reflected on in the current design standards. Therefore, the aim of this thesis is to study the combined loading of angled screws in timber-timber connections by evaluating the slip modulus and load-carrying capacity. The study investigates the behaviour of timber connections with inclined screws under various load scenarios and screw angles. The thesis utilizes experimental test results from previous studies, analytical equations from design standards and previous research, while the numerical part is carried out through finite element analysis in ABAQUS.

The results of the study indicate that the slip modulus and load-carrying capacity of timber connections with inclined screws are underestimated by Eurocode 5 in general but especially when considering certain angles. This does still remain true with the second generation of Eurocode 5. The research does however demonstrate that the use of inclined screws can significantly increase the load-carrying capacity of timber connections, as well as the stiffness and improve their overall performance. Additional research on how to implement different load-to-grain angles is suggested to improve the perfomance further.

Keywords: Timber engineering, Timber connections, Inclined screws, Slip modulus, Load carrying capacity, FE-modelling

Kombinerade laster i träförbindelser
Utvärderingsstudie av förskjutningsmodulen och lastkapaciteten i snedställda skruvar
Gustav Kullander
Alexander Sandström
Instutitionen för arkitektur och samhällsbyggnadsteknik
Chalmers Tekniska Högskola

Sammanfattning

Förbindelser spelar en avgörande roll för utformningen av träkonstruktioner eftersom de ofta presenterar komplexa lösningar och beteenden, vilket gör dem till kritiska områden under designprocessen. På grund av de ortotropa egenskaperna hos trä påverkas strukturbeteendet hos förbindeleser i hög grad av förbands- och krafters orientering. För förbindelser med snedställda skruvar återspeglas detta beteende inte fullt ut i de nuvarande designstandarderna. Därför syftar denna avhandling till att studera den kombinerade belastningen av snedskruvar i trä-trä-kopplingar genom att utvärdera förskjutningsmodulen och lastbärande kapacitet. Studien undersöker beteendet hos träförband med snedställdaskruvar under olika belastningsscenarier och skruvvinklar. Studien använder experimentella testresultat från tidigare forskning, analytiska equationer från designstandarder och tidigare studier samt numeriska metoder i ABAQUS för att utvärdera kopplingarna.

Resultaten av studien visar att styvheten och bärförmågan hos träförbindelsen med snedställda skruvar underskattas av Eurocode 5 i allmänhet, men särskilt när det gäller vissa vinklar. Detta gäller även den andra generationen av Eurocode 5, som underskattar förmågan av lutande skruvar i viss utsträckning. Forskningen visar dock att användningen av snedställda skruvar kan öka bärförmågan hos träförbindelser och förbättra deras allmänna prestanda. Ytterligare forskning om hur fler belastningsscenarier ska tillämpas föreslås för att ge en utvecklad prestanda i fler situationer.

Nyckelord: Trä, Träförbindelser, Lutande skruvar, Styvhet, Lastkapacitet, FE-modellering

Acknowledgements

This master thesis has been conducted at ELU's office in Gothenburg where we are thankful to have gotten support from our supervisor Linda Jakobsson. We would further like to thank our examiner Robert Jockwer who has helped and guided us throughout our work and answered our questions. We would also like to thank Fatima Hlal, who has patiently helped us with our Python work. We would then like to thank our opponents Albin Karlsson and Gustav Friman for their input and conversations which helped finish our work. Finally, we would like to thank our friends and family who have helped us throughout our time at Chalmers

Gustav Kullander and Alexander Sandström, Gothenburg, May 2023

List of Acronyms

Below is the list of acronyms that have been used throughout this thesis listed in alphabetical order:

BOF-model	Beam on foundation model
EC5	Eurocode 5
EC5 2G	Eurocode 5 second generation
FE	Finite element
FEM	Finite element method
SFS	Self-tapping screws
SLS	Serviceability limit state
ULS	Ultimate limit state

Nomenclature

Below is the nomenclature of indices, sets, parameters, and variables that have been used throughout this thesis.

Symbols

$F_{ax,k}$	Characteristic axial capacity of the fastener
$F_{ax,t,d,1}$	Axial design tensile resistance of an axially loaded fastener the minimum of the resistance in each timber member
$F_{ax,t,k}$	Characteristic axial tensile resistance of a a single fastener
$F_{ax,RD}$	Axial design capacity of the connection sign capacity of the connection
$F_{ax,t,RD}$	Axial design tensile resistance of the connection
$F_{c,k}$	Characteristic resistance of a screw in axial compression
$F_{D,k}$	Characteristic dowel-effect contribution per shear plane
F_{Ed}	Design tensile force transmitted by the connection
$F_{pull,k}$	Characteristic head pull-through resistance
$F_{rp,d}$	Design rope-effect contribution
$F_{sp,Rk}$	Characteristic splitting capacity of one connection
$F_{t,k}$	Characteristic tensile force
$F_{t,Ed}$	Design tensile force
$F_{r,Rd}$	Design tensile failure resistance parallel to the grain of the head tensile plane
F_{ult}	Ultimate load
$F_{v,k}$	Characteristic lateral resistance per shear plane of a single fastener
$F_{v,1,d}$	Design shear resistance per side shear plane in the timber member
$F_{v,Rd}$ / F_{RD}	Design shear capacity of the connection
$F_{90,Ed}$	Design tensile force component perpendicular to grain
$F_{90,Ed}$	Design splitting capacity

K_{ax}	Stiffness in the axial direction
K_v	Stiffness in the lateral direction
$K_{v,pulling}$	Stiffness in the lateral direction in pulling
K_{SLS}/K_{ser}	Stiffness for serviceability limit state verifications
$K_{SLS,ax}/K_{ser,ax}$	Mean stiffness per fastener per connected member in axial direction
$K_{SLS,v}$	Mean stiffness per fastener per shear plane in lateral direction
K_{ULS}	Stiffness for ultimate limit state verifications
$M_{y,RK}$	Characteristic yield moment in fastener
R_{ax}	Resistance in axial direction
R_v	Resistance in the lateral direction in shear
$R_{v,pulling}$	Resistance in the lateral direction in pulling
a	Distance or spacing
a_1	Spacing, parallel to the grain, of fasteners within one row
$a_{1,CG}$	Minimum end distance to the centre of gravity of the screw in each timber member
d	Diameter of the fastener
d_{ef}	Effective screw diameter
d_{head}	Head diameter
d_s	Diameter of the smooth part of the screw
d_1/d_{core}	Inner thread diameter
$f_{ax,k}$	Characteristic withdrawal strength
$f_{head,k}$	Characteristic head pull-through parameter
$f_{h,k}$	Characteristic embedment strength
$f_{u,k}$	Characteristic steel strength
$f_{v,d}$	Design shear strength
$f_{tens,k}$	Characteristic tensile strength
$f_{v,roll}$	Rolling shear strength
$f_{w,k}$	Characteristic withdrawal strength parameter
k_c	Factor for the buckling of the screw
k_{mat}	Factor for the material behaviour
k_{mod}	Modification factors for individual materials
k_p	Stiffness of parallel springs in the FE-Model
k_{screw}	Prefactor
k_t	Stiffness of perpendicular springs in the FE-Model
k_w	Modification factor

L_g/L_{ef}	Profiled length for nails, the length of the threaded part of screws
l_w	Withdrawal length
n	The number of fasteners
n_{ef}	Effective number of fasteners
n_p	Number of penetrated layers
t_i	The thickness of the board thickness or penetration depth.
t_h	Embedment depth
$t_{h,req}$	required minimum embedment depths in members
x_1	Reduction of effective length
α	The angle between the screw axis and to the direction parallel to the grain
α_{BT}	The angle between the screw axis and to the direction perpendicular to the grain
γ	Load to grain angle
γ_M	Partial factor for a material property
$\gamma_{M.0}$	Partial factor for material property
γ_{M1}	Partial factor for resistance of a metal fastener to instability
γ_{M2}	Partial factor for resistance to fracture of cross-sections of a metal fastener in tension to fracture
γ_R	Partial factor for resistance
ϵ	Load to grain direction
μ	Friction coefficient between the members and equals 0.25
ρ_k	Characteristic density
ρ_{mean}	Mean density

Contents

List of Figures

List of Tables

1
Introduction

This chapter presents the prerequisites for the thesis, which includes a background, purpose, objectives, method and Limitations.

1.1 Background

The popularity of using timber as a construction material in structures is growing because of the increased demand for more sustainable buildings, as well as it being a lightweight and flexible material that is easy to install, alter or remove. Connections have a deciding role concerning the design of timber structures as they often present complex solutions and behaviour, which makes them critical areas during design. Therefore, connections have become one of the most essential parts when analysing the structural integrity of timber structures. There are many factors that affect the structural safety and the final cost of timber structures, such as stress concentrations around the fasteners, multiaxial stress states, the anisotropic and brittle behaviour of wood. These factors are some of the reasons why connections play a major part in the overall structural behaviour, and as it is today, they are not fully reflected in the current design standards.

Screws as fasteners offer the benefit of transmitting loads into the wood not just perpendicular (laterally) to the screw axis but also in the axial direction, due to the screw's high withdrawal capacity. It is worth noting that the screw's highest stiffness is in its axial direction and lowest in the lateral direction. This in turn gives a big impact when choosing the direction and angle of the screw in relation to the grain and loading direction. The angled screws are in most cases exposed to a combined loading in the lateral and axial direction which presents a complex behaviour on how they act in an anisotropic material such as wood. To dimension some examples of such connections, the design standards express a combination of the two that can be used to find its structural capacity. As further reflection is needed concerning the factors that can be used in the combination, it is possible that it can be improved to further optimise the timber connections and develop design rules for further screw configurations. This can in turn result in a more effective usage of materials that can improve the efficiency during construction and the total costs of creating such a connection.

The method of fastening screws in angles other than perpendicular to the grain is somewhat unconventional for many types of timber elements. However, it is used

more frequently today in structures as the angled screws present many possibilities for complex solutions that otherwise would be harder to solve by conventional means. This method contributes to solutions that allow for more complex shapes in timber structures, which can contribute to a more advanced architectural design in newly constructed buildings or more easily constructed renovations where there are limitations on changes to the existing building. Hence, it is of interest to improve the use of angled screws in timber connections and their applicability. An optimisation of angled screws will also make the method a more economically viable solution.

1.2 Purpose and objective

The goal of this master thesis is to gain a deeper understanding of fasteners in timber connections exposed to combined loading in the lateral and axial direction, using analytical analysis, FE-modelling and experimental results. More specifically, it shall be investigated how the angle of screws in timber elements affects the structural capacity and structural behaviour within connections, how the behaviour relates to the current design rules in Eurocode (to see if the rules are unsafe, safe or too conservative), as well as how a more general and more optimal design equation would look like. As a consequence, the performance of the connections can be evaluated and optimised with regard to the economic aspect of using such a connection as well as material usage and cost during construction.

The timber connections that are analysed in this thesis are exposed to combined loading in the lateral and axial direction, which is dictated by the angle at which the screw is inserted relative to the grain direction of the timber elements and how the load is applied. All connections in this study will be between two timber elements with a screw inserted at different angles to investigate the relationship between the angle and the stiffness for given situations, a simplified sketch of such a connection can be seen in Figure 1.1 below.

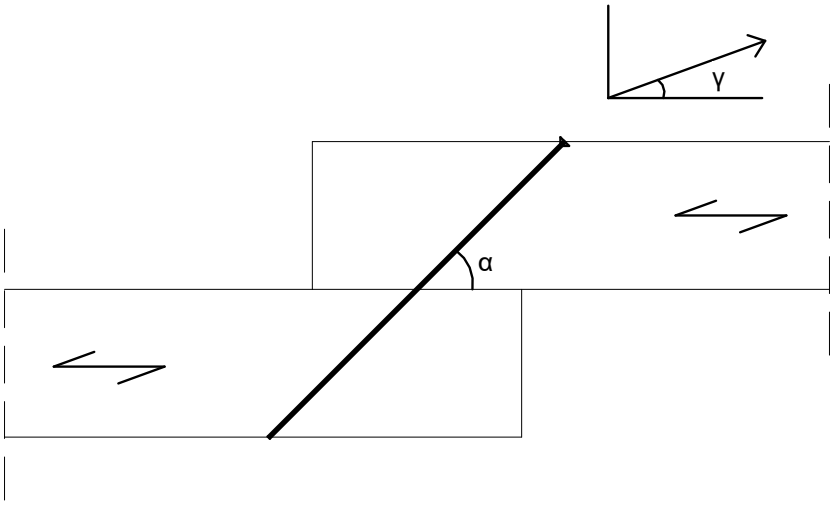

Figure 1.1: Combined loading on an angled screw

The study includes variable parameters to give a broad but isolated view of the angled screw connections, which will determine the influence that they have and from that create an understanding of how to design properly. This will be used to create insight conserning the range of applications for the connections and be used as a base to predict the behaviour in new situations.

1.3 Method

The work conducted in the master thesis covers the following steps:

1. Reviewing the state-of-knowledge on the design and structural behaviour of timber fasteners in a literature study of relevant standards, studies and experiments.

2. Collecting a database with test data on the relevant connection and identifying the main parameters of influence. This includes the assembly of analytical equations and test results in order to gain a broad overview.

3. Performing a structural analysis of the connection in FEM, then making a comparison to Eurocode and the test results.

4. Develop recommendations and conclusions. Investigate whether the existing models in Eurocode are safe and economic or if they could be developed further with factors or new equations.

1.4 Limitations

This rapport will be limited to studying the evaluation of angled screws in combined loading, more specifically how the variation of angles affects the structural capacity and structural behaviour of the connection. Comparisons between relevant reports and the assembly of relevant test data will be limited to a certain extent that can be fitted in the frame of this master thesis. The results created from the FE-models in this thesis are limited to only using one type of screw, with predefined geometry and characteristics. The type of wood chosen is limited to a certain species and strength class that is assumed to be in a climate with constant temperature and constant relative humidity. The thickness of the timber members and the screw's distance to timber edges is chosen to be sufficiently large to prevent brittle failures and to simplify the study. The number of angles between the screw axis and the grain direction that will be analysed are chosen to be the most common ones and those that can easily be compared to other reports and studies to limit the scope of the thesis. When comparing the analytical results in the form of hand calculations to FE results, a simplified FE-model will be used, this is because of limitations as previously stated in the master thesis, computer capacity as well as time constraints.

2

Material and connection properties

Timber is an organic material that has several properties which have to be taken into consideration which affects how the material can be used in the most optimal way. This chapter covers the general behaviour and considerations that need to be made when analysing timber connections.

2.1 Orthotropic material

Wood is an orthotropic material which means that it has different properties in three different directions, these are: radial-, longitudinal- and tangential direction as can be seen in Figure 2.1. This has an impact on the strength within the material, where a load applied parallel or perpendicular to the grain will give significantly different results. When the load is applied parallel to the grain direction the material will be able to withstand 10 times greater load compared to applying the load perpendicular to the grain (Swedish Wood, 2022b).

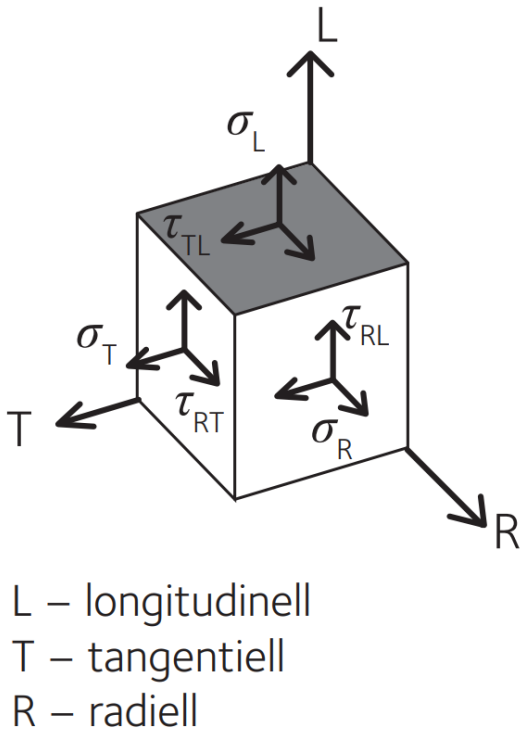

Figure 2.1: Illustrating the different directions in timber, figure from (Swedish Wood, 2022b)

2.2 Definition of angles

Throughout the thesis, the angles α, γ and ϵ are used and all of them have a relation to the grain direction of the timber, as seen in Figure 2.2. The angle between the screw axis and the grain direction is defined as α. The angle between the force direction and the grain direction, which acts on the same plane as α is defined as γ. Lastly, ϵ is the angle between the force and the grain direction in a separate plane from both α and γ.

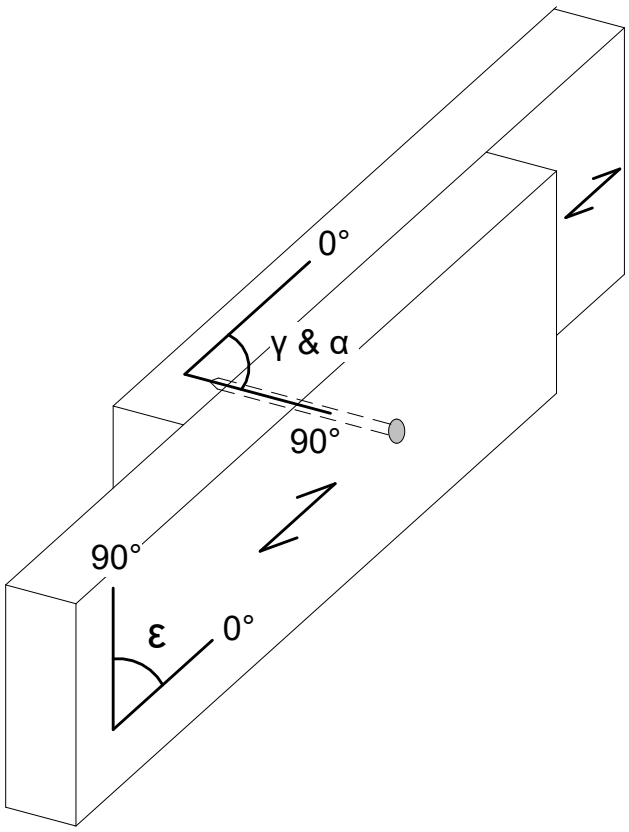

Figure 2.2: Illustrating the definition of the angles used in the study

2.3 Influence of moisture in wood

Wood as previously stated is orthotropic, which means it has different properties in different directions. This is important to consider since wood is a hygroscopic material which makes the moisture content in the wood vary with the moisture in the surrounding air. The material then swells if the moisture content increases until it reaches the fibre saturation point, therefore, the boards are dried with the Kin Drying regime to ensure drying to 12-18 % depending on the moisture conditions on-site (Swedish Wood, 2022b). If this is not taken into consideration, it can lead to splitting in the wood which is not always harmful but should be avoided. The moisture content also impacts properties such as strength and stiffness, where both properties increase linearly with lower moisture content. However, tests have shown that for full-sized timber, the tension strength is independent of moisture content in contrast to compression strength. This is taken into account through decreasing the strength class with the use of different service classes which is dependent on the highest ambient moisture content. Furthermore, it can also be seen that the moisture content has an effect on the duration of load effect, with higher moisture content resulting in a bigger loss of strength, which is expressed in the factor “kmod” which can be found in Table 2.1. Finally, moisture content also has a big impact on

creep deformations which can be further increased if there are significant moisture variations (Swedish Wood, 2022b).

Table 2.1: Strength modification factor k_{mod}

Material	Material standard	Service class	Load duration class				
			P	L	M	S	I
Glulam	EN 14080	1	0.6	0.7	0.8	0.9	1.1
		2	0.6	0.7	0.8	0.9	1.1
		3	0.5	0.55	0.65	0.7	0.9

2.4 Joints with dowelled type fasteners

Dowelled joints are mechanical fasteners which enable the transfer of shear forces in a construction, where the most common material is steel. There are several types of dowels, for example, nails, bolts, and screws, where load carrying capacity varies depending on the three parameters: the anchorage capacity which enables utilisation of tensile resistance, the yield moment and the embedment strength (Swedish Wood, 2022b).

2.4.1 Material properties

Swedish Wood (2022b) explains that the yield moment is the parameter that enables plastic moment which is needed to develop a plastic hinge in a dowel, where the value is based on the fastener diameter and the ultimate strength which depends on the material of the fastener. Embedding strength is the strain the surrounding wood of a dowel can sustain which is impacted by several parameters (Swedish Wood, 2022b). These parameters are:

- The density of wood, where higher densities give greater strength.
- The fastener diameter, which should be smaller to achieve higher embedding strength.
- The angle between the grain and load direction, where the highest strength is acquired when in compression being closer to parallel to the grain.
- The screws friction against the timber, where a rough surface is desired.
- The moisture content, which should preferably be lower to ensure high strength in general and to increase the embedded strength.
- If the hole is predrilled, which will affect how the forces are transferred.
- Withdrawal capacity, which is governed by the surface of the fastener, where screw threading severely improves the withdrawal strength. Here is both the length and depth of threading part into the material is important.
- The screw axis to grain angle is important due to the ability of the screw to transfer both axial and lateral forces.
- The number of screws acting together can also be of importance due to impacting the failure mode.

2.4.2 Johansen's failure modes

In dowel joint timber-timber connections, there are a number of failure modes that can be caused depending on the embedding strength of the material, the yield moment of the fastener or the thickness of the members, with the different modes being illustrated in Figure 2.3. The Roman letters I, II, and III represent the three failure modes from Johansen's Yielding theory, where the numbers represent the number of plastic hinges in the failure mode 0, 1 and 2 respectively (Swedish Wood, 2022b). Failure is caused by either the dowel rotating even though it is straight, the dowel bending and forming a plastic hinge, or the timber failing but the dowel remaining straight.

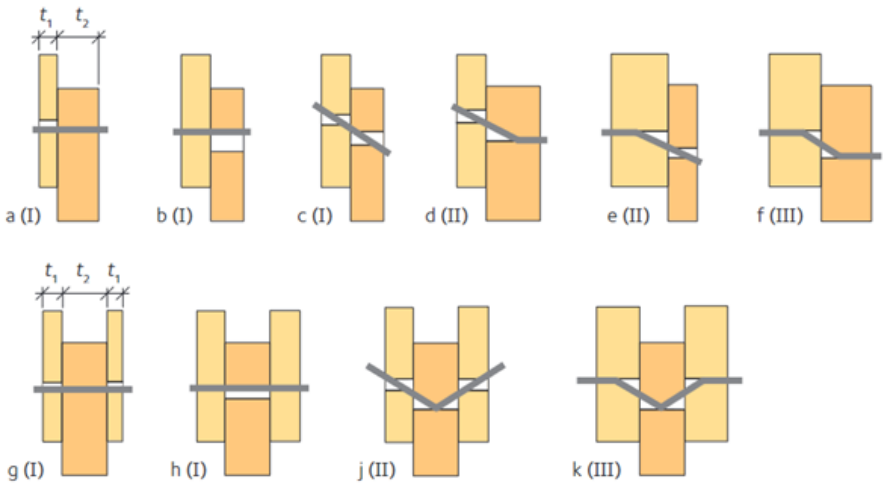

Figure 2.3: Illustrating the different failure modes in timber-timber connection, figure from (Swedish Wood, 2022b)

2.5 Brittle failure modes and group effects in dowelled joints

The existence of a joint is only considered when there are at least two fasteners in a connection, oftentimes there are several fasteners connected in a group which creates the need to have distances between fasteners as well as between fasteners and edges. Having several fasteners can also lead to more brittle failure modes (Swedish Wood, 2022b).

2.5.1 Group effect

When several fasteners are close to each other they rarely achieve their load capacity simultaneously which is due to variations in the strength of timber, the sizes of holes, misalignments of holes and sometimes uneven transfer of forces between the fasteners. This is handled in Eurocode with a factor calculating the effective number of fasteners and having a minimum spacing between the fasteners to ensure less splicing occurs (Swedish Wood, 2022b). This can be seen in equations 2.1 and 2.2.

$$n_{ef} = n^{k_{ef}} \qquad \textit{(screw } d \leq \textit{6mm, nails and staples)} \tag{2.1}$$

$$n_{ef} = \begin{cases} n \\ n^{0.9}\sqrt{\frac{a_1}{13d}} \end{cases} \qquad \textit{(screw } d > \textit{6mm, bolts and dowels)} \tag{2.2}$$

where

a_1 is the distance between fasteners parallel to the grain

and:

$$k_{ef} = \begin{cases} 1 & (a_1 \geq 14d) \\ 0.85 & (a_1 = 10d) \\ 0.7 & (a_1 = 7d) \end{cases}$$

2.5.2 Edge distances

Edge distance is set to avoid splitting and to ensure maximum strength capacity in loaded screw connections. The distances can be seen in Table 2.3 which shows different distances according to the direction in which the screw is applied. Figure 2.4 shows how the centre of gravity varies with an angle which impacts the minimum end distance.

Table 2.3: The minimum values of spacing and end/edge distance for axially loaded screws from Swedish Wood (2022b)

Min. screw spacing parallel to grain	Min. screw spacing perp. to grain	Min. end distance to centre of gravity of screw	Min. edge distance to centre of gravity of screw
a_1	a_2	$a_{1,CG}$	$a_{2,CG}$
7d	5d	10d	4d

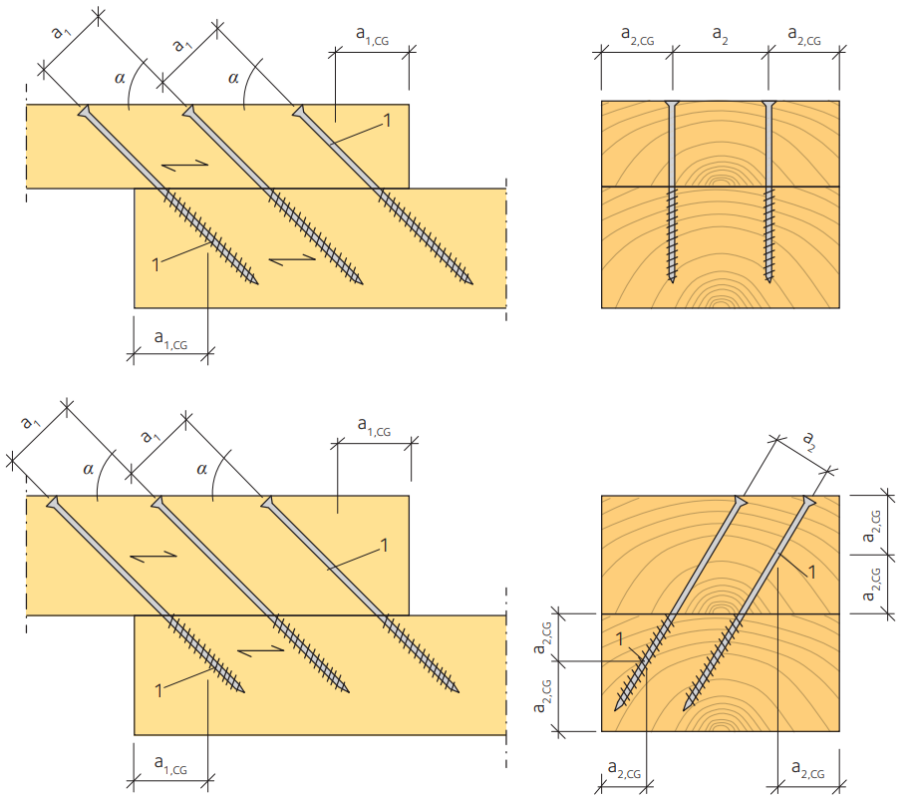

Figure 2.4: The minimum screw spacing and edge distance for angled screws, figure from (Swedish Wood, 2022b)

2.5.3 Brittle failure of connections with dowelled-type fasteners

When placing fasteners there may sometimes be a need for more fasteners than one which requires certain distances between fasteners as previously mentioned to avoid problems such as splitting. These distances can however require the timber to have bigger dimensions and therefore, use more material and as a result become more costly. According to Swedish Wood (2022b), if the distance between the fasteners is too small however it can lead to more brittle failure modes which can become an even bigger problem due to them being unexpected compared to ductile failure

modes. Swedish Wood (2022b) then continues by stating that there are five different brittle failure modes which are: row shear, block shear, net tensile failure, plug shear and splitting, which are illustrated in Figure 2.5.

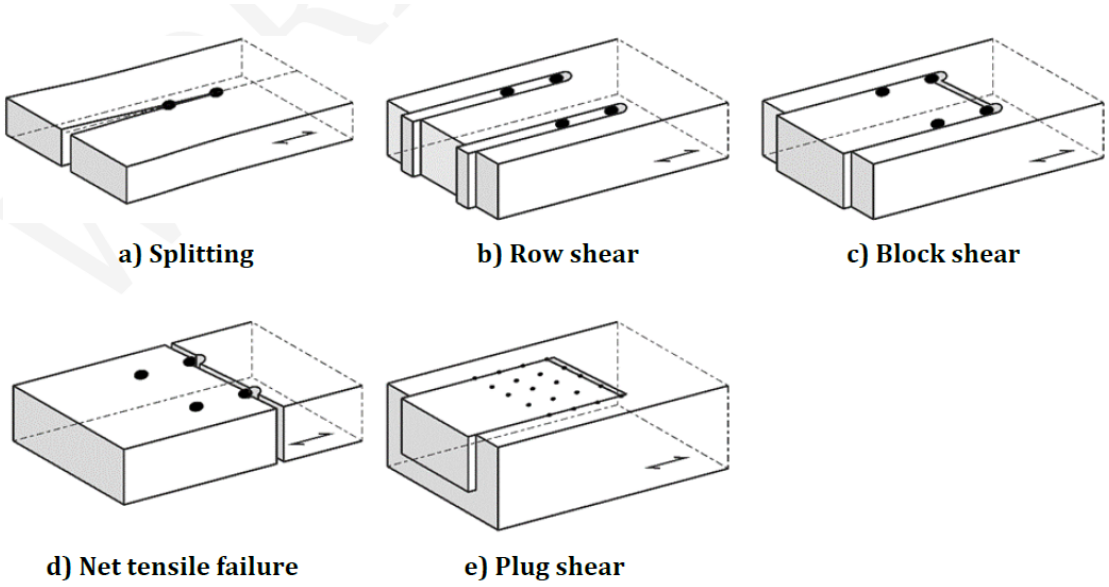

Figure 2.5: The different brittle failure modes with dowelled-type fasteners, figure from CEN (2022b)

2.5.3.1 Splitting

Splitting is a phenomenon where the wood splits across the wood fibres and for timber without cross-veneers. To avoid splitting the connection have to pass the criteria (CEN, 2022b):

$$F_{90,Ed} \leq F_{sp,Rd} \tag{2.3}$$

With

$$F_{90,Ed} = F_{Ed} \sin \alpha \tag{2.4}$$

where

F_{Ed}	is the design tensile force transmitted by the connection
$F_{sp,Rd}$	is the design splitting capacity
$F_{90,Ed}$	is the design tensile force component perpendicular to the grain as can be seen in figure 2.6

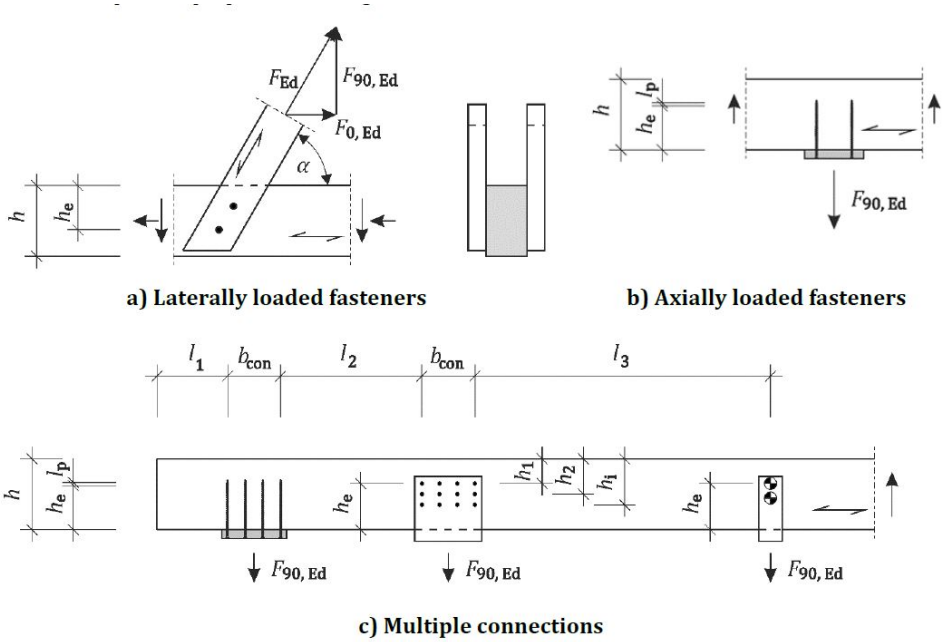

Figure 2.6: Loaded edge distance, end face distance and distances between connections, figure from CEN (2022b)

2.5.3.2 Row shear

Row shear gets cracks from a combination of in-plane shear stress and tensile forces perpendicular to the grain, this is however simplified to assume that only in-plane shear stresses are causing the cracks (CEN, 2022b). The capacity for row shear is therefore calculated with equation 2.5:

$$F_{rs,d} = 2n_{90} \cdot F_{v,1d} \tag{2.5}$$

where

n_{90} is the number of fasteners in a row perpendicular to the grain

$F_{v,l,d}$ is the design shear resistance per side shear plane in the timber member

2.5.3.3 Block shear

CEN (2022b) states that block shear occurs when the fastener penetrates the timber member and the resistance is contributed by both the tension resistance in the end face and on the shear resistance of the side faces, where the highest value of the tensile and shear strength is chosen according to equation 2.6.

$$F_{bs,Rd} = max \begin{cases} 2F_{v,la,d} \\ F_{t,d} \end{cases} \tag{2.6}$$

where

$F_{v,la,d}$ is the design shear resistance per side shear plane in the timber member

$F_{t,d}$ is the design tensile failure resistance parallel-to-grain of the head tensile plane

2.5.3.4 Plug shear

Plug shear occurs when the fastener does not fully penetrate the member and is similar to calculating block shear, but the difference is how the area A_{net} is calculated as can be seen in Figure 2.7 and the strength is calculated according to equation 2.7 (CEN, 2022b).

$$F_{ps,d} = max \begin{cases} 2F_{v,la,d} \\ F_{t,d} + F_{v,b,Rd} \end{cases} \tag{2.7}$$

where

$F_{v,la,d}$ is the design shear failure resistance per side shear plane in the timber member

$F_{t,d}$ is the design tensile failure resistance of the head plane in the timber member

$F_{v,b,Rd}$ is the design shear plane resistance of the bottom shear plane in the timber member

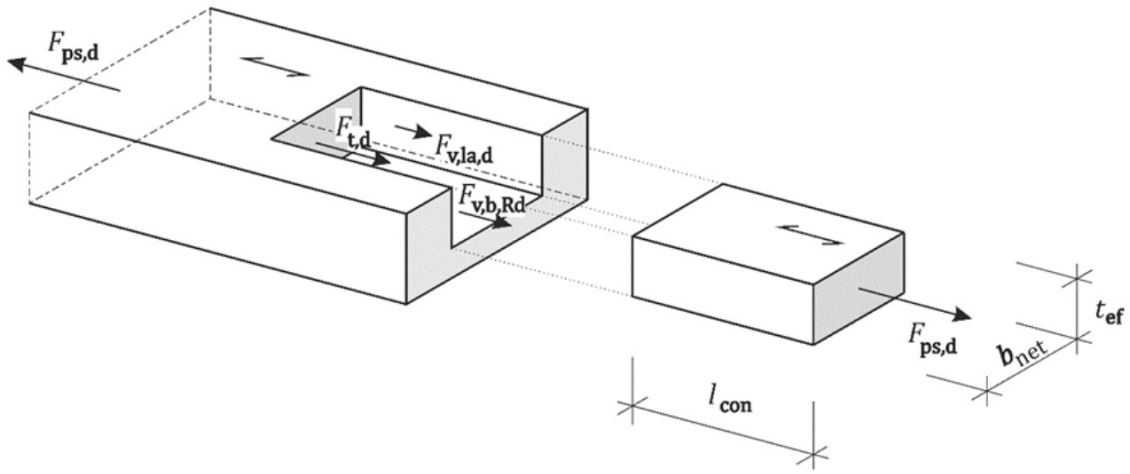

Figure 2.7: The geometries used to find the area of A_{net} in plug shear, figure from CEN (2022b)

2.5.3.5 Net tensile failure

Net tensile failure will occur if the design tensile stress parallel to the grain does not fulfil:

$$\sigma_{t.0.d} \leq f_{t,0,d}. \tag{2.8}$$

where

$\sigma_{t,0,d}$ is the design tensile stress parallel to the grain in the net cross-section at the position of the highest force and smallest cross-section

$f_{t,0,d}$ is the design tensile strength parallel to the grain and should be determined at the section presenting the largest number of fasteners perpendicular to the load direction (CEN, 2022b)

2.6 Stiffness and slip modulus

Swedish Wood (2022b) describes the stiffness as the force divided by the displacement and indicates how the member will behave as either ductile or brittle, in joints

it is described as slip modulus. The stiffness of a timber joint is dependent on several factors which are; the type of joint, the quality and strength of the surrounding materials, the direction of the grain (where parallel to the grain is the strongest), the connector force and also the duration and creep factor.

The rigidity of the connection will then play a role in the shear force stress distribution. The stiffness of the joint during SLS has an effect on the deflection where higher stiffness results in smaller deflections and which could impact the conceived safety and comfort of the habitants. The stiffness is assumed to be lower during ULS which may impact the redistribution of stresses.

Eurocode 5 describes the slip modulus K_{ser} in shear during SLS which assumes that the joint behaves linearly even if test results would show otherwise (Swedish Wood, 2022b). The slip modulus does however to some extent behave linearly assumed to be corresponding to $0.4F_{ult}$. The slip modulus varies for specific joints where the formula in SLS is according to equation 2.9.

$$K_{ser} = \begin{cases} \rho_m^{1.5} \frac{d}{23} \text{for dowels, bolts, screws, and pre-drilled nails} \\ \rho_m^{1.5} \frac{d}{30} \text{for non pre-drilled nails} \end{cases} \tag{2.9}$$

where

ρ_m	is the average density of the timber
d	is the outer thread diameter

The Ultimate limits state slip modulus K_U is calculated as two-thirds of K_{ser} which can be seen in equation 2.10 and corresponds to $\frac{2}{3}F_{Ult}$ (Swedish Wood, 2022a).

$$K_U = \frac{2}{3}K_{ser} \tag{2.10}$$

2.7 Design of connections

When calculating the design capacity (F_{Rd}) in the ultimate limit state for a wood connection, the characteristic capacity (F_{Rk}) is reduced with the partial coefficient for the material (γ_M) and the strength modification factor based on the material (k_{mod}) according to equation 2.11 (Swedish Wood, 2022a).

$$F_{Rd} = k_{mod}\frac{F_{Rk}}{\gamma_M} \tag{2.11}$$

2.7.1 Laterally loaded screws

In Eurocode, the capacity of laterally loaded screws in timber members are expressed with failure modes, as seen in Chapter 2.4.2. These failure modes concern nails, bolts, dowels, staples, screws and their resistance $F_{v,Rk}$ is calculated in equations a-f below, where the letter next to the equation is associated with the failure mode in Chapter 2.4.2 (Swedish Wood, 2022a). When the fasteners are exposed to single shear (attached to 2 timber members) the following equations can be used:

$$R_A = f_{h,1,k} \cdot t_1 \cdot d \tag{a}$$

$$R_B = f_{h,2,k} \cdot t_2 \cdot d \tag{b}$$

$$R_C = \frac{f_{h,1,k} \cdot t_1 \cdot d}{1+\beta} \cdot \left(\sqrt{\beta + 2\beta^2 \left(1 + \frac{t_2}{t_1} + \left(\frac{t_2}{t_1}\right)^2\right) + \beta^3 \cdot \left(\frac{t_2}{t_1}\right)^2 - \beta \cdot (1 + \frac{t_2}{t_1})} \right) + \frac{F_{ax,Rk}}{4} \tag{c}$$

$$R_D = 1.05 \frac{f_{h,1,k} \cdot t_1 \cdot d}{2+\beta} \cdot \left(\sqrt{2\beta(1+\beta) + \frac{4\beta(2+\beta)M_{y,k}}{f_{h,1,k} \cdot d \cdot t_1^2}} - \beta \right) + \frac{F_{ax,Rk}}{4} \tag{d}$$

$$R_E = 1.05 \frac{f_{h,1,k} \cdot t_1 \cdot d}{1+2\beta} \cdot \left(\sqrt{2\beta^2(1+\beta) + \frac{4\beta(2+\beta)M_{y,k}}{f_{h,1,k} \cdot d \cdot t_2^2}} - \beta \right) + \frac{F_{ax,Rk}}{4} \tag{e}$$

$$R_F = 1.15 \cdot \sqrt{\frac{2\beta}{1+\beta}} \cdot \sqrt{2M_{y,k} f_{h,1,k} d} + \frac{F_{ax,Rk}}{4} \tag{f}$$

$$F_{v,Rk} = min(R_A, R_B, R_C, R_D, R_E, R_F) \tag{2.12}$$

When the fasteners are exposed to double shear (attached to 3 timber members):

$$R_G = f_{h,1,k} \cdot t_1 \cdot d \tag{g}$$

$$R_H = 0.5 f_{h,2,k} \cdot t_2 \cdot d \tag{h}$$

$$R_J = \frac{f_{h,1,k} \cdot t_1 \cdot d}{1+\beta} \cdot \left(\sqrt{\beta + 2\beta^2 \left(1 + \frac{t_2}{t_1} + \left(\frac{t_2}{t_1}\right)^2\right) + \beta^3 \cdot \left(\frac{t_2}{t_1}\right)^2 - \beta \cdot (1 + \frac{t_2}{t_1})} \right) + \frac{F_{ax,Rk}}{4} \tag{J}$$

$$R_K = 1.15 \cdot \sqrt{\frac{2\beta}{1+\beta}} \cdot \sqrt{2M_{y,k} f_{h,1,k} d} + \frac{F_{ax,Rk}}{4} \tag{k}$$

$$F_{v,Rk} = min(R_G, R_H, R_J, R_K) \tag{2.13}$$

where

β	is Ratio between embedment strength of members, $f_{h,2,k}/f_{h,1,k}$
$F_{v,Rk}$	is the characteristic capacity per shear plane, per fastener
t_i	is the timber of board thickness or penetration depth, $i = (1, 2)$
$f_{h,i,k}$	is the characteristic embedment strength in wood member
d	is the fastener diameter
$M_{y,Rk}$	is the characteristic yield moment in fastener
$F_{ax,Rk}$	is the characteristic withdrawal capacity of the fastener

2.7.1.1 Embedment strength and yield moment

When calculating the embedment strength for smooth shank screws, the same equations can apply but with an effective diameter that is 1.1 times the inner screw diameter ($d_{ef} = 1.1 \cdot d_1$). If the screw is $d \leq 6$ the characteristic embedment strength can be expressed as:

$$f_{h,k} = 0.082 \cdot \rho_k \cdot d_{ef}^{-0.3} \qquad \text{(without pre-drilled holes)} \tag{2.14}$$

$$f_{h,k} = 0.082(1 - 0.01 d_{ef})\rho_k \qquad \text{(with pre-drilled holes)} \tag{2.15}$$

as well as the characteristic yield moment:

$$M_{y,Rk} = \frac{f_u}{600} 180 d_{ef}^{2.6} \tag{2.16}$$

However, for a case when $d \geq 6$, the characteristic embedment strength is expressed with equations 2.17 and 2.18.

$$f_{h,\epsilon,k} = \frac{f_{h,0,k}}{k_{90} sin(\epsilon)^2 + cos(\epsilon)^2} \tag{2.17}$$

$$f_{h,0,k} = 0.082(1 - 0.01 d_{ef})\rho_k \tag{2.18}$$

and the characteristic yield moment:

$$M_{y,Rk} = 0.3 f_u d_{ef}^{2.6} \tag{2.19}$$

where

d_{ef}	is the effective screw diameter
ρ_k	is the characteristic timber density
ϵ	is the load to grain angle
f_u	is the characteristic tensile strength

and:

$$k_{90} = \begin{cases} 1.35 + 0.015d & \text{(softwood)} \\ 1.30 + 0.015d & \text{(LVL)} \\ 0.90 + 0.015d & \text{(hardwood)} \end{cases}$$

2.7.1.2 Rope effect

According to Swedish Wood (2022b) the rope effect is taken into consideration through the term $(\frac{F_{ax,Rk}}{4})$ which is added to the shear capacity and depends on the dowel type, as can be seen in Table 2.12, where each dowel has its individual percentage of the shear capacity.

Table 2.12: Maximum contribution from the rope effect in relation to the shear strength of a single dowel-type faster

Fastener type	Percentage [%]
Round nails	20
Squared and grooved nails	25
Other nails	50
Screws	100
Bolts	25
Dowels	0

2.7.2 Axially loaded screws

There are three different failure modes that express the load-carrying capacity of screws exposed to axial loads (Swedish Wood, 2022a). The minimum of these capacities is used to get the total axial resistance ($F_{ax,Rd}$), and they are as follows:

- The characteristic withdrawal capacity ($F_{ax,Rk}$)
- The characteristic pull-through capacity ($F_{ax,Rk}$)
- The characteristic tensile capacity ($F_{t,Rk}$)

2.7.2.1 Failure mode 1: Withdrawal capacity

The first failure mode is when the threaded part of the screw loosens its attachment to the timber member and is withdrawn from the connection (withdrawal failure). If the screw has a diameter of $6mm \leq d \leq 12mm$ and an outer- to inner thread diameter ratio $0.6 \leq \frac{d}{d_1} \leq 0.75$ equation 2.20 for the characteristic withdrawal capacity can be used.

$$F_{ax,k} = \frac{n_{ef} \cdot f_{ax,k} \cdot d \cdot L_{ef} \cdot k_d}{1.2(\cos\alpha)^2 + (\sin\alpha)^2} \tag{2.20}$$

where

n_{ef}	is the effective number of fasteners
d	is the outer threading of the screw
l_{ef}	is the effective length of the threading

and:

$f_{ax,k} = 0.52d^{-0.5} \cdot l_{ef}^{-0.1}\rho_k^{0.8}$

$k_d = min \begin{cases} \frac{d}{8} \\ 1 \end{cases}$

According to CEN (2013), if the screw's dimensions are other than the requirements mentioned above, a relation between densities is used to express the capacity which can be seen in equation 2.21.

$$F_{ax,k} = \frac{n_{ef} \cdot f_{ax,k} \cdot d \cdot l_{ef} \cdot k_d}{1.2(\cos\alpha)^2 + (\sin\alpha)^2} \left(\frac{\rho_k}{\rho_a}\right)^{0.8} \tag{2.21}$$

where

$f_{ax,k}$	is the characteristic withdrawal strength
ρ_k	is the characteristic density
ρ_a	is the associated density for $f_{\alpha x,k}$
n_{ef}	is the effective number of fasteners

2.7.2.2 Failure mode 2: Pull-through resistance

The second failure mode is when the screw is sinking into the timber member as a result of the weak capacity of the timber bellow the screw head (pull-through failure). This characteristic pull-through capacity is expressed with equation 2.22.

$$F_{ax,\alpha,Rk} = n_{ef} \cdot f_{head,k} \cdot d_h^2 \left(\frac{\rho_k}{\rho_a}\right)^{0.8} \tag{2.22}$$

where

$f_{head,k}$	is the characteristic pull-through strength
d_h	is the screw head diameter
n_{ef}	is the effective number of fasteners

2.7.2.3 Failure mode 3: Tensile resistance

The last failure mode represents the yielding of the screw due to tensile forces (Tensile failure) and is expressed with equation 2.23.

$$F_{t,RK} = n_{ef} \cdot f_{tensk} \tag{2.23}$$

where

f_{tensk}	is the characteristic tensile strength
n_{ef}	is the effective number of fasteners

2.8 Hanskinsons theory

Due to timber being an orthotropic material its compressive strength varies depending on the load to grain angle (ϵ) as seen in Figure 2.8 (Swedish Wood, 2022b).

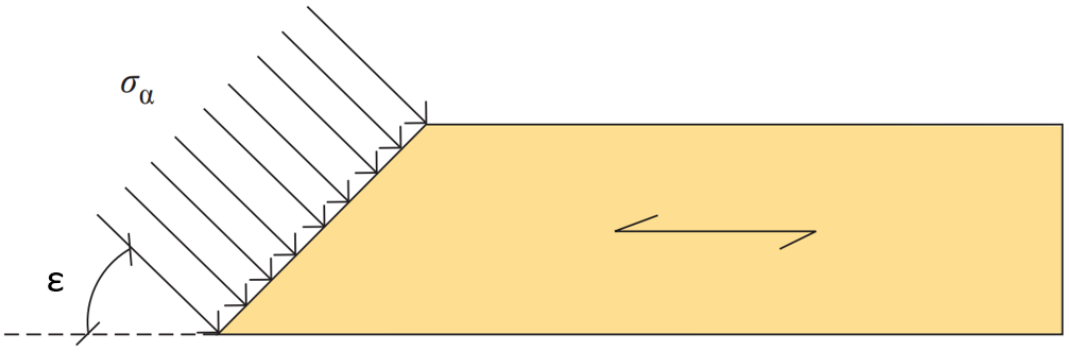

Figure 2.8: Illustrating the force to grain angle ϵ when a timber element is exposed to compression, figure from (Swedish Wood, 2022b)

Equation 2.24 defines the compressive strength at the angle (ϵ) and uses the compressive strength for a case parallel to the grain (f_0) and perpendicular to the grain (f_{90}) (Hankinson, 1921).

$$f_\epsilon = \frac{f_0 \cdot f_{90}}{f_0 sin^2(\epsilon) + f_{90} cos^2(\epsilon)} \tag{2.24}$$

Swedish Wood (2022b) states that equation 2.24 is also applicable in tension as it has shown to work well for that type of loading. With this expression, it becomes apparent that a minor deviation from the parallel direction (f_{90}) gives a major reduction of the compressive strength. This relation from Hankinson (1921) is also used as a base for equation 2.17 when calculating the embedment strength for a force-to-grain angle (ϵ).

3

Design of inclined screws

When screws experience a simultaneous loading with both axial load and shear load, an interaction of the two is needed to express the capacity of the connection. In Eurocode, this relation is shown by the following equation (Swedish Wood, 2022a):

$$\left(\frac{F_{ax,Ed}}{F_{ax,Rd}}\right)^2 + \left(\frac{F_{v,Ed}}{F_{v,Rd}}\right)^2 \leq 1 \tag{3.1}$$

where

$F_{ax,Ed}$ is the axial force

$F_{ax,Rd}$ is the axial capacity

$F_{v,Ed}$ is the lateral force

$F_{v,Rd}$ is the lateral capacity

The forces are based on geometric parameters such as the outer and inner thread diameter (d and d_1) as well as the penetration length of the threaded part (L_{ef}). They are also dependent on material properties such as the density of the timber (ρ_k), yield moment of the screws ($M_{y,Rk}$), as well as the angle between the screw axis and the grain direction (α). However, depending on the failure mode the withdrawal strength ($f_{ax,k}$), pull-through strength ($f_{head,k}$) and tensile strength ($f_{tens,k}$) are also considered (Swedish Wood, 2022a).

The parameters mentioned above all have a significant effect on the structural capacity of the screw connection. However, these parameters in the design standards are not all the factors that contribute to the overall capacity. The combination formula in Equation 3.1 does not consider the load to the grain angle as well as the stiffness of screws exposed to the interaction of both axial and shear loads (Jockwer et al., 2014b). Since the entrance of the self-tapping-screw to the market it has created a possibility for new geometries of connections with higher strength due to being able to utilise bending capacity, as well as its high withdrawal capacity (Tomasi et al., 2010). Tomasi et al. (2010) continues by stating the importance of including the "addition of the axial strength of the fastener" as well as the "resistance caused by the friction between the timber elements". As withdrawal capacity is of major importance in inclined connections, especially for axial loading (Loss et al., 2018). Longer screws give significantly higher load-carrying capacity and the load-carrying capacity is increased even further when the screw is placed at an angle of 40-70 to

the grain direction compared to being placed perpendicular to the grain direction (Bejtka & Blaß, 2002).

Screws that are exposed to a force direction that is not completely perpendicular or parallel to the screw can be seen as exposed to a combination of axial and lateral forces, as seen in Figure 3.1. This is common for inclined screws or in cases with load directions with specific angles compared to the grain direction. The force acting on the connection is divided into resultant forces, one axial ($F_{ax,Ed}$) and one lateral ($F_{v,Ed}$).

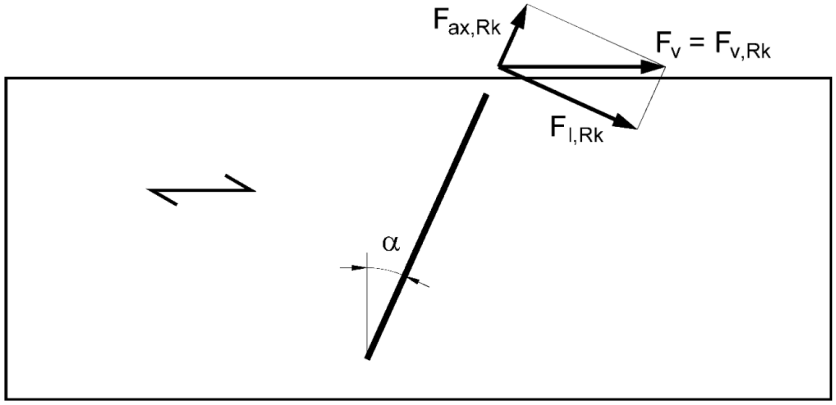

Figure 3.1: Resulting forces acting on the connection

To calculate the resulting force $F_{v,Rk}$ one can use equation 3.3 which considers the trigonometry of the screw and how its resistance will depend on the angle α (Tomasi et al., 2010). It is based on equation 3.1 from Eurocode and the dividing into resultants allows for a better way to express the forces in a connection with inclined screws.

$$F_{ax,Ek} = F_{v,RK} \cdot sin\alpha; F_{I,EK} = F_{v,Rk} \cdot cos\alpha \tag{3.2}$$

$$F_{v,Rk} = \frac{1}{[(\frac{sin\alpha}{F_{ax,Rk}})^2 + (\frac{cos\alpha}{F_{I,Rk}})^2]^{1/2}} \tag{3.3}$$

This chapter covers ways to further analyse and extend the existing expressions for the behaviour of timber connections with inclined screws. It covers how additional parameters can be implemented based on previous research and are divided into four main approaches. In this chapter, it is important to note the difference of α which is the angle between the screw to grain direction and α_{BT} which is the angle between the screw axis and the direction perpendicular to the grain, defined in (Bejtka & Blaß, 2002) and (Tomasi et al., 2010).

3.1 Bejkta and Blass Approach

The capacity of timber connections with dowel-type fasteners, which includes screws, can be determined from Johansen's yielding theory (Johansen, 1949). Where the designing load of the joints are loaded perpendicular to the screw's axis and is limited by the embedding strength of the timber elements as well as the bending capacity of the fastener. The theory has three different failure modes, where failure mode 3 represents a failure with two plastic hinges in the shear plane within the fastener which is illustrated in Figure 3.2.

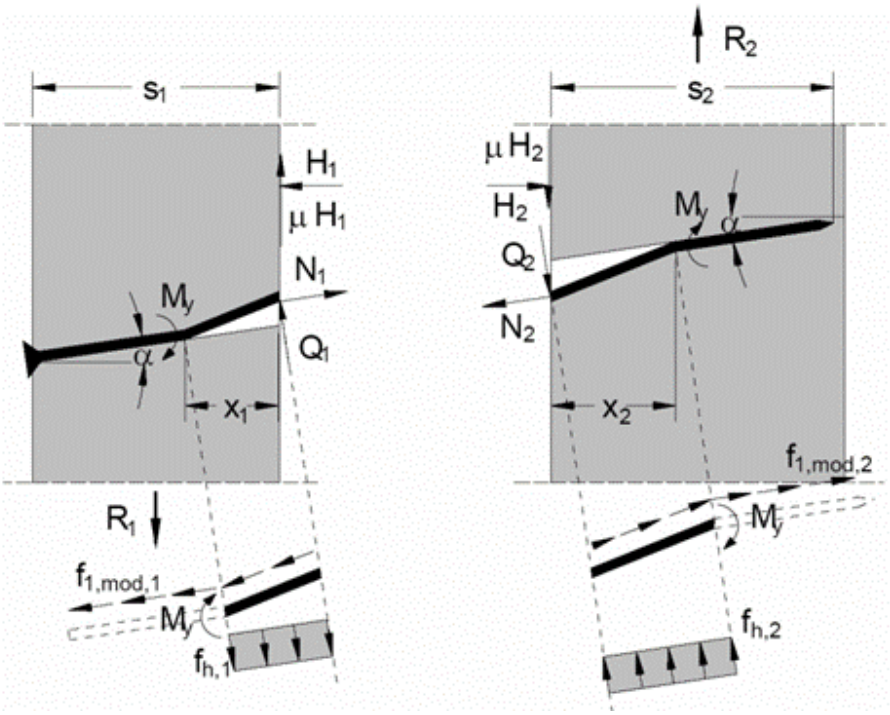

Figure 3.2: Failure mode 3 for an inclined screw connecting two timber elements, figure from (Bejtka & Blaß, 2002)

Based on Johansen's theory, Bejtka and Blaß (2002) have developed equations for the design of connections with shear loading and axial loading with inclined screws (Bejtka & Blaß, 2002). In order to build on Johansen's theory new parameters were introduced, to be able to describe the load-carrying capacity of angled screws to a further extent.

These parameters are as follows:

- The withdrawal capacity of the screw
- The angle between the screw axis and the grain direction
- The friction between the timber members

Note that the resistance from friction between the timber elements occurs in the connection from when the connection first experience loading. It is assumed through Johansen's yield theory that there is an ideal rigid plastic behaviour for the material

of the fastener in bending as well as for the timber in embedding. Load-displacement behaviour of screws that is loaded in withdrawal has been taken into consideration in the new equations from Bejtka and Blaß (2002). Although, depending on the screw displacement when reaching the ultimate force from loading, it is not certain if the screw has reached its withdrawal capacity. As a result, the shear stress acting along the screw is taken into consideration. Therefore, a reduction can be used when expressing the withdrawal capacity when considering the shear stress that is acting along the screw. The reduction of the withdrawal capacity ensures that the relationship between withdrawal and embedding capacity in fasteners for loading perpendicular and parallel to the screws can be taken into consideration as well. As this depends on failure mode, the following is assumed when Bejtka and Blaß (2002) derived their equations:

- Ideal rigid-plastic material behaviour for the timber under embedding stresses and of the fastener in bending.
- Averaged modified withdrawal parameters for different failure modes considering the withdrawal behaviour depending on the lateral load.
- The angle or the inclination α_{BT} is defined as the angle between the screw axis and the direction perpendicular to the grain (α_{BT} is denoted as α in Figure 3.2 and 3.3).

The configuration of the timber connection that is analysed in Bejtka and Blaß (2002) can be seen in Figure 3.3. This connection is the foundation for the test results as well as the calculated results in their study. For this configuration, four different angles between the screw axis and the direction perpendicular to the grain were investigated, where α_{BT} is 0°, 15°, 30° and 45° (note that α_{BT} is not the direct angle between the screw axis and the grain direction).

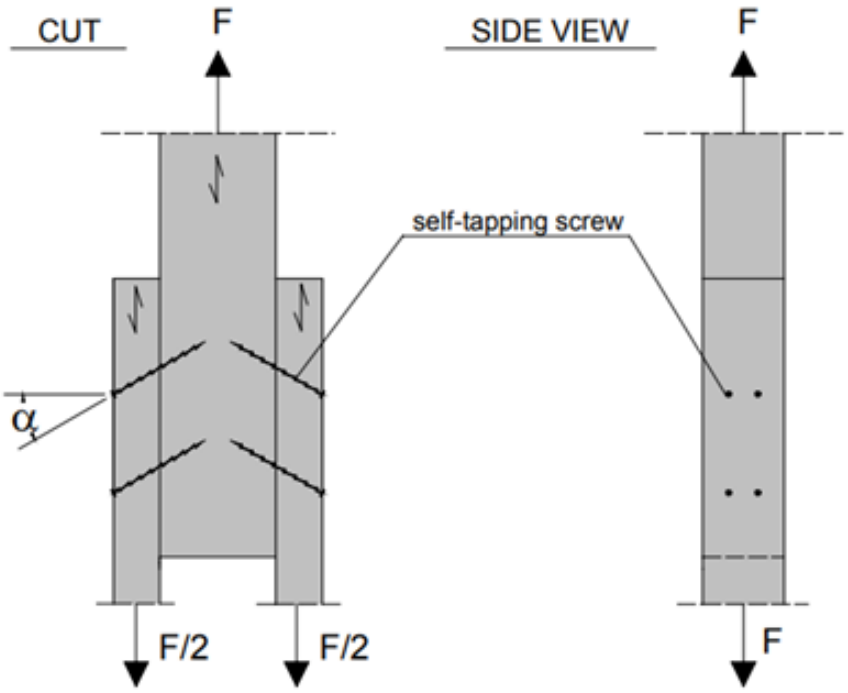

Figure 3.3: Connections between timber elements with inclined screws used during Bejtka and Blaß (2002) analysis, figure from (Bejtka & Blaß, 2002)

Equation 3.4 expresses the resistance of the connection based on both the shear- and axial resistance together with the friction force (μ) as well as the angle between the screw axis and the direction perpendicular to the grain (α_{BT}). The friction force (μ) is based on the rope effect, where surfaces between two timber elements have the friction coefficient $\mu = 0.25$. Based on failure mode 3 as seen in 3.2 above, the resistance for a single screw with an inclination loaded in axial tension (load direction is parallel to the grain) can be seen in the following equation:

$$R = R_{ax}(sin(\alpha_{BT}) + \mu cos(\alpha_{BT})) + R_v(cos(\alpha_{BT}) - \mu sin(\alpha_{BT})) \tag{3.4}$$

When the definition of the angle is changed from α_{BT} to α which is the angle between the screw axis and the grain direction, the formula is converted to equation 3.5.

$$R = R_{ax}(cos(\alpha) + \mu sin(\alpha)) + R_v(sin(\alpha) - \mu cos(\alpha)) \tag{3.5}$$

The axial resistance (R_{ax}) is taken as the characteristic withdrawal strength of the timber element. If the fastener goes through more than one wooden material, then the smallest withdrawal strength is chosen from the timber elements. This is calculated as:

$$R_{ax,k} = \begin{cases} f_{h,1} d \frac{t_1}{cos(\alpha_{BT})} \\ f_{h,2} d \frac{t_2}{cos(\alpha_{BT})} \end{cases} \tag{3.6}$$

Similar to the lateral resistance ($F_{v,Rk}$) expressed in Eurocode (equation 2.13), the lateral resistance (R) is based on the same failure modes. Bejtka and Blaß (2002) extension of the existing equations is only for fasteners loaded in single shear and can be seen in the equations a-f below. The lateral Resistance R is taken as the lowest value of the expressions according to equation 3.7.

$$R_A = R_{ax,k} \cdot sin(\alpha_{BT}) + f_{h,1,k} \cdot t_1 \cdot d \cdot cos(\alpha_{BT})) \tag{a}$$

$$R_B = R_{ax,k} \cdot sin(\alpha_{BT}) + f_{h,1,k} \cdot t_1 \cdot d \cdot cos(\alpha_{BT})) \tag{b}$$

$$\begin{aligned} R_C = R_{ax,k} \cdot (\mu \cdot cos(\alpha_{BT}) + sin(\alpha_{BT})) + \frac{f_{h,1,k} \cdot t_1 \cdot d}{1+\beta} \cdot (1 - \mu \cdot tan(\alpha_{BT})) \\ \cdot \left(\sqrt{\beta + 2\beta^2 \left(1 + \frac{t_2}{t_1} + \left(\frac{t_2}{t_1}\right)^2\right) + \beta^3 \cdot \left(\frac{t_2}{t_1}\right)^2} - \beta \cdot (1 + \frac{t_2}{t_1}) \right) \end{aligned} \tag{c}$$

$$\begin{aligned} R_D = R_{ax,k} \cdot (\mu \cdot cos(\alpha_{BT}) + sin(\alpha_{BT})) + \frac{f_{h,1,k} \cdot t_1 \cdot d}{1+\beta} \cdot (1 - \mu \cdot tan(\alpha_{BT})) \\ \cdot \left(\sqrt{2\beta(1+\beta) + \frac{4\beta(2+\beta)M_{y,k}}{f_{h,1,k} \cdot d \cdot t_1^2}} - \beta \right) \end{aligned} \tag{d}$$

$$\begin{aligned} R_E = R_{ax,k} \cdot (\mu \cdot cos(\alpha_{BT}) + sin(\alpha_{BT})) + \frac{f_{h,1,k} \cdot t_2 \cdot d}{1+\beta} \cdot (1 - \mu \cdot tan(\alpha_{BT})) \\ \cdot \left(\sqrt{2\beta^2(1+\beta) + \frac{4\beta(2+\beta)M_{y,k}}{f_{h,1,k} \cdot d \cdot t_2^2}} - \beta \right) \end{aligned} \tag{e}$$

$$\begin{aligned} R_F = R_{ax,k} \cdot (\mu \cdot cos(\alpha_{BT}) + sin(\alpha_{BT})) + (1 - \mu \cdot tan(\alpha)) \\ \cdot \sqrt{\frac{2\beta}{1+\beta}} \cdot \sqrt{2 \cdot M_{y,k} \cdot f_{h,1,k} \cdot d \cdot \cos \alpha_{BT}{}^2} \end{aligned} \tag{f}$$

$$R = F_{v,Rk} = min(R_A, R_B, R_C, R_D, R_E, R_F) \tag{3.7}$$

where

β	is the ratio between embedment strength of members, $f_{h,2,k}/f_{h,1,k}$
$F_{v,Rk}$	is the characteristic capacity per shear plane, per fastener
t_i	is the timber of board thickness or penetration depth, $i = (1, 2)$
$f_{h,i,k}$	is the characteristic embedment strength in wood member
d	is the fastener diameter
$M_{y,Rk}$	is the characteristic yield moment in fastener

$F_{ax,Rk}$ is the characteristic withdrawal capacity of the fastener

3.2 Tomasi, Crosatti and Piazza Approach

Tomasi et al. (2010) states that the stiffness of the screw is the greatest in its axial direction, but since the loading will be at an angle α it will be necessary to calculate the stiffness in both the lateral and axial direction, and then compute the resulting stiffness of K_{ser} according to equation 3.8 (Tomasi et al, 2010). Where the values for K_v and K_{ax} are received with the help of test results.

$$K_{ser} = K_v \cdot sin(\alpha) \cdot (sin(\alpha) - \mu cos(\alpha)) + K_{ax} \cdot cos(\alpha) \cdot (cos(\alpha) + \mu sin(\alpha)) \quad (3.8)$$

For equation 3.8 Tomasi et al. (2010) makes the consideration that K_v is calculated according to Eurocodes stiffness expression (equation 2.9), where the density within the equation is determined from test results. However, K_{ax} presents a more complex situation that considers the axial slip modulus, according to equation 3.9. The axial modulus represents the two threaded parts of the screw from the two timber elements it is attached to. This expression for the parallel stiffness represents a situation where both embedded parts of the screw attached to the timber elements get pulled out simultaneously. This is named the "double stiffness model". For a case where only one of the embedded parts gets pulled out from one timber element, the parallel stiffness is instead calculated according to Equation 3.10, named "single stiffness model". The double stiffness model is used when performing calculations with a screw inserted into two timber members as in Figure 3.4, as it represents the stiffness in both members. If both the timber members are of the same material the double stiffness model will generate half the stiffness than the single stiffness model.

Double stiffness model:

$$K_{ax} = \frac{1}{\frac{1}{K_{ser,ax,1}} + \frac{1}{K_{ser,ax,2}}} \quad (3.9)$$

Single stiffness model:

$$K_{ax} = K_{ser,ax,i} \quad (3.10)$$

where

$K_{ser,ax,i}$ is the axial slip modulus of the threaded part of the screw that is in the timber element (i)

There are no standards that express how $K_{ser,ax,i}$ should be calculated. Because of this Tomasi et al. (2010) propose that experimental values from withdrawal tests could be used. For a case when the screw has a homologation certificate issued by the German Institute of building technology, the instantaneous withdrawal stiffness can be expressed by equation 3.11 (Deutsches Institut fur Bautechnik, 2006).

$$K_{ser,ax,i} = 30 \cdot L_{ef} \cdot d \tag{3.11}$$

where

d	is the outer screw diameter
L_{ef}	is the embedment length

The connection between the timber elements that are analysed by Tomasi et al. (2010) is illustrated in Figure 3.4. The connections are similar to Bejtka and Blaß (2002) approach but are extended with more configurations of screw insertions, both in the number of screws and angles tested between the screw axis and grain direction. It is important to note that the calculated results from Tomasi et al. (2010) study are based on the equations that are derived from Bejtka and Blaß (2002) report. The angles that were investigated by Tomasi et al. were measured as perpendicular to the grain direction and they were 0°, 15°, 30° and 45° (note that α_{BT} is not the direct angle between the screw axis and the grain direction). This goes in two directions annotated as A and B in Figure 3.4, where the screws work under shear-compression and shear-tension respectively. If converted, the angles between the screw axis and the grain direction (α) are instead 90°, 75°, 60° and 45°.

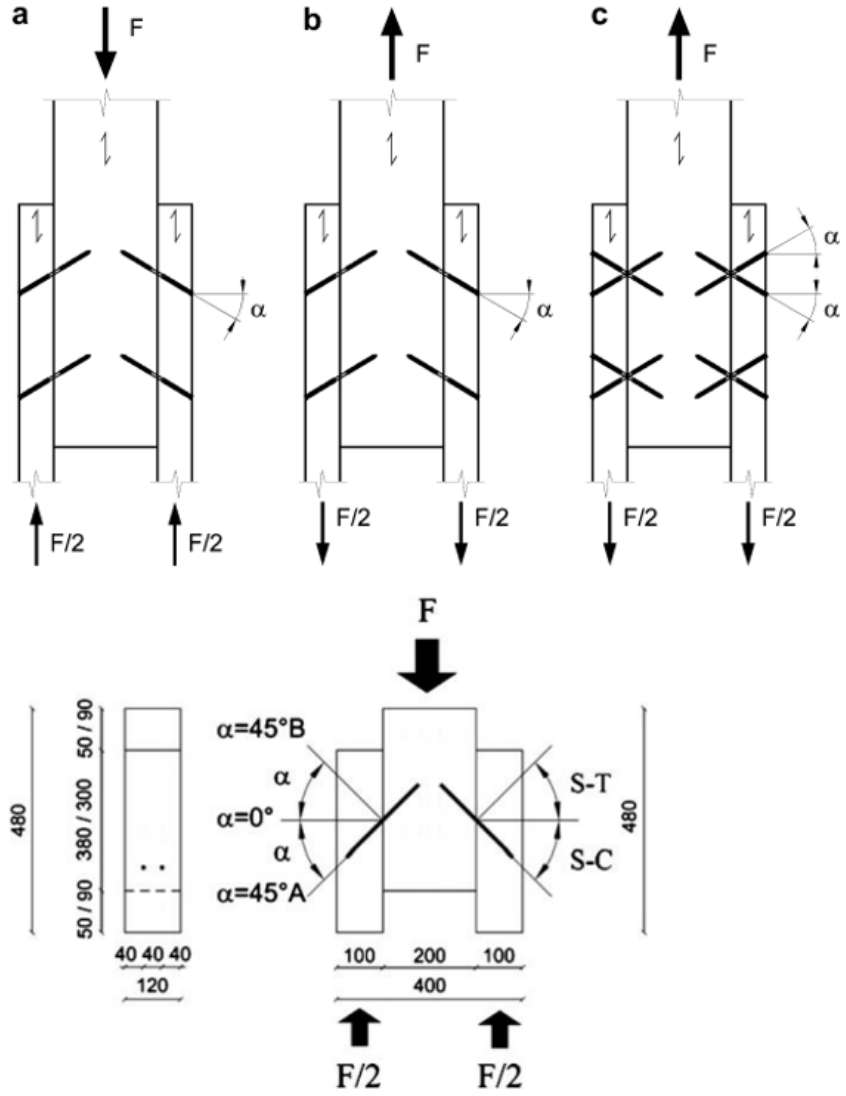

Figure 3.4: Connections between timber elements with inclined screws used during Tomasi et al. (2010) analysis, figure from (Tomasi et al., 2010).

The values achieved from Tomasi et al. (2010) test results show that screws exposed to shear-compression (Figure 3.4a) have similar stiffness as screws inserted perpendicular to the shear plane. Consequently, the stiffness calculation according to Eurocode (Equation 2.9) is proposed for the connection in shear-compression stress. While for a screw subjected to shear-tension and for the "X" configuration as seen in Figure 3.4b and Figure 3.4c, the formulas in this chapter can be used.

3.3 Jockwer, Steiger and Frangi Approach

Both the Bejtka and Blaß (2002) approach regarding resistance and Tomasi et al. approach regarding stiffness have a force acting parallel to the grain direction. This means that loads perpendicular to the grain direction are not considered. Jockwer et al. therefore handles a new loading condition which sets it apart to the previously

mentioned studies.

3.3.1 Stiffness

Based on loads perpendicular to the grain Jockwer et al. (2014) created an analytical formula, which assumes the two stiffnesses $K_{v,pulling}$ and K_{ax}, both impacted by angle and acting in series:

$$\frac{1}{K_{90}} = \frac{1}{K_{v,pulling}} + \frac{1}{K_{ax}} \tag{3.12}$$

This extension of expressing the stiffness gives an insight into the effect that the angle between the load and the grain direction has. To achieve this, Jockwer et al. (2014b) used a reduction of the effective length x_1 as seen in Figure 3.5.

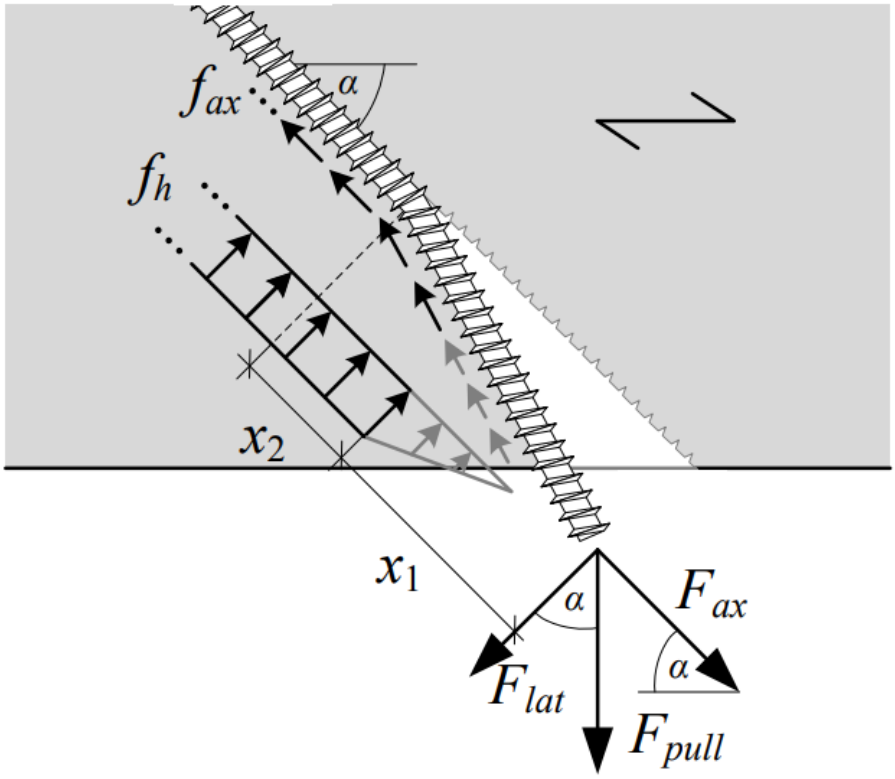

Figure 3.5: Configuration of an inclined screw exposed to a "pulling" load perpendicular to the grain, figure from (Jockwer et al., 2014b)

Here, the screw is loaded perpendicular to the grain and the embedment stress is acting downwards towards the surface of the timber. As the connection experience tension (being pulled apart), the timber surface cannot utilise full embedment strength cause of the lack of thickness in that direction. As a result, Jockwer et al. (2014b) reduce the effective length with x_1 so only the part that provides full embedment strength is considered. The reduced distance is calculated by equation 3.13. Also, for a case loaded perpendicular to the grain, the friction force (μ) is equal to zero, as no friction between the members occurs when they are being pulled away from each other.

$$x_1 = \frac{f_h d_{ef}}{2tan(\alpha) f_{v,roll}} \tag{3.13}$$

where

f_h	is the embedment strength
α	is the angle between the screw and the grain direction
d_{ef}	is the effective screw diameter
$f_{v,roll}$	is the rolling shear strength

Jockwer et al. (2014a) express the rolling shear strength as $f_{v,roll} = 1.8N/mm$ based on calculation from CEN (2013). The embedment strength f_h is calculated with Bejtka and Blaß (2005) equation 3.14 that considers the timber density (ρ) as well as the angle between the screw and the grain direction (α).

$$f_h = \frac{0.022\rho^{1.24} d^{-0.3}}{2.5cos(\alpha)^2 + sin(\alpha)^2} \tag{3.14}$$

where

ρ	is the density of the timber
d	is the screw diameter

This reduction contributes to a change in the lateral stiffness of the inclined screw. For an inclined screw loaded in perpendicular tension, the lateral stiffness is given in equation 3.15. Within this equation, the embedment strength is assumed to be nonexistent along the length x_1. It is once again important to note that the lateral stiffness is halved if it is connected to two timber members of the same material according to the "double stiffness model" in equation 3.16.

$$K_{v,pulling,i} = \frac{3E_{steel}\pi d_{core}^4}{64x_1^3} \tag{3.15}$$

Double stiffness model:

$$K_{v,pulling} = \frac{1}{\frac{1}{K_{v,pulling,1}} + \frac{1}{K_{v,pulling,2}}} \tag{3.16}$$

where

E_{steel}	is the elasticity modulus for steel
d_{core}	is the screws inner thread diameter

x_1 is the reduction of effective length

The configuration used to investigate the relation is visualised in Figure 3.6 (Jockwer et al., 2014b). Test a) shows how a force perpendicular to the grain direction pulls the timber elements fastened by an inclined screw and Test b) shows a force parallel to the grain direction. It is also worth noting that when increasing the capacity of connections through certain angles they become more brittle, and a decreased stiffness results in more ductility. It is however possible to use a combination of angles to ensure both higher capacity as well as moderate ductility (Hanna & Tannert, 2021).

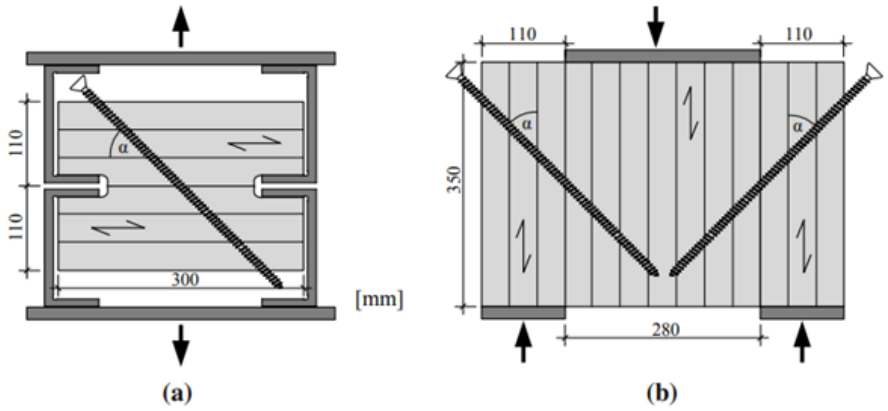

Figure 3.6: Connections between timber elements with inclined screws used during Jockwer et al. (2014b) analysis, figure from (Jockwer et al., 2014b)

For the load case with a force parallel to the grain in Figure 3.6b, Jockwer et al. (2014b) used the same method as Tomasi et al. (2010) expressed in equation 3.8 with the exception, that $K_{ser,ax,i}$ is calculated with equation 3.17 instead of 3.11. This is due to that the Deutsches Institute für Bautechnik where the equations were received, was updated between the submissions of these reports (Deutsches Institut fur Bautechnik, 2006) (Deutsches Institut fur Bautechnik, 2011). For the load case with a force perpendicular to the grain in Figure 3.6a, Jockwer et al. (2014b) came to the conclusion that the stiffness (K_{ser}) during pulling needed a larger axial stiffness (K_{ax}) than what was used for shearing. $K_{ser,ax,i}$ is calculated with equation 3.18 instead of equation 3.17 as proposed by Deutsches Institut fur Bautechnik (2011).

$$K_{ser,ax,i} = 25 \cdot l_{ef} \cdot d \qquad \textit{(shearing)} \tag{3.17}$$

$$K_{ser,ax,i} = 40 \cdot l_{ef} \cdot d \qquad \textit{(pulling)} \tag{3.18}$$

3.3.2 Resistance

For a force parallel to the grain direction Jockwer et al. (2014a) calculates the resistance with equation 3.5 but with updated expressions for the axial resistance (R_{ax}). The expression for the axial resistance (R_{ax}) is expressed with equation

3.19 and is based on a newer report from the same authors (Bejtka & Blaß, 2005). Through test results Jockwer et al. (2014b) later determined the withdrawal strength to be $f_{ax,mean} = 14.8N/mm^2$ which can be used to calculate axial resistance. Three-point bending tests were also performed by Jockwer et al. (2014a) to find the yield moment (M_y) of the screws. Through these tests, the yield moment was determined to be $M_y = 120Nm$ which shows a major increase from Deutsches Institut fur Bautechnik (2011) value of $M_y = 80Nm$.

$$R_{ax} = \frac{d \cdot l_{ef} \cdot f_{ax,mean}}{1.2cos(\alpha)^2 + sin(\alpha)^2} \tag{3.19}$$

where
$f_{ax,mean} = 0.6d^{-0.5}l_{ef}^{-0.1}\rho_{mean}$ *(Bejtka and Blaß (2005))*
$f_{ax,mean} = 14.8N/mm^2$ *(Test results)*

The way the resistance of the connection is calculated is also changed for its when the force direction is parallel to the grain. Jockwer et al. (2014a) determines the resistance with equation 3.20, which is a reformulation of equation 3.5 that is acting according to the new force direciton. The geometric relation has changed together with the fact that there is no friction force (μ) due to the opening of the gap for a case loaded perpendicular to the grain.

$$R = R_{ax}(cos(\alpha)) + R_v(sin(\alpha)) \tag{3.20}$$

The axial resistance R_{ax} according to Equation 3.19 changes in relation to force to grain angle. For a force perpendicular to the grain, it is calculated according to equation 3.21 instead due to changed orientation of the new force direction (Jockwer et al., 2014a).

$$R_{ax} = \frac{d \cdot l_{ef} \cdot f_{ax,mean}}{1.2cos^2\alpha + sin^2\alpha} * sin\alpha \tag{3.21}$$

where
$f_{ax,mean} = 0.6d^{-0.5}l_{ef}^{-0.1}\rho_{mean}$ *(Bejtka and Blaß (2005))*
$f_{ax,mean} = 14.8N/mm^2$ *(Test results)*

For the load case with a force parallel to the grain in Figure 3.6b, the lateral resistance (R_v) is calculated using the equilibrium of forces that occurs in Figure 3.6 with the plastic hinge. It is expressed as:

$$R_v = \sqrt{\frac{2\beta}{1+\beta}} \cdot \sqrt{2M_y f_h d_{ef}} \tag{3.22}$$

where

M_y	is the yield moment
f_h	is the embedment strength

d_{ef} is the effective screw diameter

β is Ratio between embedment strength of members, $f_{h,2,k}/f_{h,1,k}$

The expression for the lateral resistance changes when the load case has a force perpendicular to the grain, as illustrated in Figure 3.6. This is due to the reduced embedment length and lateral resistance ($R_{v,pulling}$) is expressed in equation 3.23. Within this equation, the embedment strength is assumed to be nonexistent along the length x_1. This is then inserted in equation 3.5, to get the resulting load-carrying capacity.

$$R_{v,pulling} = -f_h x_1 d_{ef} + \sqrt{(2M_y + f_h x_1^2 d_{ef}) f_h d_{ef}} \tag{3.23}$$

where

f_h is the embedment strength

x_1 is the reduction of effective length

d_{ef} is the effective screw diameter

M_y is the yielding moment

3.3.3 Experimental results

Jockwer et al. (2014b) performed an experimental verification of the model which is illustrated in Figure 3.6. The tests were performed with angles between the screw and the grain direction of 90°, 60°and 45°. These angles were tested for two types of timber samples, one with low density and one with high density. The tests were displacement controlled towards a total displacement of 15mm with constant movement. For the shearing test seen in Figure 3.6b, Teflon foils were placed between the middle timber element and the outer elements to negate the effect of the friction force that would otherwise occur between the elements. The stiffness, as well as the load carrying capacity, was determined for the mentioned angles for both load directions and the results are presented in Table 3.10.

Table 3.10: Test results for ultimate load and stiffness made by Jockwer et al. (2014a)

	Ultimate load	Stiffness
α [°]	F_{ult} [kN]	K_{ser} [kN/mm]
Pulling 90	21.2	28.3
60	21.6	8.9
45	17.7	3.0
Shearing 90	10.5	1.9
60	20.5	5.9
45	27.4	13.6

The full behaviour of the performed tests are illustrated in Figure 3.7. The more transparent lines in the figure represent the conducted test for both timber samples. The bold lines represent the average result from these tests and are stated in Table 3.10. A calculation of the embedment strength was performed for the shearing test at $\alpha = 90°$ which showed values of $f_h = 29.2N/mm$ and $f_h = 48.8N/mm$ for deformation of 10mm and 15 mm respectively. This shows that there was friction force acting during the shearing test despite the usage of Teflon foil between the timber members. This leads to an increased force in the connection when it goes beyond a deformation of 9mm for $\alpha = 90°$ as seen in Figure 3.7b.

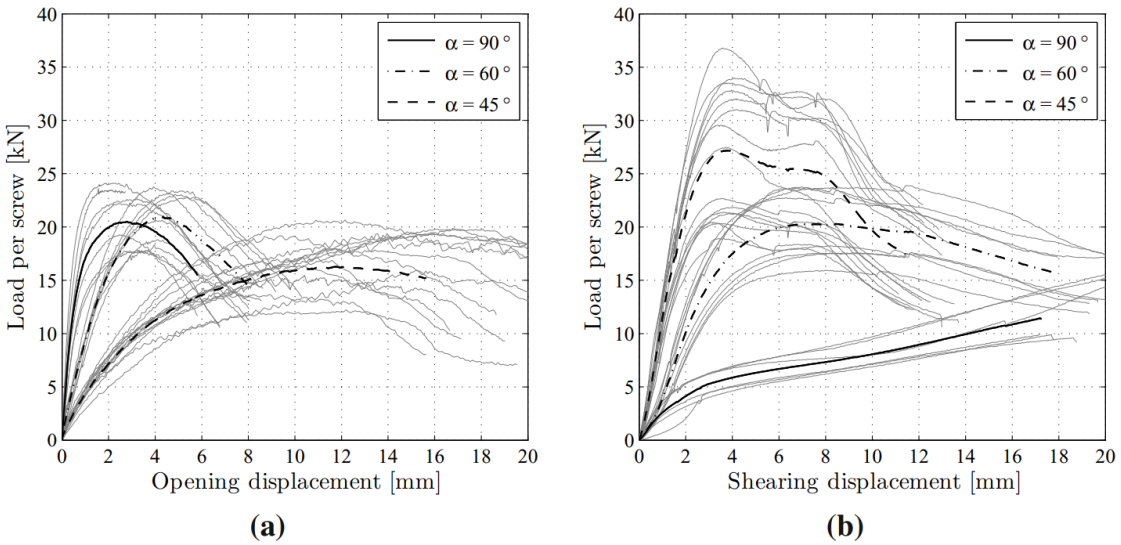

Figure 3.7: The force and displacement relation depending on different screw angles for a) pulling and b) shearing according to test results, figure from (Jockwer et al., 2014b)

3.4 Second generation of Eurocode 5

The Second generation of Eurocode utilises some equations previously mentioned in this chapter to develop the equations for both resistance and stiffness.

3.4.1 Resistance

The second generation of Eurocode is an evolution from previous standards, where it extends chapters and includes new content (CEN, 2022b). However, concerning inclined connections it is still only limited to considering shear loading.

3.4.1.1 Axial resistance

The equations for calculating the axial resistance in fasteners in the three failure modes have now been combined to be two equations which consider failure in the timber and the fastener. The axial tensile resistance $F_{ax,t,d}$ is now computed as the minimum resistance of $F_{ax,t,d,1}$ and $F_{ax,t,d,2}$ by equation 3.24 and 3.25:

$$F_{ax,t,d,1} = \frac{k_{mod}}{\gamma_R} max \begin{cases} F_{pull,k} \\ F_{w,k} \end{cases} \tag{3.24}$$

where

$F_{ax,t,d,1}$ is the axial tensile resistance

K_{mod} is the modification factor which considers the duration of load and moisture content

γ_R is the partial factor for resistance

$F_{pull,k}$ is the characteristic head pull-through resistance and can be seen in Table 3.14

$F_{w,k}$ is the characteristic withdrawal resistance

$$F_{ax,t,d,2} = \frac{F_{t,k}}{\gamma_{M2}} \tag{3.25}$$

where

$F_{t,k}$ is the characteristic tensile resistance of a fastener

γ_{M2} is the partial factor for resistance to fracture of cross-sections of a metal fastener in tension to fracture

The axial compression resistance $F_{ax,c,d}$ of an axially loaded screw, rod with wood screw thread or bonded-in rod is calculated as the minimum of the resistances calculated by the following equation:

$$F_{ax,c,d} = \frac{k_{mod}}{\gamma_R} min \begin{cases} F_{w,k} \\ F_{c,k} \end{cases} \tag{3.26}$$

where

$F_{c,k}$ is the characteristic compression resistance of a fastener

Another factor to consider is the head pull-through resistance which can be seen in Table 3.14

Table 3.14: Head pull-through resistance for cross-laminated timber

Material	**Limits**	$F_{pull,k}$
SL, PL and CL	$t_1 \geq 4d$	$F_{pull,k} = \begin{cases} f_{head} A_{head} & \text{for } A_{head} \leq 4072 \text{ mm}^2 \\ 3 f_{c,90,k} A_{head} & \text{for } A_{head} > 4072 \text{ mm}^2 \end{cases}$ (1) $f_{head} = 19 \exp\left(-\frac{d_{head}}{50}\right)\left(\frac{\rho_k}{350}\right)^{0,8}$ (2) NOTE $A_{head} = 4072$ mm² equals $d_{head} = 72$ mm for nails $F_{pull,k} = 15\, d_{head}^2 \left(\frac{\rho_k}{350}\right)^{0,8}$ (3)

The withdrawal resistance $F_{w,k}$ is the withdrawal resistance of a fastener can be calculated with the equation:

$$F_{w,k} = \pi \cdot d \cdot L_w \cdot f_{w,k} \qquad \textit{(for nails and screws)} \tag{3.27}$$

where

L_w is L_{ef} which is the withdrawal length

$f_{w,k}$ is the characteristic withdrawal strength taken from Table 3.16

d is the outer diameter of the fastener

Table 3.16: Characteristic withdrawal strength for cross-laminated timber

Screws and rods with woodscrew thread 3,5 mm ≤ d ≤ 22 mm and 0,55d ≤ d_1 ≤ 0,76d			(5)
SL, PL, CL and LVL and GLVL	$l_w \geq 5d$ $\rho_k \leq 700$ kg/m^3 $d \geq 8$ mm for CLT	$f_{w,k} = k_{screw} k_w k_{mat}\, d^{-0,33} \left(\frac{\rho_k}{350}\right)^{k_\rho}$ N/mm^2 For materials not mentioned specifically $k_w = k_{mat} = 1,0$ Categorie [a] k6 k7 k8 k9 k10 k_{screw} 6 7 8 9 10 $k_w = \begin{cases} 1,0 & \text{for } 30° \leq \varepsilon \leq 90° \\ 1 - 0,01(30 - \varepsilon) & \text{for } 0° \leq \varepsilon < 30° \end{cases}$ $k_{mat} = \left\{1 + \frac{\ln(n_p)}{12} \leq 1,15 \quad \text{for PL and CL}\right.$ $k_\rho = \begin{cases} 1,10 & \text{for softwoods and } 15° \leq \varepsilon \leq 90° \\ 1,25 - 0,05d & \text{for softwoods and } 0° \leq \varepsilon < 15° \\ 1,6 & \text{for hardwoods and } 0° \leq \varepsilon \leq 90° \end{cases}$	(6) (7) (8) (9)

The tensile resistance should be taken from either the technical product specification or the following formula:

$$F_{tk} = 0.9 A_s f_{u,k} \tag{3.28}$$

where

As is the nominal stress area

f_{uk} is the characteristic steel strength

The compressive resistance shall be applied to a metal dowel-type fastener with 6 mm ≤ d ≤ 22 mm and is calculated with the following equation:

$$F_{ck} = \frac{\gamma_R}{\gamma_{M1}} k_c N_{pl,k} \tag{3.29}$$

3.4.1.2 Lateral resistance

The characteristic lateral resistance per shear plane is a result of the contribution from the dowel effect per shear plane and by the characteristic rope-effect contribution. The resistance is expressed with equation 3.30.

$$F_{v,k} = F_{D,k} + F_{rp,k} \tag{3.30}$$

where

$F_{D,k}$ is the characteristic dowel-effect contribution per shear plane and can be seen in equation 3.31 and which is based on the European Yield Model (Swedish Wood, 2022b)

$F_{rp,k}$ is the characteristic rope-effect contribution and can be seen in equation 3.32

$$F_{D,k} = 1.15\sqrt{\frac{2\beta}{1+\beta}}\sqrt{2M_{yk}f_{h,\alpha,k}d}min\begin{cases} t_{h,1}/t_{h1,req} \\ t_{h,2}/t_{h2,req} \\ 1 \end{cases} \tag{3.31}$$

where

$f_{h,1,k}$	is the characteristic embedment strength of member 1 and can be seen in Table 3.20;
$M_{y,k}$	is the characteristic yield moment
d	is the diameter of the fastener;
t_{h1}, t_{h2}	are the embedment depths in members 1 and 2 and can be calculated in Table 3.21;
$t_{h1,req}, t_{h2,req}$	are the required minimum embedment depths in members1 and 2;
$f_{h,1,k}, f_{h,2,k}$	are the characteristic embedment strengths of members 1 and 2

and:

$\beta = \frac{f_{h,2,k}}{f_{h,1,k}}$

Table 3.20: Characteristic embedment strength f_{hk}

Material	Characteristic embedment strength
SL, PL, CL	$f_{h,\alpha,k} = \frac{0.019\rho_k^{1.24}d^{-0.3}}{2.5cos^2\alpha+sin^2\alpha}$

Table 3.21: Required minimum embedment depth which ensures failure mode f

Failure mode	member 1	member 2
	Single shear	
(f)	$t_{h1,req} = 1.15\cdot 2\sqrt{\frac{M_{y,k}}{f_{h,1,k}d}}(\frac{\sqrt{\beta}}{\sqrt{1+\beta}}+1)$	$t_{h1,req} = 1.15\cdot 2\sqrt{\frac{M_{y,k}}{f_{h,1,k}d}}(\frac{\beta}{\sqrt{1+\beta}}+1)$

$$F_{rp,k} = min\begin{cases} k_{rp,1}F_{ax,t,k} \\ k_{rp,2}F_{D,k} \end{cases} \tag{3.32}$$

with:

$$F_{ax,t,k} = min \begin{cases} F_{pull,k} \\ F_{w,k} \\ F_{t,k} \end{cases} \tag{3.33}$$

where

$k_{rp,1}$ is the factor for rope effect in general and can be found in Table3.23

$k_{rp,2}$ is a limitation factor which can be found in Table 3.24

$F_{D,k}$ is the design dowel effect contribution

$F_{ax,k}$ is the characteristic axial capacity

Table 3.23: Factors $k_{rp,1}$ for the rope effect contributions from CEN (2022b)

Fastener type and connection type	$k_{rp,1}$
General and uncoated staples	0,25
Ring shank nails and coated staples	0,4

Table 3.24: Limitation factors $k_{rp,2}$ for the rope effect contributions from CEN (2022b)

Fastener type	$k_{rp,2}$
Dowels	0
smooth round nails and uncoated staples	0.15
Smooth square nails and bolts	0.25
Ring shank nails and coated staples	0.5
Screws, rods with wood screw thread and laterally loaded bonded-in rods	1.0

3.4.1.3 Combination of axial and lateral loading

When calculating a combination of axial and lateral loading the formula remains mostly the same as the older generation of Eurocode. However, there is now an addition of the parameter (p) as can be seen in the equation 3.3. The parameter (p) has a value between 1.0-2.0 as shown in Table 3.26 and is based on the type of fastener as well as the failure mode the connection has.

$$\left(\frac{F_{ax,Ed}}{F_{ax,Rd}}\right)^p + \left(\frac{F_{v,Ed}}{F_{v,Rd}}\right)^p \leq 1 \tag{3.1}$$

where

$F_{ax,Ed}$ is the axial force.

$F_{ax,Rd}$ is the axial capacity

$F_{v,Ed}$ is the lateral force

$F_{v,Rd}$ is the lateral capacity.

p is an exponent taken from Table 3.26

Table 3.26: Exponent p for combined loading in both axial and lateral direction from CEN (2022b)

Fastener	p	Failure modes
Smooth nails, uncoated staples and bolts	1,0	-
Ring shank nails, coated staples, bonded-in rods	2,0	-
Screws and rod with wood screw thread	1,0	Mode unknown
	1,0	Mode (a) and (b) - no plastic hinge
	1,5	Mode (d) and (e) - one plastic hinge
	2,0	Mode (f) two plastic hinges

The equation can also be written in the following way for screws with the use of trigonometry:

$$F_{v,Rk} = \frac{1}{[(\frac{sin\alpha}{F_{ax,Rk}})^2 + (\frac{cos\alpha}{F_{D,Rk}})^2]^{1/2}} \tag{3.3}$$

3.4.2 Slip modulus

The slip modulus $K_{SLS,v,mean}$ in the new generation of Eurocode now differentiates between lateral, axial, as well as a combined slip modulus. This is in contrast to the previous expression for stiffness which was only valid for shear connections with laterally loaded fasteners inserted perpendicular to the grain. The total slip modulus of a connection is also included in the Eurocode with the equation 3.34 which now takes the combination of different fasteners as well as the number of shear planes per fastener as can be seen in equation 3.34.

$$K_{SLS} = \Sigma_{i=1}^{n \cdot m} K_{SLS,i} \tag{3.34}$$

where

n	is the number of fasteners
m	is the number of shear planes per fastener
$K_{SLS,i}$	is the slip modulus of a single fastener per shear plane

3.4.2.1 Lateral slip modulus

The equation for lateral slip modulus for a screw is calculated with equation 3.35 and is dependent on the diameter of the fastener. It should be reduced by half when loaded perpendicular to the grain.

$$K_{SLS,v,mean} = 60(0.7d)^{1.7} \tag{3.35}$$

where

d	is the diameter of the fastener

In Eurocode 2G, it is stated that "in general, for connection members loaded perpendicular to the grain ($\alpha = 90°$) the values of the mean lateral slip modulus $K_{SLS,v}$ should be reduced by 50%. For intermediate angles linear interpolation may be applied" (p. 194)

3.4.2.2 Axial slip modulus

The axial slip modulus is as previously mentioned included in the new generation of Eurocode 5 and is calculated with the equation 3.36. As can be seen in the equation, the axial slip modulus is dependent on the mean density of the material, the screw diameter and the withdrawal length. The effective withdrawal length is defined as the length of the threaded part of the screw that is embedded into the timber element as seen in Figure 3.8.

$$K_{SLS,ax} = 160(\frac{\rho_{mean}}{420})^{0.85} d^{0,9} \cdot l_w^{0.6} \tag{3.36}$$

where

d	is the diameter of the screw in mm
l_w	is the withdrawal length in mm
ρ_{mean}	is the mean density in kg/m^3

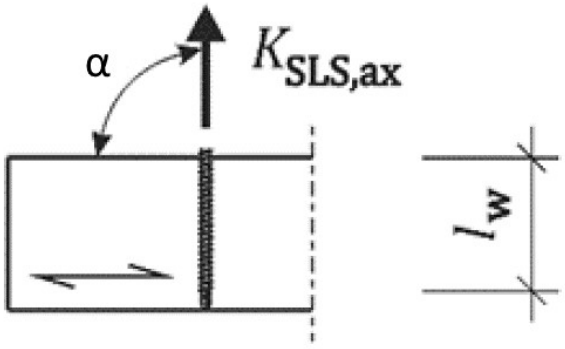

Figure 3.8: The slip modulus in an axially loaded fastener, figure from (CEN, 2022b)

3.4.2.3 Combination of axial and literal slip modulus

When calculating the combination of axial and lateral slip modulus which can be calculated with the equation 3.37, one could see that there is a clear similarity to the equations of Tomasi et al. (2010) and Jockwer et al. (2014b). The differences in equation 3.37 is how the axial slip modulus is expressed, as it has a factor of $\frac{1}{2}$ included.

$$K_{SLS} = K_{SLS,v} \cdot \sin\alpha(\sin\alpha - \mu\cos\alpha) + \frac{1}{2}K_{SLS,ax} \cdot \cos\alpha(\cos\alpha + \mu\sin\alpha) \quad (3.37)$$

where

$K_{SLS,v}$	is the mean slip modulus per fastener per shear plane in the lateral direction
$K_{SLS,ax}$	is the mean slip modulus per fastener per connected member in the axial direction
α	is the angle between the screw axis and the grain direction
μ	is the friction coefficient between the timber members and is equal to 0.25

4

Modelling procedure

The finite element analysis in this study was performed in the program Abaqus where an elastic foundation model was used to simplify the analysis of the connections. A Beam-on-Foundation model (BOF) which was developed by De Santis and Fragiacomo (2021), was used to create an appropriate model that considers additional parameters that can more accurately describe the behaviour of the connection. In this model, the screw was represented by a beam which was embedded in both parallel and perpendicular non-linear springs. The springs were used to describe the stiffness of the timber in different directions. This was done by letting the springs represent the stiffness parallel and perpendicular to the grain direction. The FE-model can therefore be used to get more correct results of screw connections behaviour compared to Eurocode 5.

The modelling procedure was divided into two main steps. Firstly to validate the model for it to produce an accurate representation of the behaviour of the screw, and secondly to apply the validated model to new situations. To ensure that the model was viable it was verified with test results from previous experiments in studies conducted by Jockwer et al. (2014b).

4.1 Conditions

In this analysis, it was assumed that there was a constant relative humidity and temperature in order to preserve the constant behaviour of the timber. These conditions were also used because previous experiments have been made in labs with controlled inside conditions, which makes the results easier to compare. The friction force (μ) that could occur between the timber elements in the connection was not applied in the Abaqus model due to the usage of Teflon foils in the physical test model, note that for shearing friction occurred despite the Tefonl foil which could increase some values.

For every configuration of the screw connection, no matter the effective screw length, the number of springs attached to the screw remains the same. The number of springs and the distance between the springs were then studied in a convergence study which was covered in Chapter 5.

4.2 Geometry

The model consisted of two timber members which had a self-tapping screw connecting them at an angle α, as illustrated in Figure 4.1. The stiffness of the horizontal spring (k_p) and the vertical spring (k_t) differs according to which material they were attached to. However, for this thesis, only one material was studied, and it was the same for both two timber elements through all configurations, which means that $k_{p1} = k_{p2}$ and $k_{t1} = k_{t2}$.

In the validation procedure, the investigated angles between the screw and the grain direction α were limited to the angles used for the experimental results in Jockwer et al. (2014b). These angles were 90°, 60°, and 45°. These angles were also used in previous tests conducted throughout Chapter 3, which enables easier comparison to previous research. Both of the two force directions used in Jockwer et al. (2014b) experiments were also modelled in Abaqus together with the mentioned angles.

The effective lengths L_{ef} that were used in the simulation for the validation procedure were the same lengths as the ones used in the experiments from Jockwer et al. (2014b). As seen in Figure 3.6 the geometry of the timber members remains constant for all insertion angles of the screw. As a result, the effective lengths L_{ef} were 110 mm, 127 mm and 155 mm for the angles 90°, 60°, and 45°respectively. When then simulating other angles than the previously mentioned ones, the effective length was calculated with the use of trigonometry. In Abaqus the screw was modelled as a small cylinder without threading, to compensate for this the diameter was expressed as $d_{ef} = d1 \cdot 1.1$ to consider the relationship between the outer and inner diameter.

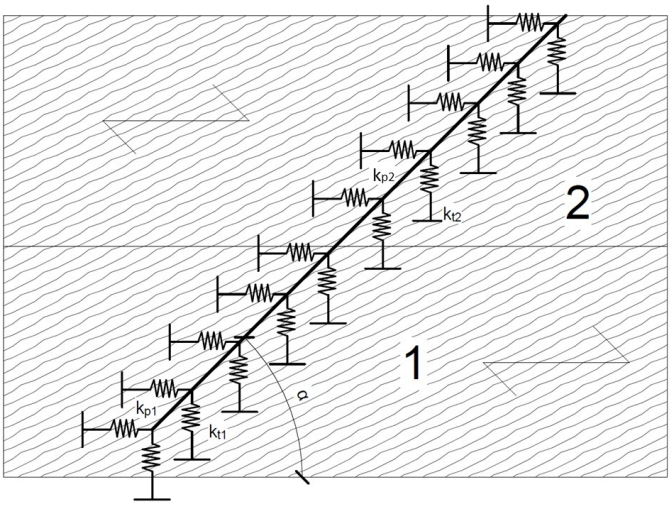

Figure 4.1: The spring configuration used for the screw in the FE-analysis

4.3 Material properties

The two timber members were made of glued laminated timber beams with the strength class GL24h with boards of timber with a strength class of C24. The screw used in the model was a self-tapping screw of type SFS WR-T-13xL400 with an outer thread diameter of $d = 13$ mm, an inner diameter $d_1 = 8.5$ mm and a screw length of 400 mm (Deutsches Institut fur Bautechnik, 2011). The characteristic yield moment for the screw was $M_{y,k} = 80Nm$ and the yield stress was $f_{yk} = 900MPa$. Furthermore, the screw had a characteristic withdrawal capacity, $f_{ax,k} = 80 \cdot 10^{-6} \cdot \rho_k^2$. Other material properties were taken from Bejtka and Blaß (2002).

4.4 Configuration in Abaqus

When configuring the BOF-model into Abaqus, nonlinear springs were attached to a 2D-Beam, as seen in Figure 4.2 (note that only a few springs were used in the Figure to give a better illustration of the assembly). The 2D beam represents the screw and the springs represent the stiffness in the connection between the wood and screws in both grain directions. Each spring was fastened to a separate boundary which corresponds to the attachment between the timber and the screw. The springs were made non-linear by defining the initiation of plastic deformation after the stiffness threshold had been reached. This was done for both directions respectively as the stiffness was lower in the perpendicular direction compared to the parallel direction. The nonlinear behaviour of the screw was initiated when the yield stress for the screw was reached.

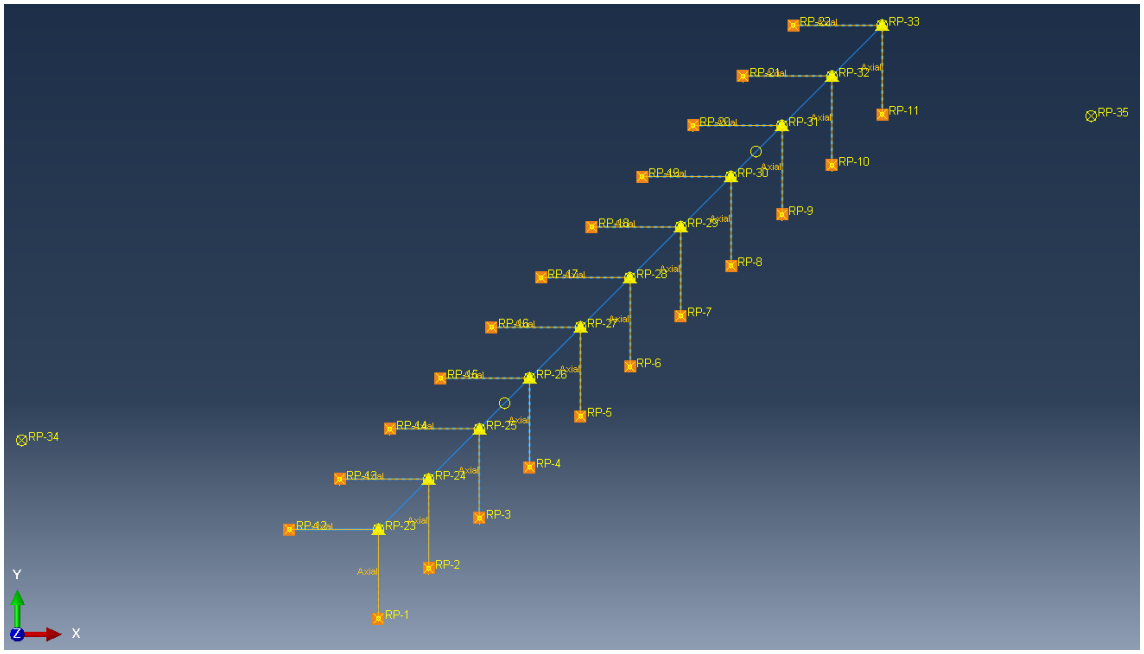

Figure 4.2: The FE-model for the timber connection with a 2D beam attached to nonlinear springs

In Figure 4.2 and 4.3 the screw angle was 45°while the connection was exposed to

shearing by being pulled in opposite directions. Similar configurations were applied to the different scenarios explained in Chapter 4.2. Figure 4.3 shows in detail the main principle of how the configuration works in Abaqus and how the different elements interact.

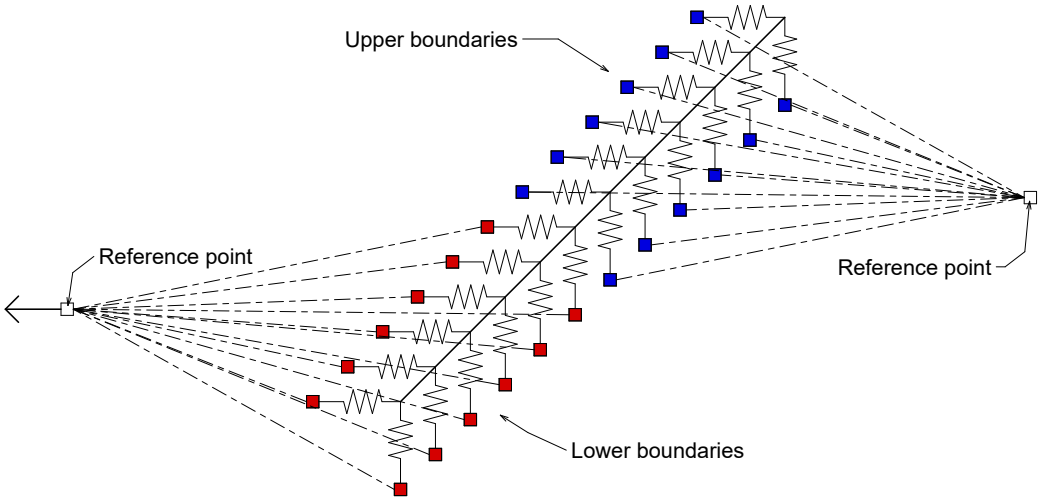

Figure 4.3: Principal configuration for the FE-model in shearing

For the shear test, a deformation-controlled analysis was used in Abaqus by assigning movement to the boundaries to which the springs were attached. The lower boundary points (marked with red) were attached to a reference point with a constraint equation, as seen in equation 4.1.

$$1 \cdot RP_{left} - 1 \cdot B_{red} = 0 \tag{4.1}$$

where

B_{red} are the boundaries which were connected to the lower part of the screw, as seen in Figure 4.3

RP_{left} is the left reference point to which all lower boundary conditions were attached, as seen in Figure 4.3

This allows the movement of the reference point to evenly move the positions of the red boundary points at the same distance. As the constraint equation makes them move uniformly, it will represent the effect of a screw being pulled along with the timber that it is fastened to. The reference point was set to move a distance of 15mm to the left to simulate this, which makes the model displacement controlled. The same relation was performed for the upper boundaries (marked with blue) to another reference point. However, the displacement of this point was fully restricted which locked the upper boundaries in their place. Similarly to the lower boundaries, it simulates the screw's attachment to the timber, as the reaction force of this upper

part was equal to the force generated in the lower part.

For the pulling test, a very similar configuration was provided with the only difference being that the reference point moves in a different direction as seen in Figure 4.4. The reference point attached to the lower boundaries (marked with red) was instead dragged downward to simulate the timber element being pulled apart from each other. The other reference point (marked with blue) was also fully restricted similar to the shearing test.

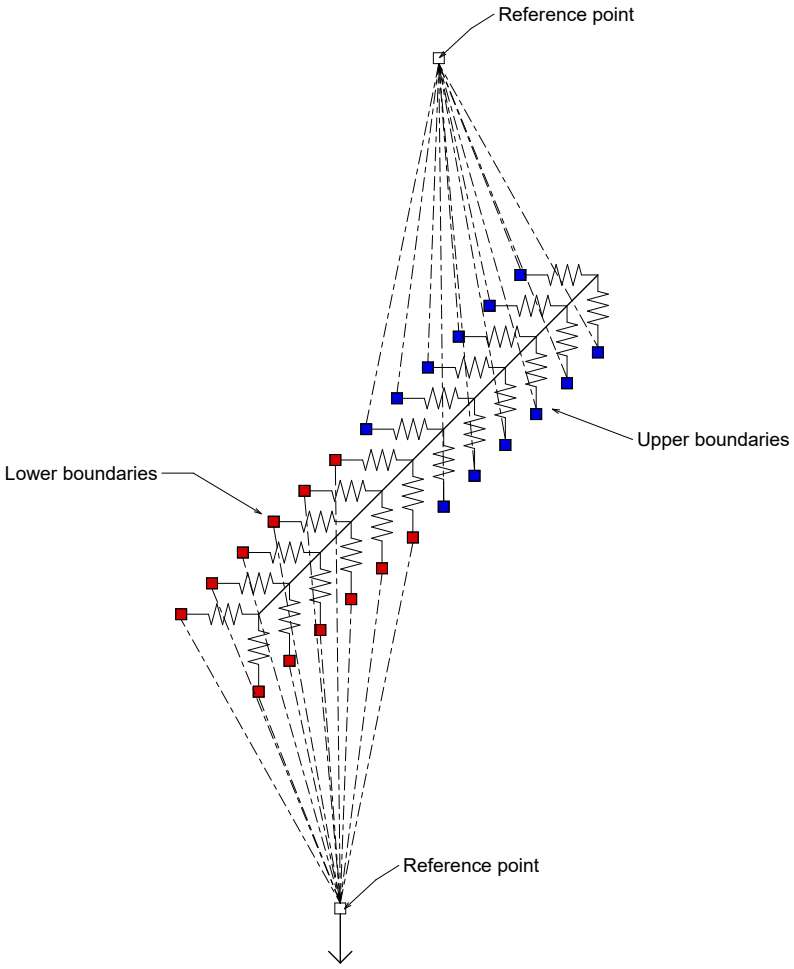

Figure 4.4: Principal configuration for the FE-model in pulling

The forced movement in the boundary condition results in stresses which creates a critical part in the model located in the area where the two timber elements meet. The resulting major displacement and stresses cause the screw to reach yielding here first. The method of separating the boundaries was to ensure that a double plastic hinge occurs in the model according to Johansen (1949) third failure mode, as seen in Figure 4.5. With this configuration, the behaviour of an inclined screw becomes

similar to the real case, which allows for the creation of force/displacement diagrams that can be used to express the resistance and the stiffness.

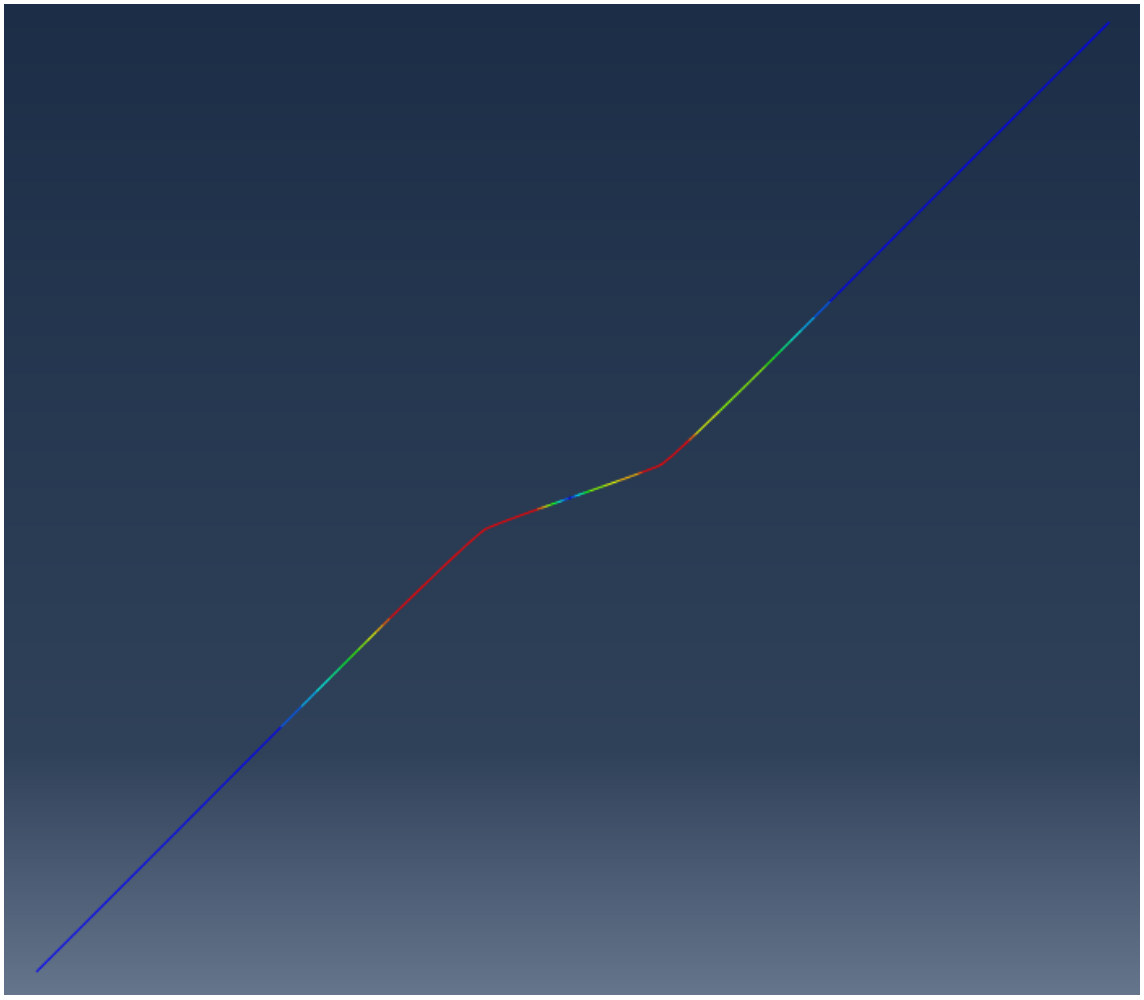

Figure 4.5: FE-model of the timber connection where two plastic hinges were created due to yielding

Values for the force were obtained by observing the reaction force of the lower reference points. Together with the predefined displacement, the values that were extracted represent the average displacement and the total force acting on the screw in that direction. From these values, the force/displacement diagrams were created from which K_{ser} and F_{ult} can be extracted, where the x-axis represents the deformation and the y-axis represent the reaction force. An example of this is illustrated in Figure 4.6.

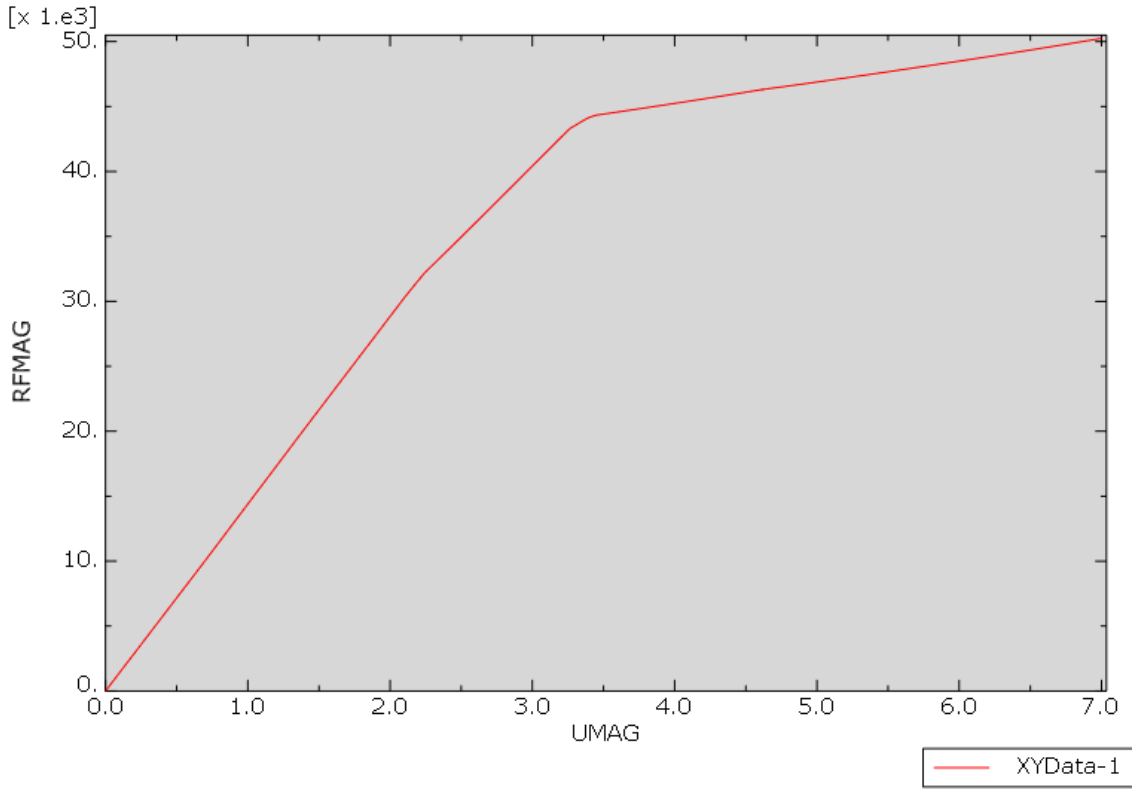

Figure 4.6: An example of a force/displacement-curve for an inclined screw in Abaqus

When this curve was created the values for the ultimate force (F_{ult}) and the stiffness in service state (K_{ser}) can be obtained. According to CEN (1991) the ultimate force was the total maximum value created from the simulation within a deformation of 15 mm, which translates to the highest visible value in the force/displacement diagram in that displacement range. The effective stiffness was achieved by analysing the range between $0.1F_{ult} - 0.4F_{ult}$ through linear regression. This was calculated according to equation 4.2.

$$K_{sls} = \frac{0.4 * F_{ult} - 0.1 * F_{ult}}{\upsilon_{0.4} - \upsilon_{0.1}} \tag{4.2}$$

where

F_{ult}	is the maximum load the connection is exposed to
$\upsilon_{0.1}$	is the displacement of the connection at a load of $0.1F_{ult}$
$\upsilon_{0.4}$	is the displacement of the connection at a load of $0.4F_{ult}$

In the FE-model the stiffness was defined to be fully linear until plasticisation takes place. For the range between $0.1F_{ult} - 0.4F_{ult}$, it remains linear and as a result, the ratio between $\frac{0.1F_{ult}}{\upsilon_{0.1}}$ and $\frac{0.4F_{ult}}{\upsilon_{0.4}}$ was used to calculate K_{sls}.

4.5 Defining stiffness parameters

The values used for the stiffness parameters k_p and k_t were uniform which means that all parallel springs defined in one model had the same stiffness and all the perpendicular spring had the same stiffness as well. In order to simulate the stiffness in the service state (K_{ser}) only the linear relation was needed as the spring in this state had not reached plasticity. As a result, the input for k_p and k_t could in this case be limited to one Force-Displacement relation that expresses the linearity. However, the ultimate load was reached when the connection had entered a non-linear state as the screw and the springs started plasticisation as seen in Figure 3.7. The connection behaved differently in its non-linear state depending on the angle and the force direction. Simulating this behaviour created the need to express the damage to the connection within the input parameters. This was done by creating several Force-Displacement relations with the springs in order for the correct behaviour to be simulated.

5
Validation of FE-model

To be able to simulate the behaviour of the connection in Abaqus, the model needs to be calibrated. The model becomes validated and verified by the process illustrated in Figure 5.1.

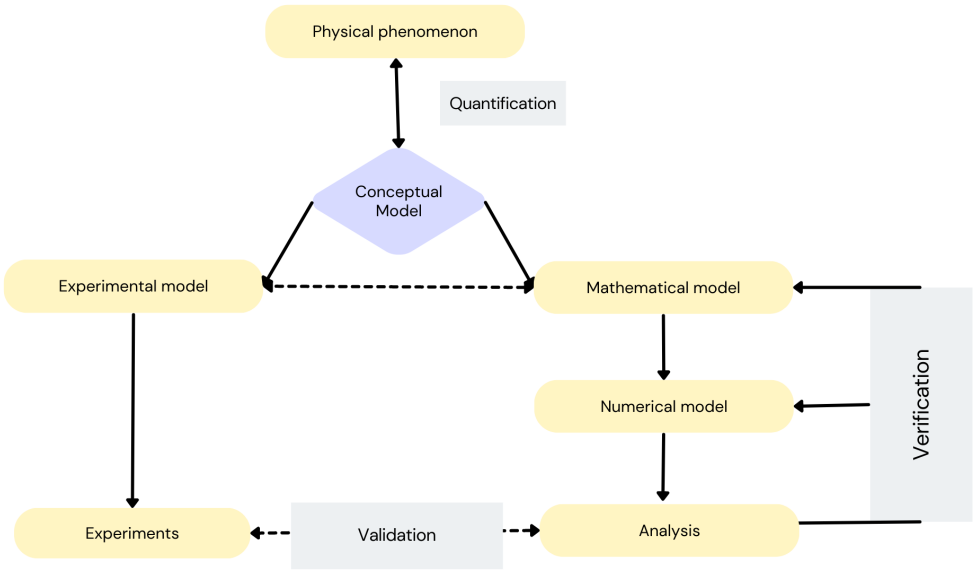

Figure 5.1: Interpretation of a validation and verification process (CEN, 2022a)

The verification of the numerical model is done by initiating a convergence and sensitivity study. It was conducted by increasing the number of springs connected to the beam until the values converged, as well as investigating the behavioural changes caused with different spring stiffnesses and how they relate to the section. The values were then validated against test results from previous experiments created by Jockwer et al. (2014b), as seen in Table 3.10 and illustrated in Figure 3.7. The validation is then completed when the Abaqus model produces the same behaviour for the connection as presented in the test results. To achieve this, the input parameters for the parallel and perpendicular spring stiffness (k_p and k_t) need to be calibrated according to the model constructed by De Santis and Fragiacomo (2021). This is followed by a convergence study where different a number of springs are used, which determined the amount of finite elements. These are evenly distributed to avoid convergence problems and can be seen in Figure 5.6. The validation procedure was conducted for all configurations tested in Jockwer et al. (2014b) to establish a relation between the input parameters and the stiffness (K_{ser}).

5.1 Shearing test validation

The FE-models created from the shearing tests reached the ultimate loads and stiffnesses according to the experimental values from Jockwer et al. (2014b) as can be seen in Table 5.1 and 5.2. Force-Displacement diagrams from the FE-model that represent the connection's behaviour for different angles are visualised in Figure 5.2. Since the force-displacement relationship only has minor deviations, the model can work as a basis on which further extrapolation can be conducted to extend the use of the model.

Table 5.1: Result for validation of stiffness in shearing

	Stiffness test in shear		
Angle	FE results $[kN/mm^2]$	Experimental results $[kN/mm^2]$	Difference [%]
45	13.8	13.6	0
60	6.0	5.9	2
90	2.0	1.9	5

Table 5.2: Result for validation of resistance in shear

	Stiffness test in Pulling		
Angle	FE results $[kN]$	Experimental results $[kN]$	Difference [%]
45	29.6	27.4	8
60	20.0	20.5	-2
90	10.5	10.5	0

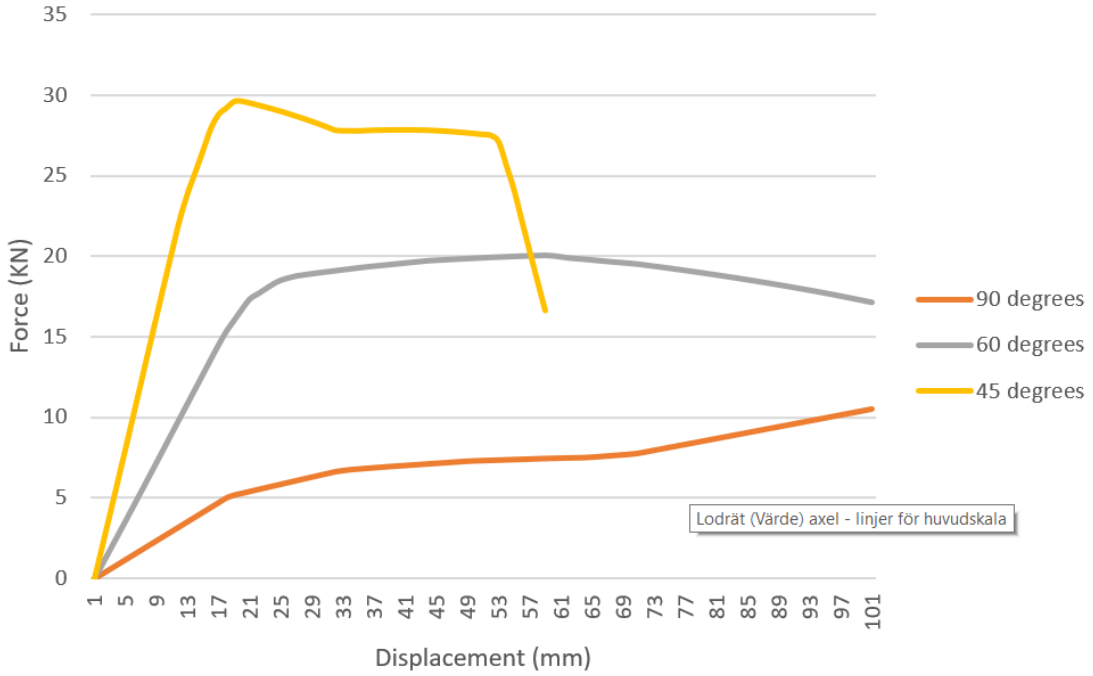

Figure 5.2: Force and displacement relation from FE-model depending on different screw angles for shearing

The linear behaviour of the connection was achieved with the input values for k_p and k_t as seen in Figure 5.3. For the tested angles it becomes apparent that the defined stiffness for the parallel direction is significantly larger than the perpendicular stiffness, and that the difference increases with a lower angle.

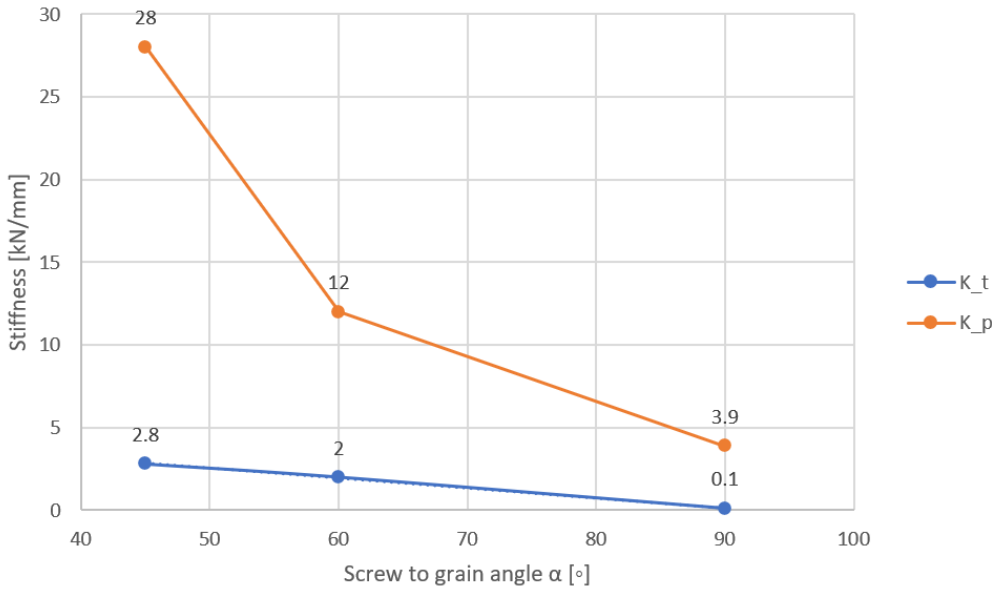

Figure 5.3: Input parameters for the parallel and perpendicular spring stiffness (k_p and k_t) when loaded in shearing in Abaqus that creates the desired stiffness (K_{ser})

As mentioned before, to simulate the non-linear behaviour in the connections, several force-displacement relations for the springs are defined. These are defined as 5 different displacements values which consist of 0, 1, 4, 10 and 16 mm. The stiffness for the springs k_p and k_t can be seen illustrated in Figure A.1 and A.2 respectively in Appendix A. These values represent the non-linear behaviour of the springs at different displacement stages for different angles during shearing.

5.2 Pulling test validation

The finite element pulling tests result was similar to the shearing test compared to the experimental results from Jockwer et al. (2014b) and a comparison of the stiffness and ultimate resistance can be found in tables 5.3 and 5.4 respectively. Force-Displacement diagrams from the FE-model can be seen in Figure 5.4. Since the force-displacement relationship only has minor deviations, the model was used as a basis on which further extrapolation could be conducted to extend the use of the model.

Table 5.3: Result for validation of stiffness in pulling

	Stiffness test in Pulling		
Angle	FE results $[kN/mm^2]$	Experimental results $[kN/mm^2]$	Difference [%]
45	3.0	3.0	0
60	8.8	8.9	-1
90	28.1	28.3	-1

Table 5.4: Result for validation of resistance in pulling

	Resistance test in Pulling		
Angle	FE results $[kN]$	Experimental results $[kN]$	Difference [%]
45	17.7	17.7	0
60	21.6	21.6	0
90	20.4	21.2	-4

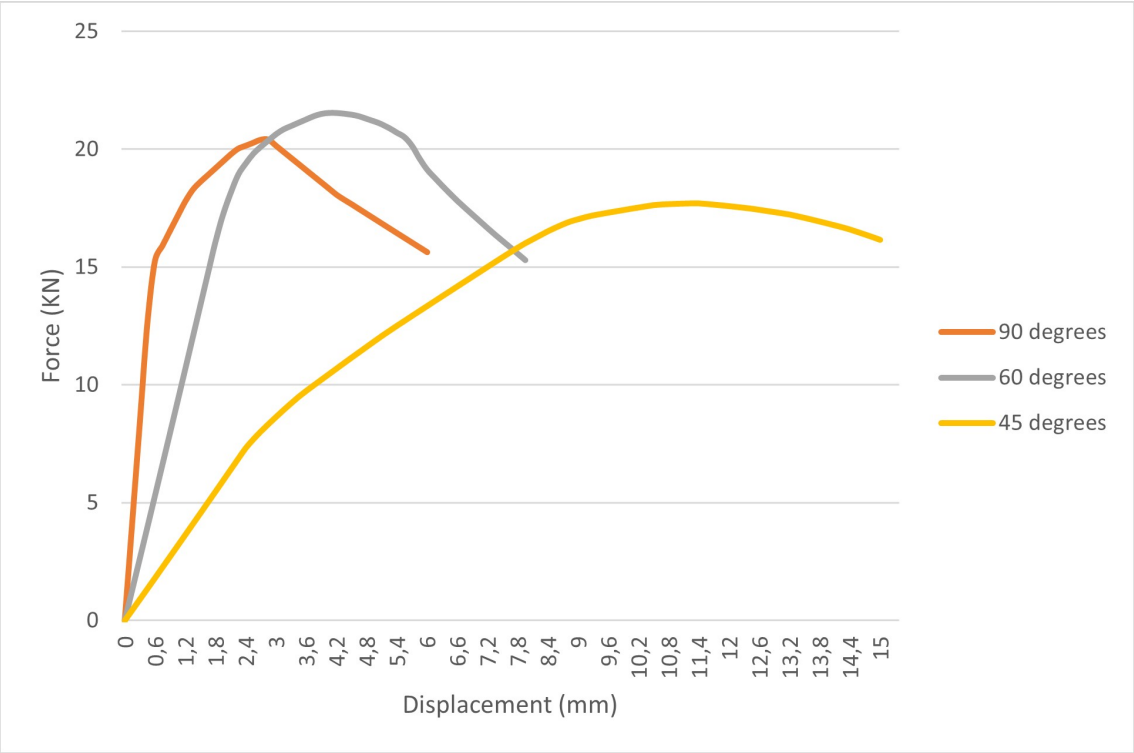

Figure 5.4: Force and displacement relation from FE-model depending on different screw angles for pulling

The linear behaviour of the connection was achieved with the input values for k_p and k_t as seen in Figure 5.5. For the tested angles it becomes apparent that the result is nearly the opposite of the shearing results, whereas in the pulling test, the perpendicular stiffness increases with an increased angle and the parallel stiffness decreases.

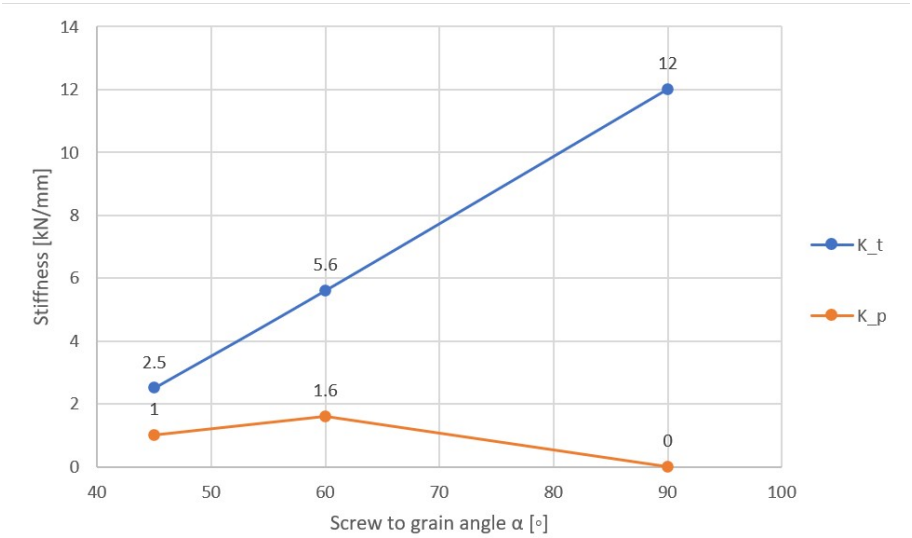

Figure 5.5: Input parameters for the parallel and perpendicular spring stiffness (k_p and k_t) when loaded in pulling in Abaqus that creates the desired stiffness (K_{ser})

In the same way done as with shearing, to simulate the non-linear behaviour in the connections, several force-displacement relations for the springs were defined. The stiffness for the springs k_p and k_t is illustrated in Figure A.3 and A.4 respectively in Appendix A. These values represent the non-linear behaviour of the springs at different displacement stages for different angles during pulling. With these input values the full force-displacement diagram shown in Figure 5.4 was created.

5.3 Comparison of behaviour in validation

When observing the behaviour in the figures throughout chapters 5.2 and 5.3 it becomes apparent that the horizontal stiffness (k_p) is dominant in shearing and the vertical stiffness (k_t) is dominant in pulling. This is due to that the spring stiffnesses need to resist the movement of the force in the direction they are oriented. A clear example of this behaviour is that for shearing with an angle of 90 degrees, k_t becomes negligible, as seen in Figure 5.3. In other words, pure shearing exerts a force that only the horizontal stiffness k_p can resist, because they have the same orientation. The opposite applies for k_p and k_t for the case with pulling.

k_p and k_t are fixed, while K_{ax} and K_v are changing direction with the screw. As the springs need to resist the force relative to their orientation, they have a relation to each other depending on the screw-to-grain angle. As a result, one can to a certain extent predict how the input parameters in Abaqus will behave in different situations.

As mentioned in Chapter 3.3, a configuration that has a force perpendicular to the grain should theoretically have a reduction of the effective screw length (x_1) due to unfulfilled utilisation of embedment strength. This reduction in pulling, together with the influence of friction force in shearing is neglected in the FE-models configuration. The input parameters (k_p and k_t) are fitted to act as the reduction.

The test for pulling in a 90°angle between the screw to the grain direction has significantly higher stiffness (k_{ser}) compared to all other test results. This means that the linear slope at the beginning of the force-displacement diagram is relatively steep. As a result, the force-displacement relations needed to be altered to smaller intervals to express the behaviour of the screw. Only the vertical spring stiffness is active for this configuration and the centre of mass pulling the screw is directly above and below the screw. This causes the diagram to consist of linear lines that follow the input parameter (k_t) as there is no interaction for parallel and perpendicular stiffness.

5.4 Convergence study

The number of non-linear springs that exist in the FEM configuration influences the accuracy at which the result can be measured and affect if the results converge. A more representative connection between the timber elements and the screw will be

achieved as more springs are present in the model. To determine a suitable number of springs needed to produce a desirable precision in the results. a convergence study is then conducted. For this study, the non-linear springs are evenly distributed along the screw. The study is being performed on a configuration with shearing at a screw-to-grain angle of 45°and the results are illustrated in Figure 5.6. The result shows that at around 100 springs per axis both the resistance and the stiffness had fully converged.

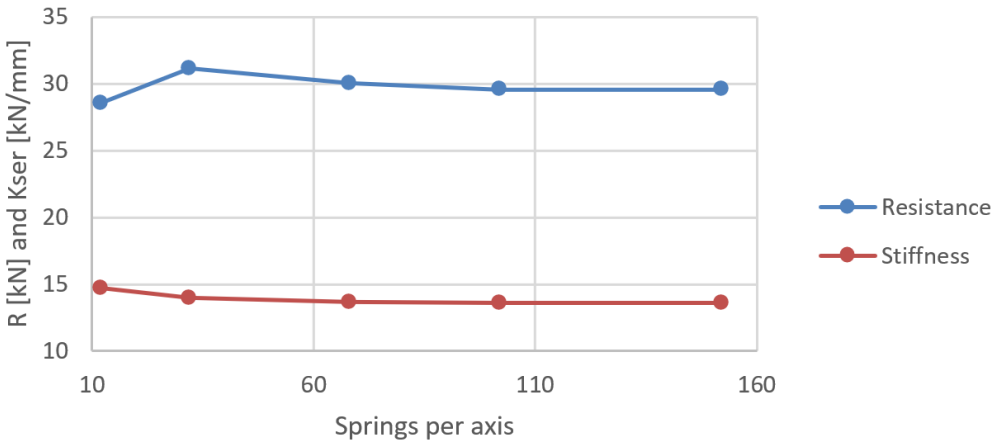

Figure 5.6: The stiffness and resistance for a screw exposed to shearing at $\alpha = 45°$ depending on the amount of springs in the FE-model

6

New model applications for studying joint behaviour

Once the FE-model is verified and validated it can be used to study further applications which can be of use when compared to new theoretical models.

6.1 Parameterisation of joint behaviour

Once the FE-model is defined and validated against experimental test results, a parametric study was conducted using Python with ABAQUS to explore the behaviour of the screw within the angles 45°to 90 °, where there is no physical test data. The goal of this study is to investigate the impact of screw-to-grain angle on slip modulus and resistance. The study is then divided into several parts, with the first part focusing on the screw's behaviour under shear, the second on the screw's behaviour under pulling and subsequently for new force to grain angles.

With the input values generated through parameterisation, the full force-displacement diagram shown in Figure 5.2 was created. The red line in Figure 6.1 and 6.2 represents an angle of 75° based on the validated force-displacement relations. This value acts as an example of how the input parameters (k_p and k_t) could vary for a new screw-to-grain angle through interpolation. This interpolation is a pure interpolation between the input values created from angles 60° and 90°. It works as an estimation of how the input parameters should change depending on the angle and is used to generate new values for stiffness and resistance in new angles with our model.

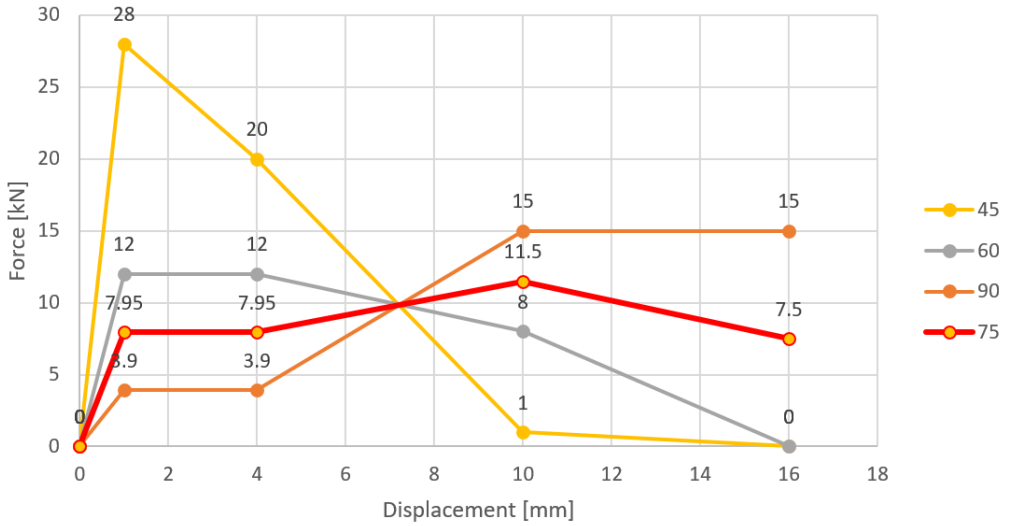

Figure 6.1: Input parameters for the parallel spring stiffness (k_p) in Abaqus that describes the screw behaviour in shear

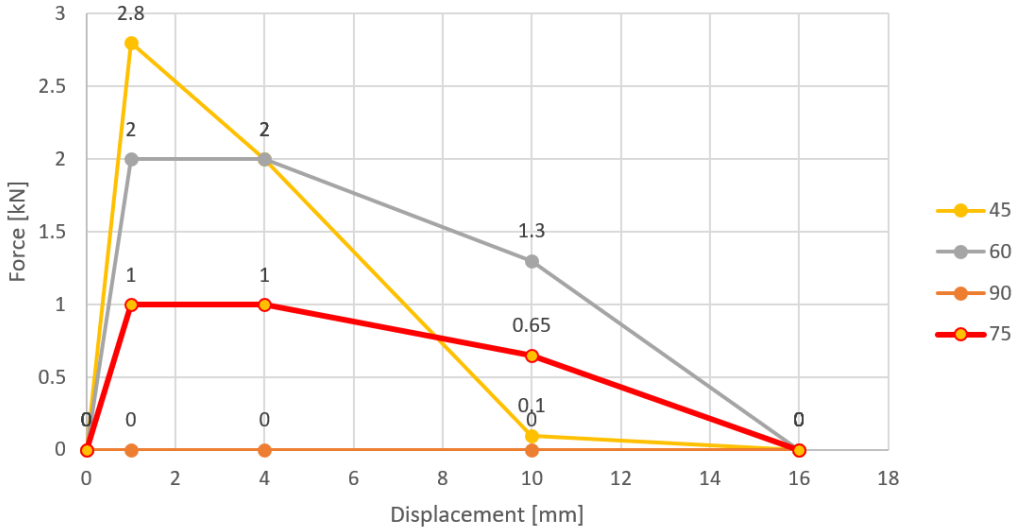

Figure 6.2: Input parameters for the perpendicular spring stiffness (k_t) in Abaqus that describes the full screw behaviour in shearing in shear

When applying the model to pulling, an application was made in 75° which is represented by the red line in Figure 6.3 and 6.4. Where the values for the input parameters (k_p and k_t) are interpolated for a new screw to grain angle of 75°. The model shows a behaviour which seems realistic and which fits into the other angles.

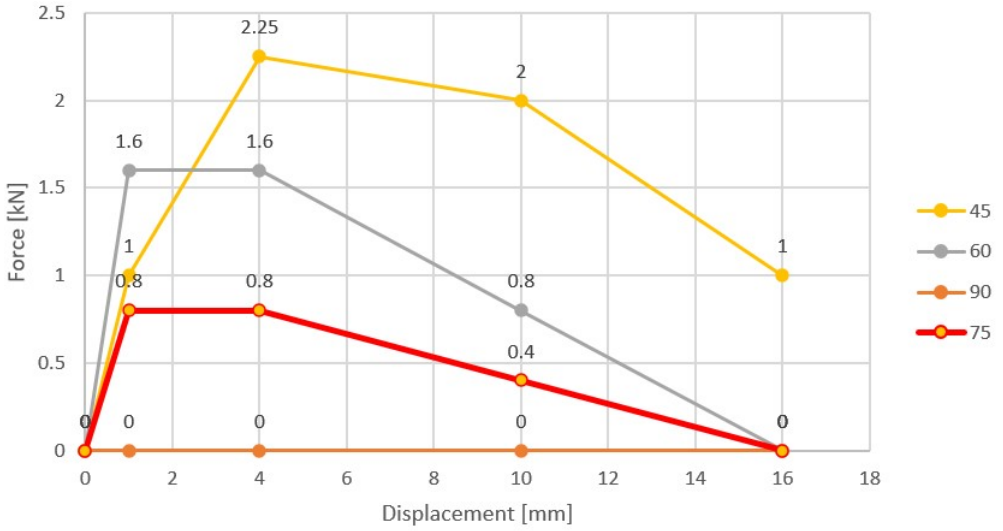

Figure 6.3: Input parameters for the parallel spring stiffness (k_p) in Abaqus that describes the screw behaviour in pulling

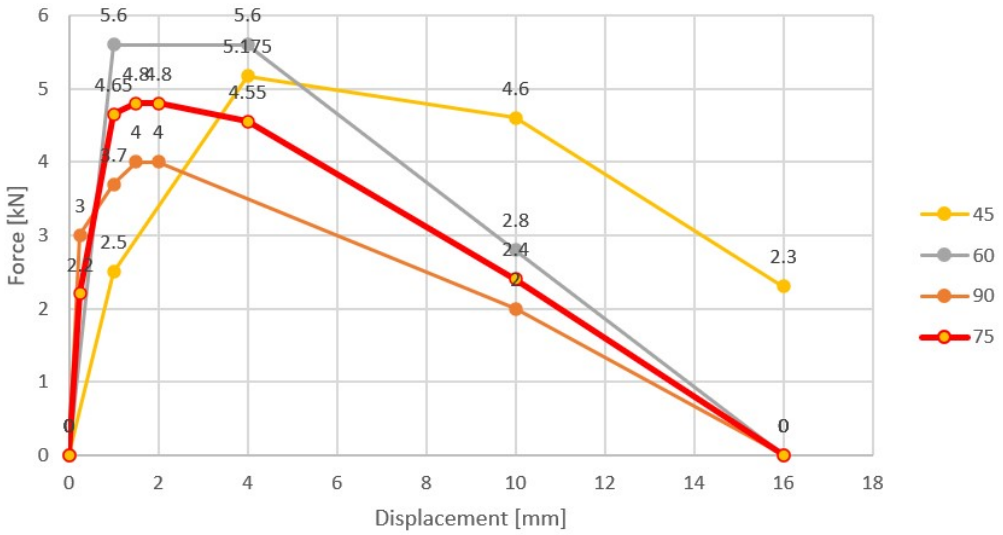

Figure 6.4: Input parameters for the perpendicular spring stiffness (k_t) in Abaqus that describes the full screw behaviour in pulling

6.2 Extension below 45°

The test results from Jockwer et al. (2014b) limit the investigated range of the screw to grain angle (α) to 45°-90°. In order to extrapolate values below 45° the trend from the extrapolated results between 45°-90° could be used and verified with theoretical behaviour explained in chapter 3.

The first thing that needs to be considered is that the model presented in Jockwer et al. (2014b) has an increasing effective length of the screw the lower the angle

becomes. If this relation would continue it would mean that the effective length would go towards infinity as α approaches zero degrees. The screw used in Jockwer et al. (2014b) experiments have a total screw length of 400mm, which means that a screw-to-grain angle of approximately 35° would utilise the full screw length. Everything below 35° would require a longer screw to penetrate through both timber elements as seen in Figure 3.6a. If the screw angle is too low it also brings the risk of failure as the screw is too close to the gap between the timber elements, as well as losing its capability to connect two timber elements and transferring forces. The angles used in the extrapolation are therefore only investigated down to 35° as they are plausible to investigate and can be practically constructed in reality.

6.3 Extension of force direction

To create an expression that describes the behaviour in a new force direction a few things need to be considered. Firstly, as the force to grain angle rises above 0° to a certain degree the friction force will disappear due to the opening of the joint. A reduction of the effective length should also exist to a certain extent as the connection cannot utilise the full embedment strength due to the force direction to some extent pulling it apart.

As the axial stiffness can be taken as $K_{ser,ax,i} = 25L_{ef}d$ for shearing according to Deutsches Institut fur Bautechnik (2011) and $K_{ser,ax,i} = 40L_{ef}d$ for pulling according to Jockwer et al. (2014a), the axial stiffness for a new force angle could be hard to estimate as there is no physical test data to prove the behaviour. If one of these existing expressions were to be chosen for a new force direction (γ), it would represent the stiffness more accurately the closer γ is to the force angle the expression is based on. As an example, $K_{ser,ax,i} = 25L_{ef}d$ would represent a more accurate value when $\gamma = 2°$ and would represent an inaccurate value if $\gamma = 88°$. As no definition has been stated for an axial stiffness (K_{ax}) for an angle between $\gamma = 0° - 90°$ an estimation through interpolation is performed as seen in equation 6.1, could not be linear. Note that this is an estimation of K_{ax} based on the expressions made from test results for force angles 0° and 90° which are later needed to be verified through physical test results.

$$K_{ser,ax,i,\gamma} = (\gamma \cdot \frac{40-25}{90} + 25) \cdot L_{ef} \cdot d \qquad \textit{(double stiffness model)} \tag{6.1}$$

The expression for the embedment strength in equation 3.14 from Blaß et al. (2006) is only dependent on the screw-to-grain angle (α) and independent on the force-to-grain angle (γ). However, in equation 2.17 which is based on Hankinson (1921) theory, the embedment strength is dependent on the load to grain angle (ϵ). By following the principles and results from Hankinson (1921) the angle (ϵ) at which the force is applied in relation to the grain direction will have an effect on the embedment strength of the timber. As a result, the embedment strength should also experience a change of force-to-grain angle (γ) that is acting on another plane than (ϵ). As equation 3.14 is used for a force-to-grain angle of ($\gamma = 0$) it can

be reformulated with equation 2.17 to achieve the embedment strength for a new force-to-grain angle (γ) as follows:

$$f_{h,\gamma} = \frac{f_h}{k_{90} sin(\gamma)^2 + cos(\gamma)^2} \tag{6.2}$$

where

f_h is calculated according to equation 3.14

6.3.1 Extension based on shearing formula

Using the stiffness and resistance equations for shearing as a base (equation 3.8 and equation 3.5 respectively), a new expression for a different force direction could be created. The main change would be the geometrical relation that describes the lateral and axial effect on the screw. If the new force direction is the angle γ (°) then the lateral and axial components would experience a change of force according to that angle. The stiffness could then be expressed with equation 6.3 and the resistance would be according to equation 6.4. The effect of the friction force (μ) is difficult to estimate for new force directions, as $\mu = 0.25$ for shearing and $\mu = 0$ during pulling. When γ increases above 0°the friction force (μ) will subside successively until it reaches a certain angle of γ which is unknown and then becomes negligible.

$$\begin{aligned} K_{ser,\gamma,0} = K_v \cdot |sin(\alpha-\gamma)| \cdot (|sin(\alpha-\gamma)| - \mu|cos(\alpha-\gamma)|) \\ +K_{ax} \cdot |cos(\alpha-\gamma)| \cdot (|cos(\alpha-\gamma)| + \mu|sin(\alpha-\gamma)|) \end{aligned} \tag{6.3}$$

$$R = R_{ax}(|cos(\alpha-\gamma)| + \mu|sin(\alpha-\gamma)|) + R_v(|sin(\alpha-\gamma)| - \mu|cos(\alpha-\gamma)|) \tag{6.4}$$

where

K_v is calculated according to equation 2.9 in double stiffness model

K_{ax} is calculated according to equation 6.1 in double stiffness model

R_v is calculated according to equation 3.22

$$R_{ax,\gamma} = \frac{d \cdot L_{ef} \cdot f_{ax,mean}}{1.2cos(\alpha)^2 + sin(\alpha)^2} * |sin(\alpha-\gamma)| \tag{6.5}$$

6.3.2 Extension based on pulling formula

Equation 6.3 and 6.4 do not take into account a reduction of the effective length (x_1). Therefore, the theory based on Jockwer et al. (2014b) extension for a force perpendicular to the grain can be used to include the reduction. Equation 6.6 for the stiffness would be the same as equation 3.12, but with the exception that

some components that are based on the screw-to-grain angle (α) would include an expression with the new force direction γ. These components are the reduction of the effective length (x_1) expressed with equation 6.8 as well as the axial resistance ($R_{ax,\gamma}$) in equation 6.5. Equation 6.6 does however not take friction into consideration due to it being related to pulling which in theory does not generate any friction and is therefore not included.

$$\frac{1}{K_{ser,\gamma,90}} = \frac{1}{K_{v,\gamma,90}} + \frac{1}{K_{ax}} \tag{6.6}$$

where

K_{ax} is calculated according to equation 6.1 in double stiffness model

$$K_{v,\gamma,90,i} = \frac{3 * E_{steel}\pi d_{core}^4}{64 x_{1,\gamma}^3} \qquad \textit{(double stiffness model)} \tag{6.7}$$

$$x_{1,\gamma} = \frac{f_{h,\gamma} d_{ef}}{2tan(|\frac{\pi}{2} + (\alpha - \gamma)|) f_{v,roll}} \tag{6.8}$$

Note that the reduction of the effective length (x_1) can only apply if the $\gamma > \alpha$ as those are the only possible angles where the full embedment strength of timber can not be utilised. This is illustrated in Figure 6.5, as the angle of the screw is 45°, the only force-to-grain angles between 45° and 90° can cause a reduction of the effective length.

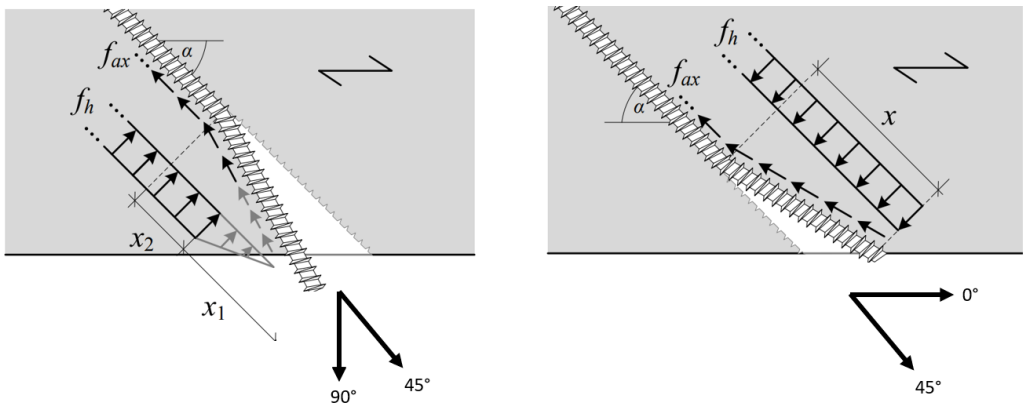

Figure 6.5: The force to grain angles that causes a reduction of the effective length for screw angles at 45° to the grain, adapted from (Jockwer et al., 2014b)

The resistance for a case with a new force direction acts according to equation 3.20 but with changed geometric relation for the new angle. It can be expressed with equation 6.9 below. All components within this equation that are based on the

screw-to-grain angle (α) would once again include an expression with the new force direction γ.

$$R = R_{ax,\gamma} \cdot |cos(\alpha + \gamma)| + R_{perp,\gamma} \cdot |sin(\alpha + \gamma)| \tag{6.9}$$

where

$R_{ax,\gamma}$ is calculated according to equation 6.5

$$R_{perp,\gamma} = -f_h x_{1,\gamma} d_{ef} + \sqrt{(2M_y + f_h x_{1,\gamma}^2 d_{ef}) f_h d_{ef}} \tag{6.10}$$

7
Results

This chapter presents the results created through simulations in Abaqus based on the configurations and material properties presented in Chapter 4. These results are compared to previous test results from Jockwer et al. (2014b) as well as values obtained through the theoretical equations in chapter 3 from Tomasi et al. (2010), Bejtka and Blaß (2002) and Jockwer et al. (2014b) as well as with current guidelines from CEN (2013) and future guidelines from CEN (2022b).

7.1 Behaviour in shearing and pulling

As the experiments from Jockwer et al. (2014b) presents values during shearing and pulling for α=0°, 45° and 90°, the investigated range during validation is between a screw to grain angle of 45°-90°. After tailoring the FE-model with the input parameters (k_p and k_t) to act according to the test results, new input parameters could be interpolated for other angles in the range between 45°-90°. As mentioned in Chapter 5, this is done through interpolation between the validated input parameters.

7.1.1 Stiffness

The resulting stiffness achieved through the extrapolation in the FEM model is shown in Figure 7.1 and 7.2.

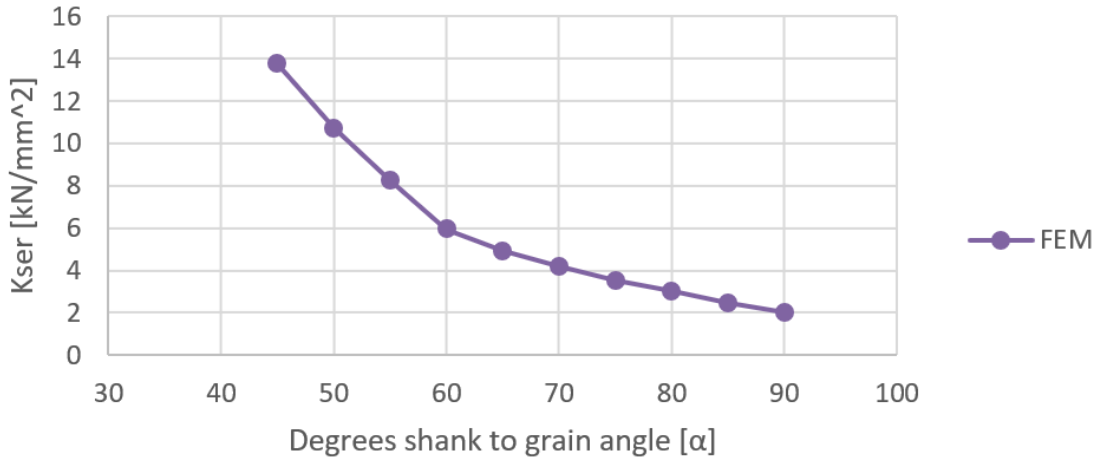

Figure 7.1: The stiffness for a connection exposed to shearing based on the FE-model

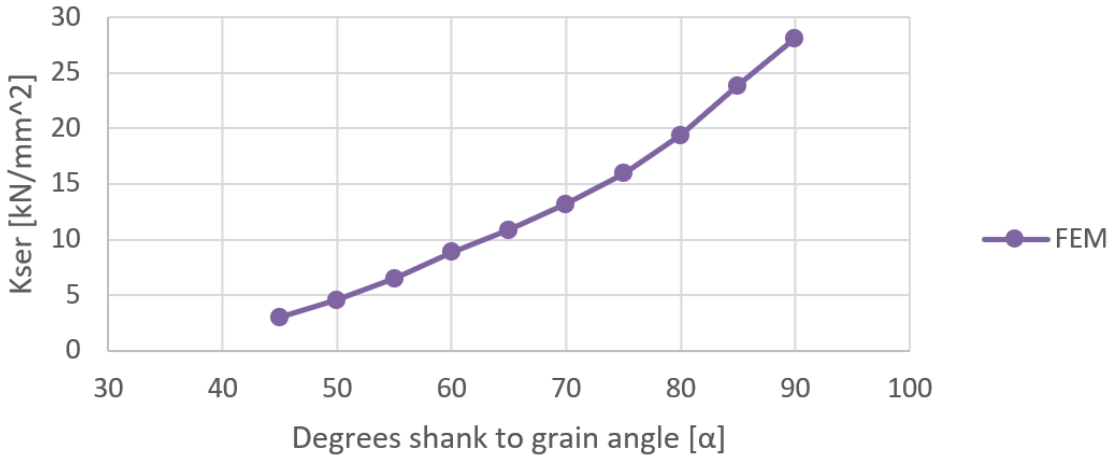

Figure 7.2: The stiffness for a connection exposed to pulling based on the FE-model

The results created in the FE-model follow the main theoretical behaviour for the stiffness as it becomes stiffer when the screw-to-grain angle (α) comes closer to the force-to-grain direction (γ). This symbolises the increase of stiffness created by the withdrawal strength of the screw, as well as the influence of the axial stiffness compared to the lateral stiffness for this type of fastener. Figure 7.3 and 7.4 presents the FEM results marked with the experimental test results from Jockwer et al. (2014b) together with the theoretical procedures presented in chapters 2 and 3. The trend line called "EC5" is the current method used to calculate the stiffness in Eurocode 5. The line remains constant as it is only dependent on the density, and screw diameter, and is only valid for shearing. The lines "EC5", "Tomasi", "Jockwer" and "EC5 2nd gen" is created using the equations presented in chapter 2.7. 3.2, 3.3 and 3.4 respectively. The test results and the FEM interpolation is similar to the results from the second generation Eurocode between angles of $\alpha = 60° - 90°$, where below 60° the results increase at a higher rate.

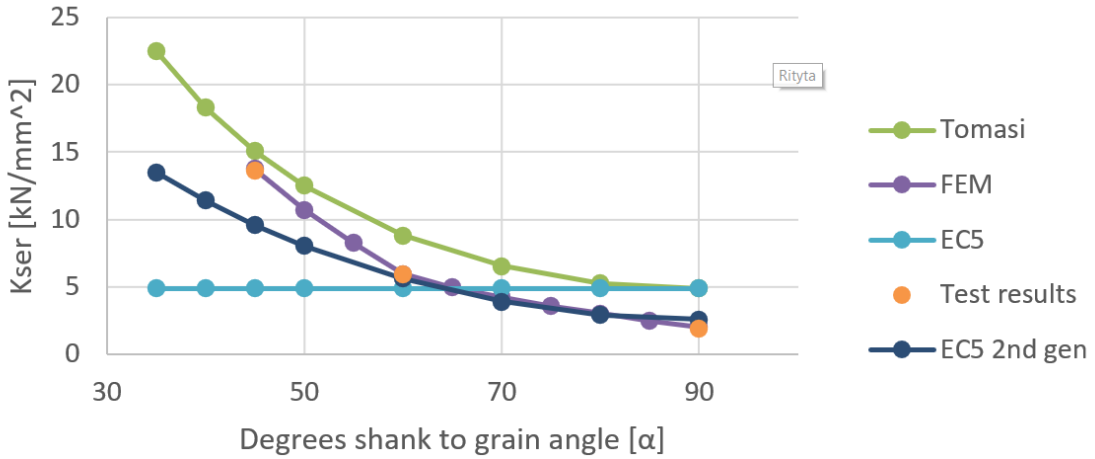

Figure 7.3: Stiffness in shearing based on different models and results with an increasing screw length

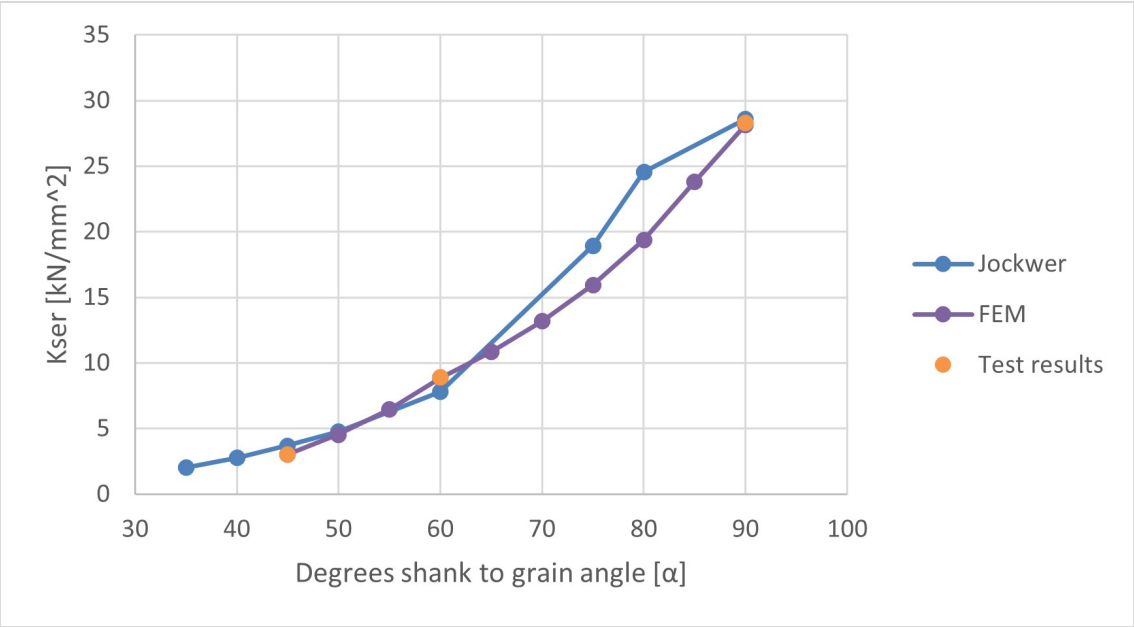

Figure 7.4: Stiffness in pulling based on different models and results with an increasing screw length

The stiffnesses for the connection expressed by the different approaches in figure 7.3 and 7.4 follow the same fundamental behaviour except for the current Eurocode standard. In shearing the difference between Tomasi et al. (2010) theory and the second generation of Eurocode 5 is an overall higher stiffness for all screw-to-grain angles. The main reason the stiffness is higher in Tomasi et al. (2010) approach is due to the lateral stiffness component is being defined according to equation 2.9, which is the same as in Eurocode 5. This could also be seen in Figure 7.3 as the line "Tomasi" is equal to line "EC5" for $\alpha = 90°$, when only the lateral stiffness contributes to the total stiffness. The lateral stiffness in the second generation of Eurocode is defined according to equation 3.35, which represents a value similar to the test results. If Tomasi et al. (2010) would use the same expression for the lateral stiffness, its relation to the tested values would be considerably more accurate. This can be seen in Figure 7.5, where the lateral stiffness for Tomasi et al. (2010) approach is expressed with equation 3.35 instead of equation 2.9.

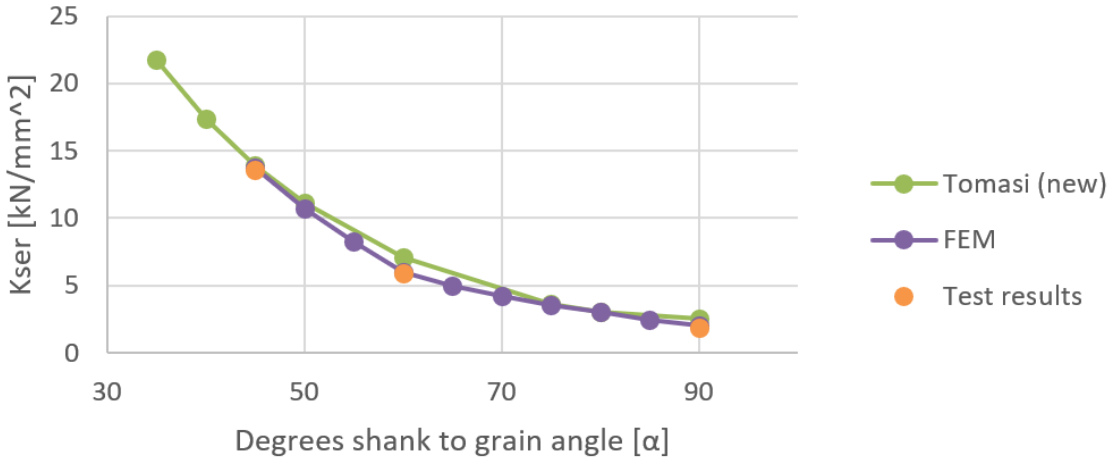

Figure 7.5: Stiffness in shearing based on Tomasi et al. (2010) approach with a new lateral stiffness and results with an increasing screw length

7.1.2 Behaviour below 45°

When extrapolating values below a screw to grain angle of 45°, as previously stated, the trend from the interpolated results between 45°-90° could be used and verified with theoretical behaviour shown in Figure 7.3 and 7.4. As the lateral stiffness becomes more dominant, the changes in stiffness depending on α become more similar between the different approaches. This is true both during pulling and shearing. For shearing it can be seen as α is getting closer to 90°, and for pulling as α is getting closer to 0. The test results, the FEM extrapolation and the theoretical approach from Jockwer et al. (2014b) during pulling show a similar behaviour of how the stiffness in the connection would act below 45°. An extension for pulling below the range of 45°-90° of the test results could therefore follow the theoretical approach from Jockwer et al. (2014b). This would mean the stiffness would continue to decrease but at a lower pace below 45°. For shearing the behaviour differs more between the approaches as seen in Figure 7.3. The main difference between Tomasi et al. (2010) theory and the second generation of Eurocode 5 is as mentioned the lateral stiffness, but the axial stiffness also increases at a higher rate at lower angles during shearing for "Tomasi". If Tomasi et al. (2010) approach would have a changed expression for lateral stiffness, as seen in Figure 7.5, the change in stiffness below 45°would act similarly to the trend from the FEM extrapolation. This would result with that the stiffness would continue to increase but at a higher rate below 45°.

7.1.3 Resistance

The resulting resistance generated in the FEM model is shown in Figure 7.6 and 7.7. The extrapolated resistance from the FE-model shows a behaviour similar to the theoretical foundation, as the load-carrying capacity increases when the screw-to-grain angle (α) comes closer to the force-to-grain direction (γ). This shows how the resistance is being influenced by the withdrawal strength of the screw, as it gets larger when the force is aligned with the screw axis. Note that the screw length is

increasing at lower screw-to-grain angles which also results in an increased resistance.

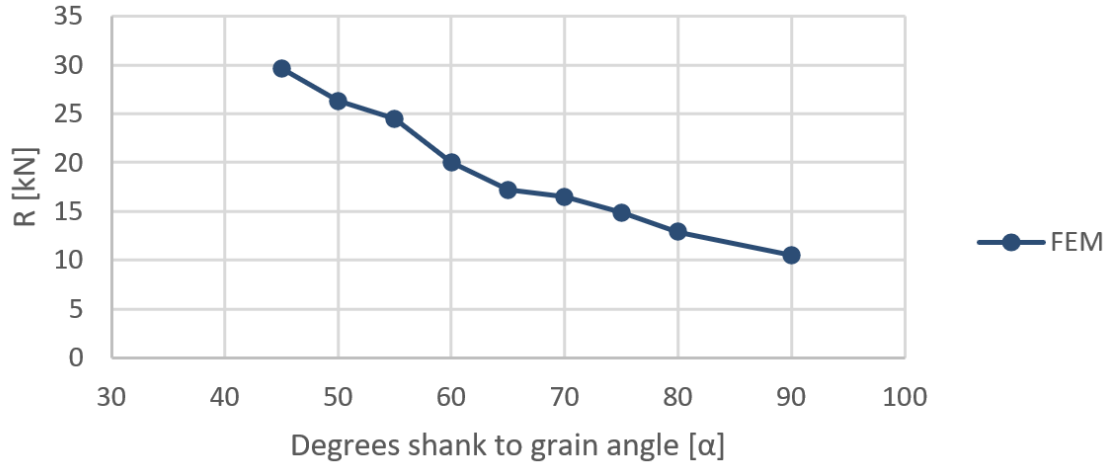

Figure 7.6: The resistance for a connection exposed to shearing based on the FE-model

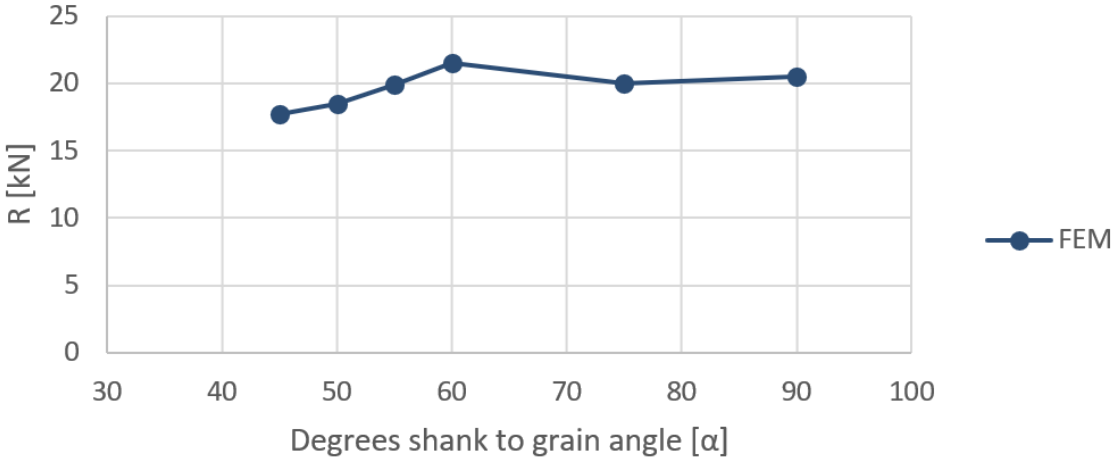

Figure 7.7: The resistance for a connection exposed to pulling based on the FE-model

The results from FEM, the experimental test results and the theoretical procedures presented in chapters 2 and 3 are shown in Figure 7.8 and 7.9. The lines "EC5", "Bejtka", "Jockwer" and "EC5 2nd gen" are created using the equations presented in chapters 2.8, 3.1, 3.3 and 3.4 respectively. Similar to the stiffness, the numerical results from ABAQUS act according to the main theoretical behaviour as the resistance increases the closer the screw-to-grain angle (α) gets to the force-to-grain direction (γ). EC5, Bejtka and Blaß (2002) approach and Jockwer et al. (2014b) approach underestimate the resistance greatly when compared to the test results. For shearing the line "Bejtka" is considerably lower and for "EC5" is about half of the measured numerical values. The test result values from Jockwer et al. (2014a) that the numerical values are based on have a significant increase partly because

of the friction that occurred during the shearing test. As the Teflon foil did not fully negate the friction force it was hard to estimate its contribution to the total resistance during shearing. The line "jockwer" in shearing represents the theoretical resistance based on the measured embedment strength that increased due to the acting friction force. With this considered a better representation of the resistance is formed.

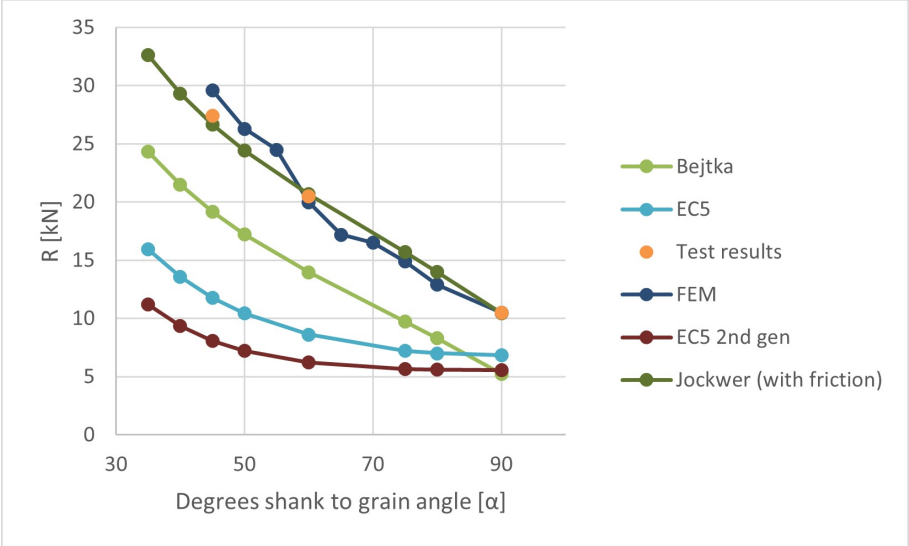

Figure 7.8: Resistance in shearing based on different models and results with an increasing screw length

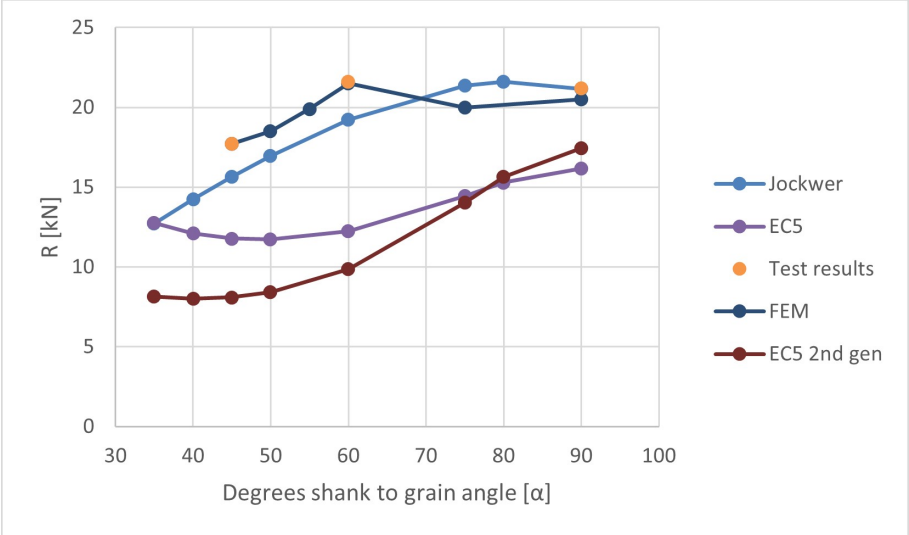

Figure 7.9: Resistance in Pulling based on different models and results with an increasing screw length

7.2 Overview of results

The results can also be seen in Table 7.1 and 7.2 where it can be seen how all values vary with the angle in both shearing and pulling. It can be seen that in pulling a higher resistance is achieved with a higher angle. Jockwer's equation seems to be the equation which follows the test results the most in pulling. In shearing the resistance increases in lower angles. EC5 2G seems as the equation which follows the test results the most.

Table 7.1: The load-carrying capacity from the different procedures

	Load carrying capacity					
	Tests	[Blaß]	[Jockwer]	FE	EC5	EC5 2G
α	F_{ult}	$R_{int,k}$	R_{mean}	R_{mean}	R_{mean}	R_{mean}
[°]	[kN]	kN	kN	kN	kN	kN
Pulling 90	21.2	18.7	18.7	20.4	16.2	17.4
75			18.4	20.2	14.4	14.0
60	21.6		16.3	21.6	12.3	9.9
45	17.7		15.3	17.7	11.8	8.1
35			15.5		12.8	8.2
Shearing 90	10.5	5.2		2.0	6.8	5.6
75		9.7		3.6	7.2	5.7
60	20.5	14.0		6.0	8.6	6.2
45	27.4	19.2		13.8	11.8	8.1
35		24.3			16.0	11.2

Table 7.2: The stiffness from the different methods

	Stiffness					
	Tests	[Tomasi]	[Jockwer]	FEM	EC5	EC5 2G
α	K_{ser}	K_{ser}	K_{ser}	K_{ser}	K_{ser}	K_{ser}
[°]	[kN/mm]	[kN/mm]	[kN/mm]	[kN/mm]	[kN/mm]	[kN/mm]
Pulling 90	28.3		17.9	28.1		
75			13.7	16.0		
60	8.9		6.9	8.9		
45	3.0		3.5	3		
35			2.0			
Shearing 90	1.9	4.9		2.0	4.9	2.6
75		5.8		3.6	4.9	3.3
60	5.9	8.8		6.0	4.9	5.6
45	13.6	15.1		13.8	4.9	9.6
35		22.5			4.9	13.5

7.3 Behaviour force direction extension

The resulting behaviour of the new force-to-grain directions overall seems to coincide between the theoretical applications and the FE-model.

7.3.1 Behaviour of the extension in theory

A force direction of 45° was set to get perspective for how a new force direction would behave between 0° and 90°. Figure 7.10 presents the stiffness from both formulas according to equation 6.3 and 6.6 for constant screw length and increasing screw length. The equivalent is presented in Figure 7.11 but for the resistance according to equation 6.4 and 6.9. All results following the extension based on pulling formulation from Jockwer et al. (2014b) experience a reduced value in all cases due to the reduced effective length of the screw ($x_{1,\gamma}$). The further away α is from 45°, the larger the reduced length becomes and as a result, $\alpha = 90°$ produces the lowest value in terms of stiffness and strength. When the screw-to-grain angle (α) equals the force-to-grain direction (γ) the connection is exposed to pure axial resistance (R_{ax}). The screw's highest stiffness is in its axial direction which becomes apparent with a constant screw length in Figure 7.10b. The stiffness for Figure 7.10a continues to increase at lower angles as the effective length of the screw continues to rise.

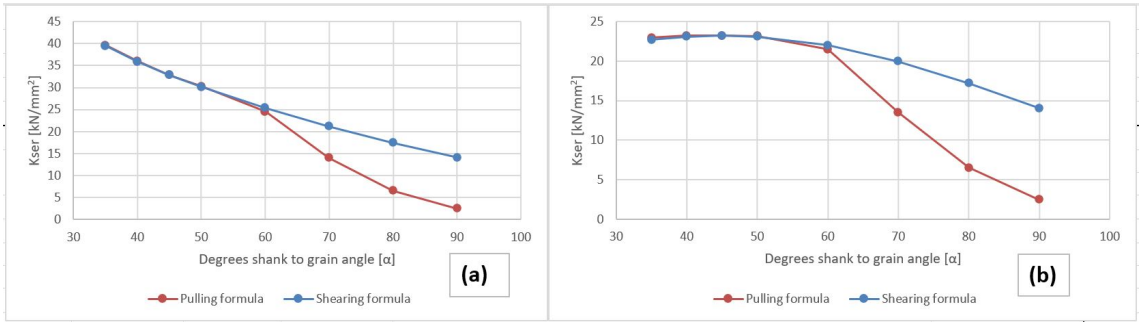

Figure 7.10: Stiffness for a 45° force direction based in the pulling and shearing formulas, where (a) has an increasing screw length and (b) a constant screw length

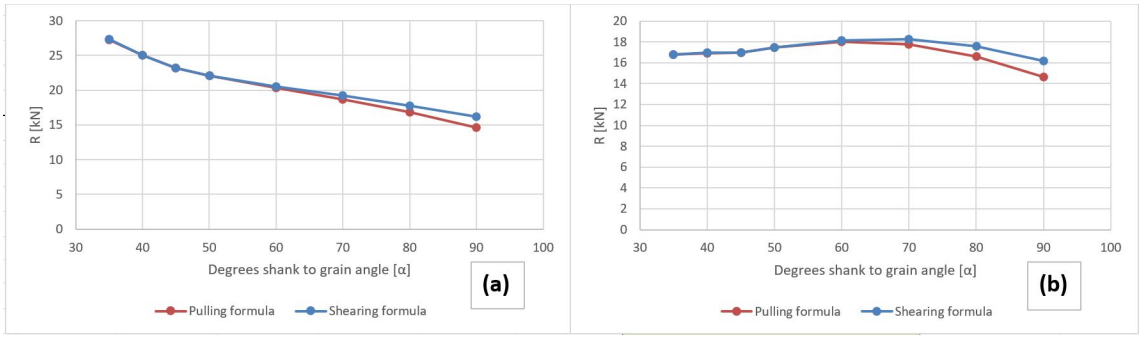

Figure 7.11: Resistance for a 45° force direction based in the pulling and shearing formulas, where (a) has an increasing screw length and (b) a constant screw length

At the force-to-grain angle $\gamma = 45°$ the connection should in theory not be able to utilise full embedment strength for all angles of α as it to some extent is being pulled apart. Therefore the extension based on the pulling formula should present a more true representation of reality. Figure 7.12 shows the stiffness for the force-to-grain angles $\gamma = 0°$, 45° and 90° at different screw-to-grain angles (α). These values are calculated from Tomasi et al. (2010) during shearing, Jockwer et al. (2014b) for pulling and equation 6.6 for $\gamma = 45°$. The equivalent is shown for the resistance in Figure 7.13.

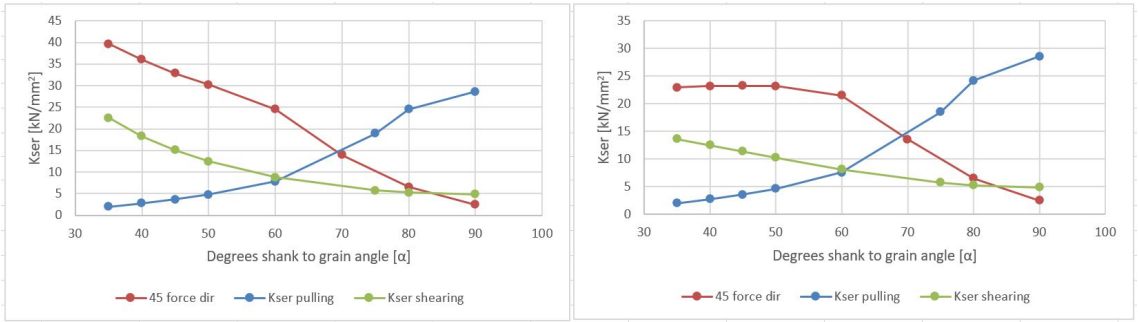

Figure 7.12: Stiffness for force directions 0°, 45°, 90°, where (a) has an increasing screw length and (b) a constant screw length

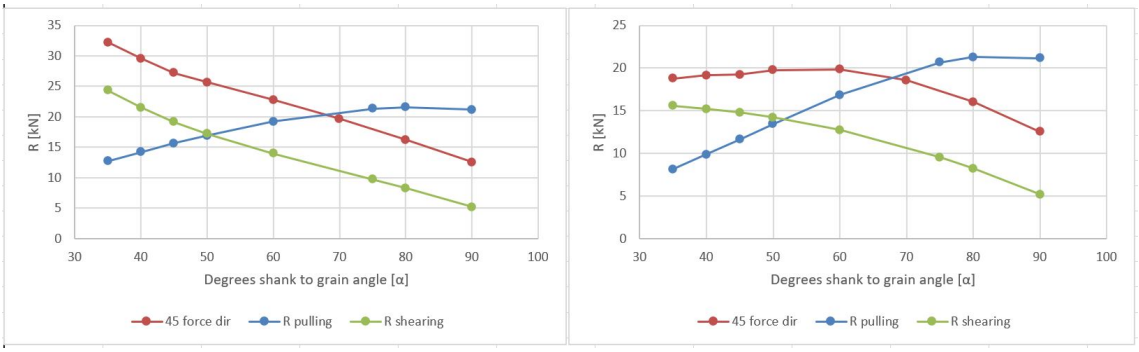

Figure 7.13: Resistance for force directions 0°, 45°, 90°, where (a) has an increasing screw length and (b) a constant screw length

7.3.2 Numerical behaviour of extension

The expressions in chapter 6.3.2 that define the stiffness and resistance for a force-to-grain direction of 45° work as a base for estimating the behaviour in the FE-model. Together with the theoretical formulas and validated test results an extrapolation of simulated values were created for the new force-to-grain direction. Figure 7.14 and Figure 7.15 represent the estimation of stiffness and resistance for a 45°force to grain angle. The red line represent pure analytical calculation from chapter 6.3.2 and the blue lines represent the numerical results from ABAQUS.

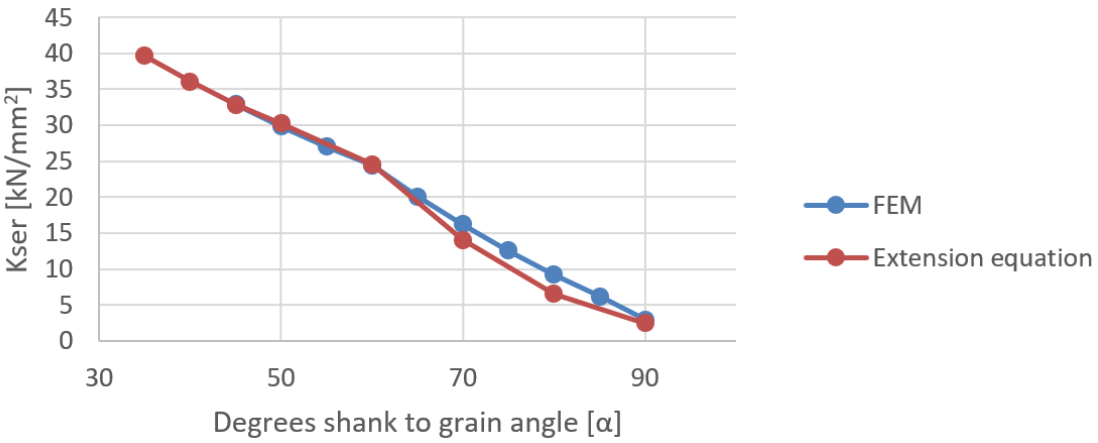

Figure 7.14: Comparison of the stiffness of a screw in the load-to-grain angle of 45°

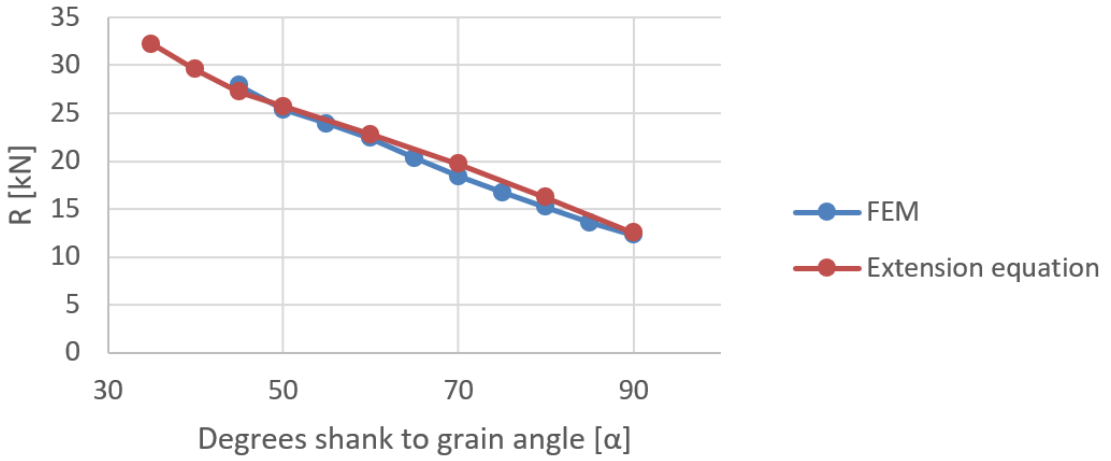

Figure 7.15: Comparison of the resistance of a screw in the load-to-grain angle of 45°

It can be seen that the FE-model and the extension equations coincide well, this in turn indicates that the created model works for new force directions and that the extended equations might be able to be used further on if verified. It is clear that the lower the angle is the higher the stiffness and resistance becomes. Similar to the shearing case this is due to the increasing screw length as well as the high withdrawal strength that the self-tapping screw withholds.

8

Discussion

In this chapter, the theory will be compared to the numerical results made in the parametric study, where the slip modulus as well as the resistance will be discussed to answer the aim and objectives of this thesis.

8.1 Slip modulus

The resulting slip modules can be seen in Table 7.2 where it is clear that the EC5 drastically both overestimates and underestimates the stiffness in connections, especially in certain angles. This is due to EC5 not considering axial stiffness and does not take the effects of angles into consideration, which results in constant values through all angles of α. It can also be seen that EC5 2G is the one equation which most consequently has similar values to the FE-analysis for shearing. Tomasi et al. (2010) equations become an accurate representation of the test results if the lateral stiffness is reduced by using equation 3.35 in EC5 2nd generation, as illustrated in Figure 7.5.

Based on the relation to the test results and the simulated values in FEM, it becomes apparent that the current definition of the slip modulus in EC5 is insufficient as major differences occur for different screw-to-grain angles. The new generation of Eurocode and Tomasi et al. (2010) approach represents the behaviour of the connection better as they consider screw-to-grain angles and axial stiffness. The calculation standard as it is now and as it is proposed in the draft for the new generation is limited to only one force direction (shearing). This limits the situations to which the slip modulus can be applied in the calculation standard, which is a major drawback as the results show major differences in stiffness depending on force direction. Jockwer et al. (2014b) extension of the slip modulus equation in pulling enables calculations for another load case. As shown in Figure 7.4, Jockwer et al. (2014b) method with a new axial stiffness of $K_{ser,ax,i} = 40 \cdot l_{ef} \cdot d$ follows the tested results well with similar behaviour to the numerical results created from the FE-model. The concept for stiffness with new load-to-grain directions as seen in Chapter 6.3.1 and 6.3.2 presents a possibility to extend the application of stiffness. This is however an area which has not been experimented with sufficiently and can therefore be hard to validate. Although the theoretical behaviour created with the extension is shown to follow the principle behaviour that has been validated with test results for shearing and pulling. That principle is, as mentioned earlier in the report, an increased stiffness due to the influence of the axial stiffness of the

connection. Through all investigated force directions, the stiffness increases when the force-to-grain direction is in close alignment with the force-to-screw direction. This is due to the high withdrawal capacity of self-tapping screws.

8.2 Resistance

In EC5, when expressing the lateral resistance through equation 2.12 the rope effect is defined with the expression $\frac{F_{ax}}{4}$ which makes it only dependent on the axial resistance. However, EC5 2G has an addition of the rope effect in equation 3.31 based on either the axial resistance or the dowel contribution. Due to the usage of Teflon foil between timber elements, all analysed values in this thesis were studied without the effect of rope effect or friction force. If it would have been included the resistance would have increased further.

The calculated values for the resistance can be seen in Table 7.1 where it becomes apparent that EC5 underestimates the resistance of the connection at all screw-to-grain angles for both shearing and pulling. The same applies to EC5 2G which generates a similar result to the current Eurocode standard. For the experimental results in shearing the load-carrying capacity is increased as friction force occured between the timber elements despite the use of the Teflon foil. This means that the test results as well as the FEM results which are based on the test results have a larger gap to the theoretical values from EC5, EC5 2G and Bejtka and Blaß (2002) equations. Figure 7.9 illustrates that 7.8 method with new values for the withdrawal strength (f_{ax}) and yield moments of the screw (M_y) shows a more accurate representation of the resistance of the connection in pulling. The same can be seen in Figure 7.8 as the updated equation for embedment strength (f_h) provides a similar value to the results for shearing. This in turn also shows that the previous values from Blaß et al. (2006) are too low in order to generate values similar to the given test results.

During shearing, the current Eurocode and the second generation of Eurocode 5 produce more valid results at $\alpha = 90°$. This is probably true for Eurocode 5 due to the design standards not considering self-tapping screws which can be used in more angles than other fasteners. However, EC5 and EC5 2G does have an equation for a combination of loads according to equation 3.1 but do little to consider the effect of angles. For this reason Tomasi et al. (2010) did a derivation of the equation for combined loading to equation 3.3 as mentioned previously, which is derived with the use of trigonometry to calculate the resultant forces. With this implemented, EC5 and EC5 2G can more accurately describe the behaviour of the load capacity but is still low in comparison with the test results.

8.3 Model

The numerical model used in this thesis is based on the model created by De Santis and Fragiacomo (2021) and is comprised of a solid 2D-beam element which simulates the screw to be able to describe bending and bending failure satisfactorily, which is needed to accurately simulate the screw. The surrounding timber is then simulated as two sets of springs (kp and kt) and each set of springs are assumed to have the same stiffness, which might not be a representative case compared to reality. The stiffness, which is expressed in springs along the screw, might in reality differ as different parts of the screw are subjected to higher stresses in shear and bending for different load cases. In reality, the springs closer to the shear plane could also be further embedded than the springs closer to the outer edge, depending on the connection. The principle layout of the FE-model is depending on the boundary points, to which the springs are attached, that has their movement in unison. This configuration is a simplified representation of how the timber elements move and their attachment to the screw, which might cause a different general behaviour compared to reality.

As the FE-model is in 2D, the angles that are investigated and changed through parametrisation coincide with all the theoretical calculation models mentioned in this thesis, making it easier to compare the results. The FE-model does however not take the effect of friction into consideration. This is due to its validation that is compared to the test results, which include Teflon foil between the timber elements to negate the friction. In order for the validation to create similar behaviour between the FE-model and the real tests it needed to be neglected, which limits the study's ability to show the influence of friction. If friction would be included, it would result in different stiffnesses and resistances than what was measured. Including it would be more representative of the behaviour in a real case as friction is an important factor, especially during full shearing.

Furthermore, the screw would probably not only be applied by itself but rather be applied together with another screw. Since the model does not consider group effect, the distance between screws or take the edge/end distance into account, this model is in its base incomplete and would need another verification if one would want to study these phenomena. The experiments against which the model is validated does not take this into account either ergo it would require new experiments to explore further.

One of the bigger differences between the FE-model and hand calculations is that the FE-model considers non-linearity in the screws and has the capacity to express the stiffness outside of SLS and in ULS. Furthermore, the numerical results are more thorough compared to the analytical results and can for example show how the forces may vary inside the screw.

8.4 Extension of the current models

When extending the FE-model to try on new load-to-grain angles assumptions are made about how the model will react. One such assumption is how the rope effect will impact the resistance of the connection due to it being related to the timber member's friction which might decrease when the members have less connection. The change of embedment strength for new force angles is an estimation based on equation 3.14 and Hankinson (1921) theory. Equation 3.14 based on tests from Blaß et al. (2006) produced stiffness values below 1kN/mm for a force direction of $\gamma = 45°$, which seemed improbable and went against the theoretical behaviour of the connection. As a result, equation 6.2 was formed to give a better estimation of the embedment strength. This extension is not proven with experimental tests which only makes it an estimation of the behaviour, but it was chosen as it seemed to represent a behaviour more in line with the theory. The axial stiffness in equation 3.17 showed an accurate behaviour for shearing when used in Tomasi et al. (2010) equations, while the axial stiffness in equation 3.18 gave a similar behaviour of the stiffness in pulling with Jockwer et al. (2014b) equations. Since the new equation is made through interpolation between the previous stiffness equations it might not correspond to a realistic representation of how the stiffness varies in new load-to-grain angles. Since there is so little research on the subject it is hard to verify the assumptions made when modelling, which can make one question the validity of the results. The same is true regarding modelling the different screw axis-to-grain angles which do not have experimental test results. The results can not be certain unless they are verified with experiments.

8.5 Economical evaluation

When comparing the experimental results with the current calculation standards, EC5 underestimates the resistance of connections in all investigated screw-to-grain angles both for shearing and pulling, as well as the stiffness in lower angles. This is especially true for shearing at 45 degrees where both EC5 values for stiffness and resistance are less than half of the experimental values. This is of interest since it indicates that the fastener can be used in a less-than-optimal way when designed according to Eurocodes guidelines. If there would be a need for high-stiffness connections the standards would present a solution that is more demanding to achieve low ductility in the connection and therefore not optimising the performance of the building. As the load-carrying capacity of all investigated connections are significantly higher than the limitations set by the current calculation standards, it would suggest that there is an unnecessary use of material, something which might lead to increased costs and increased environmental impact. Using a more correct equation will therefore lead to a better understanding of how the connections behave and to create more correct usage of material. Using equations which underestimate the capacity of inclined screws might in some situations create the assumption that screws as a fastener is a less than valid option. This would narrow the possibilities

of flexible construction solutions and limit the ways one can construct connections. The lack of knowledge and optimisation in this area might in turn create an overall more expensive building since the contractor might look to other more expensive connections as alternatives, which might in turn lead to less innovation and development of screws. Having a more correct calculation of inclined screws might also improve the safety of the building since there might not be a clear understanding of how much the building can withstand with these types of connections. Having an incorrect understanding could potentially make the building behave differently than desired and could result in accidents.

8.6 Implementing

If one were to implement the forthcoming equations from Eurocode 5 second generation, the key takeaway from this report is that when using self-tapping screws, an angle of 35-50 degrees for the screw-to-grain angle is preferred in shearing. If one has the screw in this angle the screws have an increased resistance due to the screw's axial capacity which can enable the use of fewer screws for the connection. One can also use two screws in a cross-wise fashion to enable the connection to handle both compression and tension in a satisfactory way. It also creates both high stiffness and a ductile connection due to their combined attributes while still having a high resistance. In pulling it is wise to have a screw-to-grain angle closer to 90 degrees to be able to utilise the axial strength and stiffness in the most optimal way. It is crucial to note that as of writing this thesis, the second generation of Eurocode is still a draft and has not reached its final completion. New research and development could, and probably will create changes to the draft before its planned release in 2025.

For new force-to-grain angles (γ) a general guideline for inserting screws is to place them at an angle close to the force direction as the high withdrawal capacity generally dominates the contribution of stiffness and load-carrying capacity. Since some connections are exposed to loading scenarios which are not idealised (not pure shear or pulling) the connections might handle the loads better when designed crosswise due to their wide application capability.

9
Conclusion

The analysis of inclined screw's behaviour is something which is complex to simulate correctly and difficult to create analytical expressions for due to the orthotropic characteristics of the wood. However, there are several simplified analytical equations which can be used to express the behaviour of a connection for both stiffness and resistance. The results from physical experiments as well as the numerical result indicate that some analytical approaches are more correct depending on the situation. Where Jockwer et al. (2014a) approach represents the most similar values to the test results for resistance in shear and pulling. For stiffness in shear Tomasi et al. (2010) approach provided the best representation of the results if the expression for lateral stiffness (R_v) was changed to the new expression from the second generation of Eurocode. The stiffness in pulling only had one applicable analytical approach which was from Jockwer et al. (2014a) and showed to be relatively accurate to the tested results.

It is clear that the equations from Eurocode underestimate the stiffness in connections with inclined screw for certain angles due to its disregard for the separation between axial and lateral stiffness. Eurocode second generation is therefore a big improvement when calculating stiffness as it takes this into consideration along with additional factors. The second generation together with the current standard does however not take pulling into consideration as of writing this thesis, which put limits to the situations where they can be applied.

The resistance is relatively underestimated for all angles in the current calculation standard which indicates the posibillity of a major reduction of material use, regarding screws as fasteners. The economical gain and the increased range of application for connections with inclined screws are apperent if the standards are improved. If the extension based on new force directions are developed further, verified through additional research and experimental test results, further improvement regarding cost and applicability could be made.

9.1 Further research

When conducting this thesis we analysed several different load-to-grain angles (γ) for different screw-to-grain angles (α) in a FE-model and through analytical equations. To verify all the results gathered in this thesis there should be further studies performing experimental tests, expecially for new force to grain angles (γ). Further

tests should also consider screws with different material properties and geometries in order to consider their impact on resistance and stiffness. This becomes apparent as Jockwer et al. (2014a) suggested a change to the withdrawal capacity and yielding moment of the screw for it to be more relatable to the test results during pulling. This report is focused on individual inclined fasteners in timber-timber, therefore it is of interest to conduct additional studies with several fasteners in different inclinations and cross-wise.

The numerical model in this thesis is based on the beam-on-foundation approach according to De Santis and Fragiacomo (2021) and does in this case not take friction into consideration. Further research could therefore be made on how to implement friction accurately in a FE-model in order to develop the model further. It could then be of interest how the friction coefficient varies with different load-to-grain angles (γ).

Bibliography

Bejtka, I., & Blaß, H. J. (2002). Joints with inclined screws. *Bejtka I., Blaß H.J. (2002): Joints with inclined screws. In: Proc. of the CIB-W18 Meeting 35, Kyoto, Japan,Paper No. CIB-W18/35-7-4.*

Bejtka, I., & Blaß, H. J. (2005). Verstärkung von Bauteilen aus Holz mit Vollgewindeschrauben. *Fakultät fürBauingenieur-, Geo- und Umweltwissenschaften, Universtität Karlsruhe, Karlsruhe, Germany.*

Blaß, H. J., Bejtka, I., & Uibel, T. (2006). *Tragfähigkeit von Verbindungen mit selbstbohrenden Holzschrauben mit Vollgewinde.*

CEN. (2013). *EN 14080: Timber structures - Glued laminated timber and glued solid timber.*

CEN. (1991). EN 26891: Timber structures - Joints made with mechanical fasteners - General principles for the determination of strength and deformation characteristics.

CEN. (2022a). *prEN 1993-1-14; Eurocode 3: Design of Steel Structures—Part 1–14: Design Assisted by Finite Element Analysis; CEN/TC 250/SC 3 N 3723.*

CEN. (2022b). *prEN 1995-1-1: Eurocode 5 Design of timber structures — Part 1-1: General rules and rules for buildings. . CEN/TC 250/SC 5 N 1650, 12-2022.*

De Santis, Y., & Fragiacomo, M. (2021). Timber-to-timber and steel-to-timber screw connections: Derivation of the slip modulus via beam on elastic foundation model. *Engineering Structures*, *244*. https://doi.org/10.1016/j.engstruct.2021.112798

Deutsches Institut fur Bautechnik. (2006). Allgemeine baufsichtliche Zulassung, SFS Befestiger WT-T-6,5, WT-T-8,2, WT-R-8,9 als Holzverbindungsmittel.

Deutsches Institut fur Bautechnik. (2011). Z-9.1-472, Allgemeine bauaufsichtliche Zulassung, SFS Befestiger WT-S-6,5; WT-T-6,5; WT-T-8,2; WR-T-9.0 und WR-T-13 als Holzverbindungsmittel.

Hankinson, R. (1921). *Investigation of crushing strength of spruce at varying angles of grain.* Air Force Information Circular No. 259, U. S. Air Service, USA.

Hanna, D., & Tannert, T. (2021). Glulam connections assembled with screws in different installation angles. *Maderas: Ciencia y Tecnologia*, *23*, 1–14. https://doi.org/10.4067/s0718-221x2021000100454

Jockwer, R., Steiger, R., & Frangi, A. (2014a). *Design model for inclined screws under varying load to grain angles Timber-concrete composite slabs with micro-notches.* https://www.researchgate.net/publication/278671728

Jockwer, R., Steiger, R., & Frangi, A. (2014b). Fully Threaded Self-tapping Screws Subjected to Combined Axial and Lateral Loading with Different Load to

Grain Angles. *RILEM Bookseries*, *9*, 265–272. https://doi.org/10.1007/978-94-007-7811-5{_}25

Johansen, K. (1949). Theory of timber connections. https://doi.org/10.5169/seals-9703

Loss, C., Hossain, A., & Tannert, T. (2018). Simple cross-laminated timber shear connections with spatially arranged screws. *Engineering Structures*, *173*, 340–356. https://doi.org/10.1016/j.engstruct.2018.07.004

Swedish Wood. (2022a). *Design of timber structures, Rules and formulas according to Eurocode 5, Volume 2*. www.swedishwood.com.

Swedish Wood. (2022b). *Design of timber structures: Rules and formulas according to Eurocode 5, Volume 1*. www.swedishwood.com.

Tomasi, R., Crosatti, A., & Piazza, M. (2010). Theoretical and experimental analysis of timber-to-timber joints connected with inclined screws. *Construction and Building Materials*, *24*(9), 1560–1571. https://doi.org/10.1016/j.conbuildmat.2010.03.007

A

Input parameters for non-linear springs

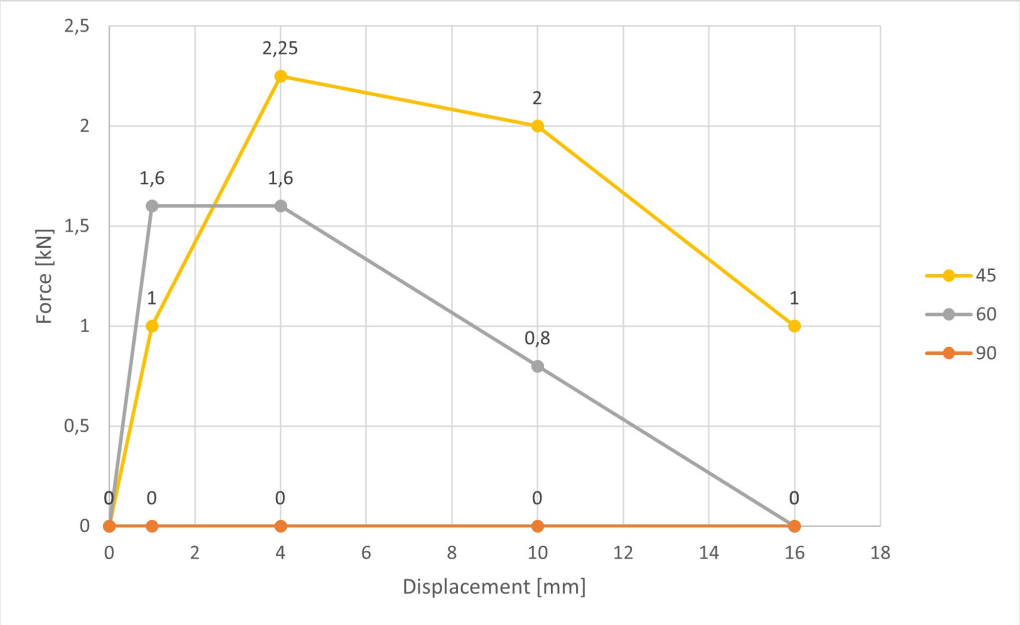

Figure A.1: Input parameters for the parallel spring stiffness (k_p) in Abaqus that describes the screw behaviour in shear

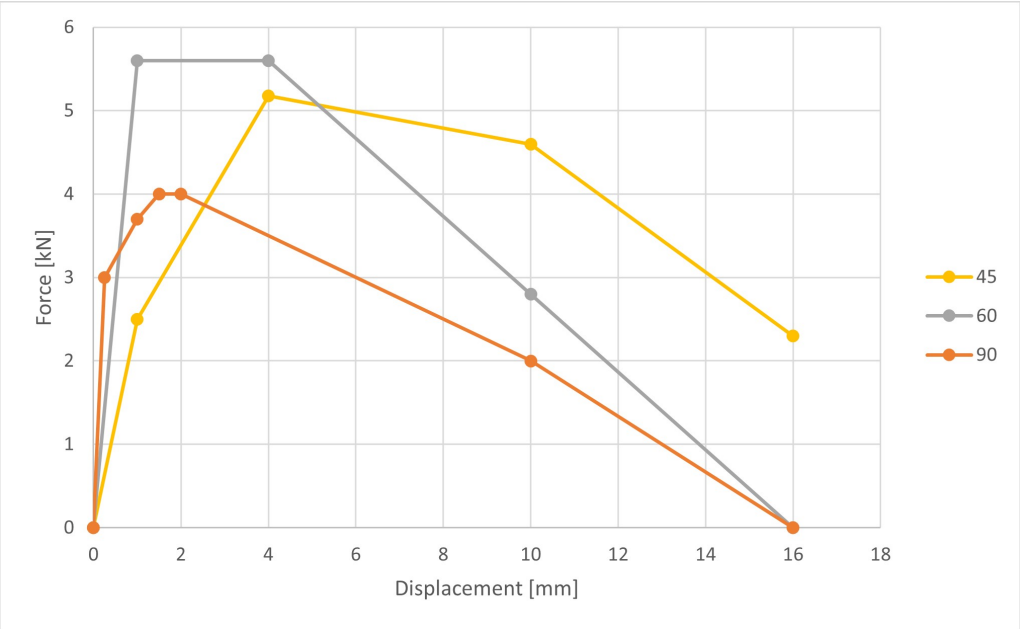

Figure A.2: Input parameters for the perpendicular spring stiffness (k_t) in Abaqus that describes the full screw behaviour in shearing in shear

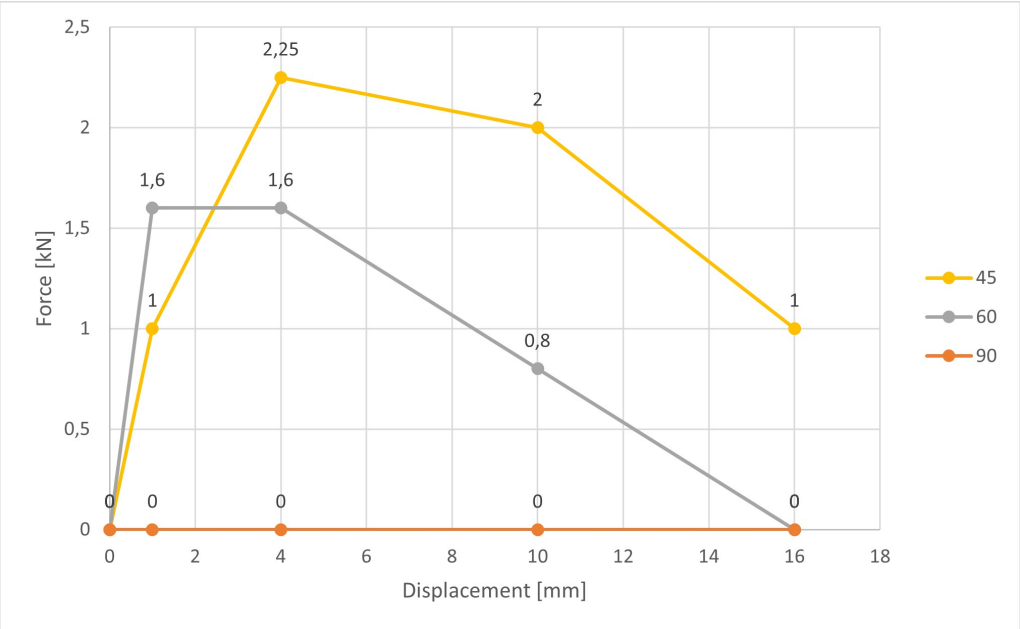

Figure A.3: Input parameters for the parallel spring stiffness (k_p) in Abaqus that describes the screw behaviour in pulling

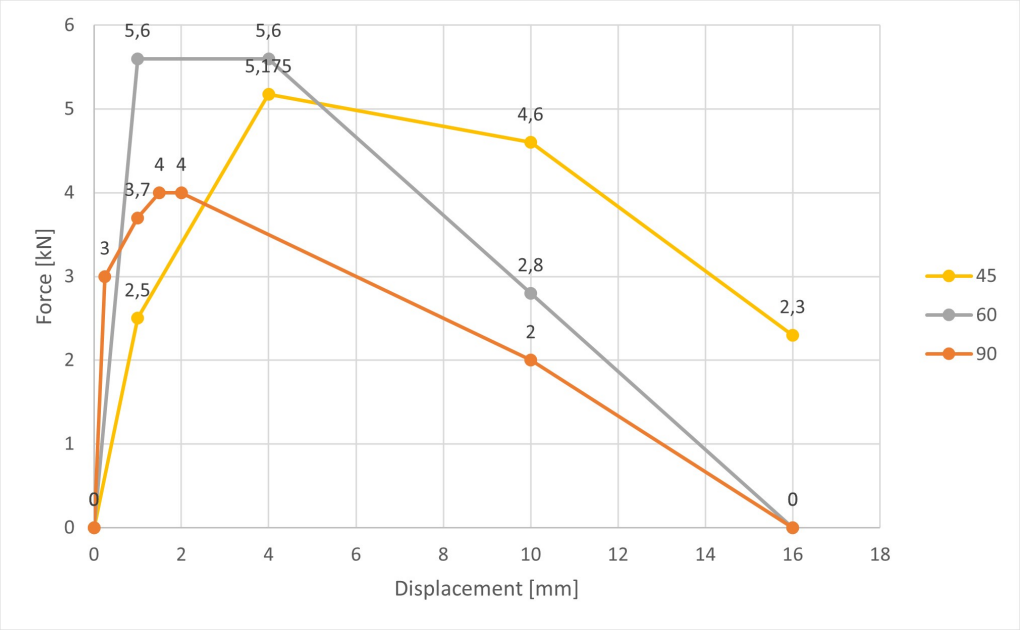

Figure A.4: Input parameters for the perpendicular spring stiffness (k_t) in Abaqus that describes the full screw behaviour in pulling

DEPARTMENT OF SOME SUBJECT OR TECHNOLOGY
CHALMERS UNIVERSITY OF TECHNOLOGY
Gothenburg, Sweden
www.chalmers.se

CHALMERS
UNIVERSITY OF TECHNOLOGY